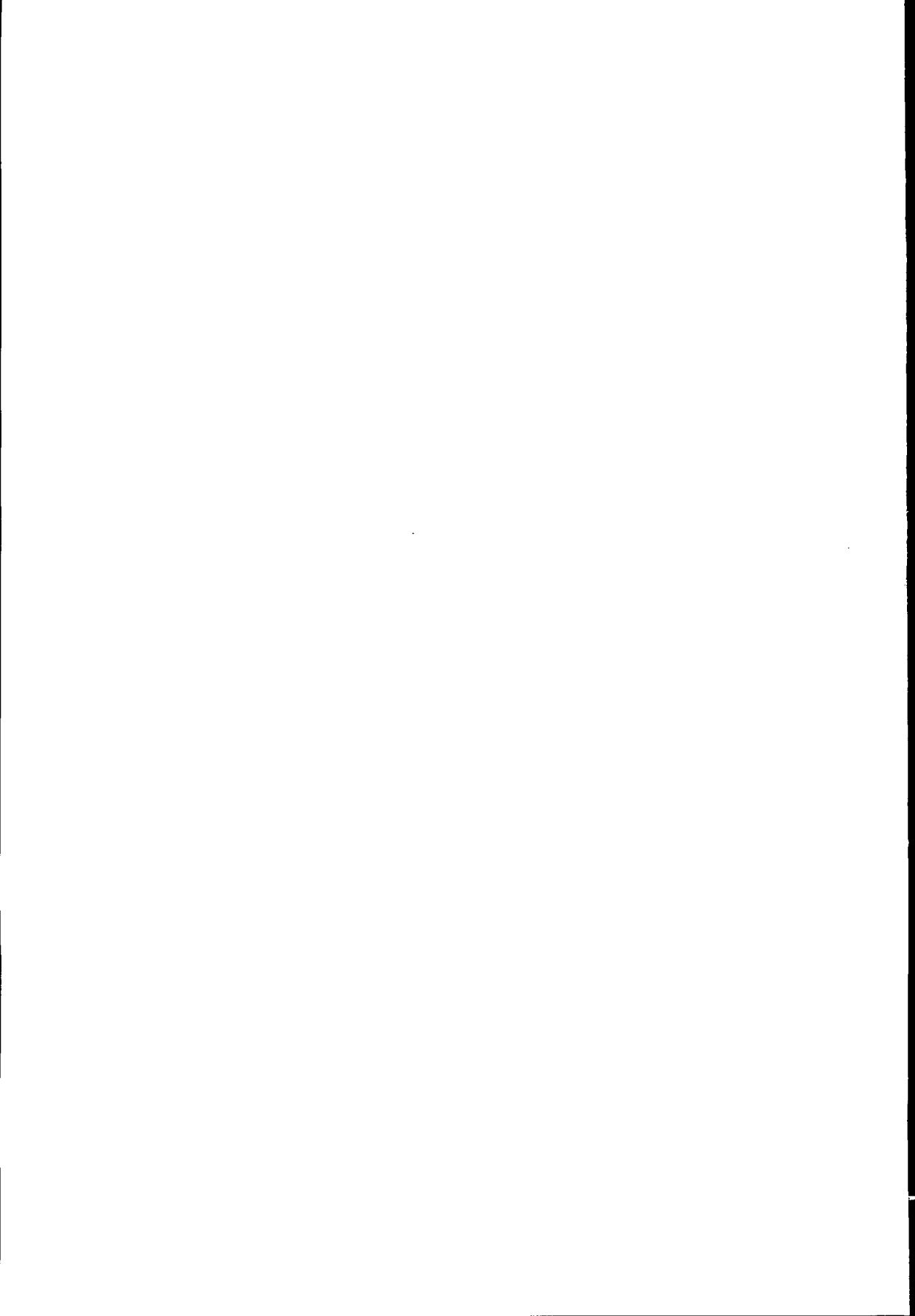


# SATEM 2002: Software for Aquifer Test Evaluation



ILRI publication 57

# SATEM 2002: Software for Aquifer Test Evaluation

J. Boonstra

R.A.L. Kselik



International Institute for Land Reclamation and Improvement/ILRI  
P.O. Box 45, 6700 AA Wageningen, The Netherlands, 2001

This book is published in the ILRI Publication Series. The main characteristic of this series is that the books are "practical" in the sense that they can be used in the day-to-day work of those professionals (mostly engineers) who are involved in irrigation and drainage.

The aims of ILRI are:

- To collect information on land reclamation and improvement from all over the world;
- To disseminate this knowledge through publications, courses, and consultancies;
- To contribute – by supplementary research – towards a better understanding of the land and water problems in developing countries.

© International Institute for Land Reclamation and Improvement/ILRI, Wageningen, The Netherlands.

This book or any part thereof may not be reproduced in any form without the written permission of ILRI.

ISBN 90-70754-54-1

Printed in The Netherlands

# Preface

Since ILRI Publication 48 *SATEM: Selected Aquifer Test Evaluation Methods*, A microcomputer program was published in 1989, the software has been updated many times, but the accompanying manual has merely been reprinted. Now, at last, here is the new book *SATEM 2002: Software for Aquifer Test Evaluation*. Readers familiar with ILRI Publication 48 will note a number of changes to the text and the accompanying software of this book.

What are these changes? In the first place, there are now distance-drawdown analyses to complement the time-drawdown analyses of piezometers and step-drawdown analyses to analyse the time-drawdown data of the pumped well itself. In addition, step-drawdown analyses provide valuable information for exploitation wells. Secondly, we have also included a large number of aquifer and step-drawdown test analyses based on field data. Finally, we have made a special effort to make the software more user-friendly, by providing a clear and complete interface and ample on-line help.

The underlying philosophy of this latest version of the SATEM software is the same as that of the earlier versions: a diagnostic plot of the field data is presented on-screen. SATEM 2002 also enables users to check their analysis by presenting a match between the drawdowns observed in the field and the theoretical drawdowns found from the analysis. Hence, the matching itself is still performed by the user. This approach combines the advantages of manual analysis (i.e. professional judgement and a 'feel' for the local hydrogeological conditions) with the advantages of the computer (i.e. data can be analysed quickly and accurately, sensitivity analyses that represent possible combinations of aquifer and well conditions are easily performed, and hard copies of the data curve and the best-fitting theoretical curve can be produced and used directly as report-ready figures).

Using SATEM 2002, tests in unconsolidated aquifers that are confined, leaky, or unconfined can be analysed, providing that the pumped well penetrates the aquifer fully. SATEM 2002 can be used for confined and unconfined aquifers with partially penetrating wells. It can also be used to evaluate the drawdown data observed during the pumping period and the residual drawdown data observed during the subsequent recovery period. The data can be taken from observation wells, or from the pumped well, or from both.

Although we have written this book primarily for professionals, we are confident that it will also be valuable to students and teachers. For them, we have included not only the computer-aided analyses, but also the manual procedures. In addition, the book offers professionals, students and teachers alike the opportunity to deepen their insight by making their own sets of test data with the auxiliary program SDG (Synthetic Data Generator) and solving them with the SATEM 2002 program package.

The authors

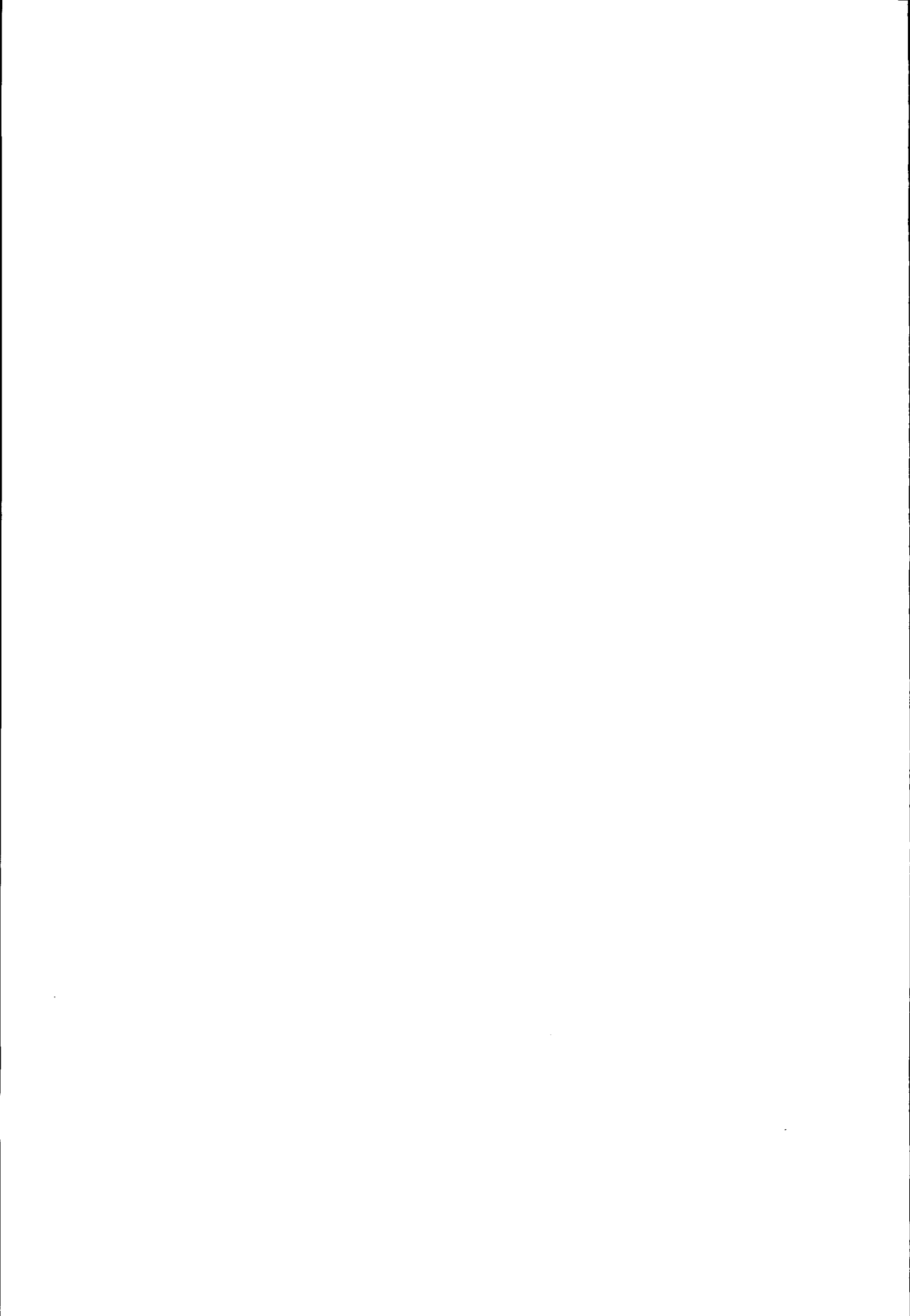


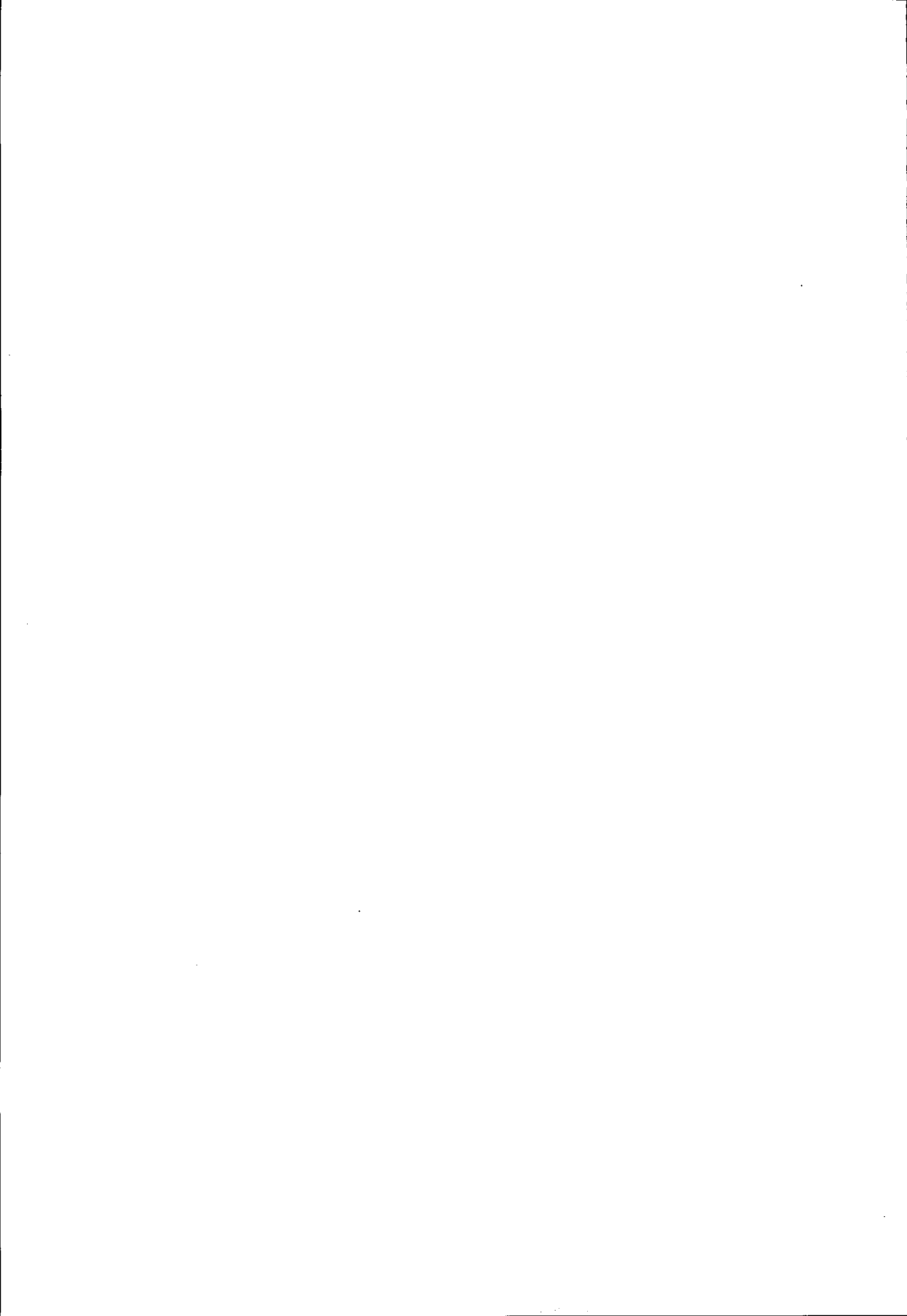
# Table of contents

1	Introduction	11
2	Basic concepts and definitions	13
	2.1 Types of water-bearing layers	13
	2.2 Aquifer types	13
	2.3 Hydraulic head	15
	2.4 Darcy's law	16
	2.5 Anisotropy and heterogeneity	18
	2.6 Physical properties	19
	2.6.1 Hydraulic conductivity (K)	19
	2.6.2 Saturated thickness (H, D')	20
	2.6.3 Transmissivity (KH or T)	20
	2.6.4 Specific storage ( $S_s$ ) and storativity (S)	20
	2.6.5 Specific yield ( $S_y$ )	21
	2.6.6 Hydraulic resistance (c)	22
	2.6.7 Leakage factor (L)	22
3	Performing an aquifer test	23
	3.1 General	23
	3.2 Measurements	24
	3.3 Duration of a pumping test	26
	3.4 Reporting and filing the data	28
4	Theory of aquifer test analysis	31
	4.1 Confined aquifers	31
	4.1.1 Theis-Jacob's method	32
	4.1.2 Thiem-Jacob's method	34
	4.2 Leaky aquifers	36
	4.2.1 Hantush's inflection-point method	37
	4.2.2 Hantush-Jacob's method	40
	4.3 Unconfined aquifers	42
	4.4 Partially penetrating wells	44
	4.4.1 Jacob-Hantush's method	46
	4.5 Recovery tests	48
	4.5.1 Theis's recovery method	49
	4.6 Single-well tests	52

5	Theory of step-drawdown test analysis	55
5.1	Well and aquifer losses	55
5.2	Well efficiency	57
5.3	Diagnostic plots	58
5.4	Jacob's method	59
5.5	Rorabaugh's method	61
6	SATEM 2002 software package	63
6.1	Installation procedure	63
6.2	Type of analysis	64
6.3	Input	64
6.3.1	General test features	65
6.3.2	Features of data sets	66
6.3.3	Data set specific features	67
6.3.4	Units	68
6.4	Analysis	69
6.5	Output	71
7	Familiarising yourself with SATEM 2002	73
7.1	Using Theis-Jacob's method	73
7.2	Using Hantush's inflection-point method	76
7.3	Using Jacob-Hantush's method	79
7.4	Using Theis's recovery method	81
7.5	Applicability of time-drawdown methods	82
7.5.1	Theis-Jacob's method	83
7.5.2	Hantush's inflection-point method	85
7.5.3	Jacob-Hantush's method	87
8	Time-drawdown analyses	91
8.1	Using Theis-Jacob's method	91
8.2	Using Hantush's inflection-point method	95
8.3	Using Jacob-Hantush's method	98
8.4	Using Theis's recovery method	100
8.5	Guidelines	102



9	Distance-drawdown analyses	107
	9.1 Using Thiem-Jacob's method	107
	9.2 Using Hantush-Jacob's method	110
	9.3 Guidelines	111
10	Step-drawdown analyses	115
	10.1 Using Jacob's method	115
	10.2 Using Rorabaugh's method	118
	10.3 Guidelines	121
11	Case studies	125
	11.1 Aquifer test in an unconfined aquifer	125
	11.2 Aquifer test in a confined aquifer	128
	11.3 Aquifer test in a leaky aquifer	131
	11.4 Single-well test in an unconfined aquifer	134
	References	137
	List of principal symbols and units	139
	Appendix	141
	Index	145



# 1 Introduction

The SATEM 2002 software package can be used to (1) estimate hydraulic properties of water-bearing layers from exploration wells and (2) determine the optimum production capacity of exploitation wells and analyse the well performance over time, to facilitate maintenance and rehabilitation.

There are numerous examples of groundwater-flow problems whose solution requires a knowledge of the hydraulic properties of water-bearing layers. The problem may be to predict the future water table if one or more wells are pumped for water supply. Or it may be a more regional problem of determining how much water can be withdrawn from a large groundwater basin. Or it may be one of determining the seepage flow into a waterlogged area, as in a groundwater balance study.

One of the most effective ways of determining the hydraulic properties of water-bearing layers is to perform an aquifer test. The procedure is simple: water is pumped from a well in the aquifer for a certain time and at a certain rate, and the effect of this pumping on the water table is measured at regular intervals in the well itself and in a number of piezometers nearby.

Aquifer tests are so costly that in most studies of regional groundwater resources, the number of aquifer tests that can be performed must be restricted. It is possible, however, to perform an aquifer test without using piezometers, thereby cutting costs. Of course, one must then accept a certain, sometimes appreciable, error. To distinguish such tests from the normal aquifer test, they are often called single-well tests.

To determine the hydraulic properties of water-bearing layers from a single-well test or an aquifer test, the data collected during the test are substituted into an appropriate well-flow equation. This manual deals only with the well-flow equations incorporated into SATEM 2002. For well-flow equations that cover a wider range of conditions, see Kruseman and de Ridder (1990).

Aquifer tests are commonly preceded by step-drawdown tests to determine the appropriate discharge rate for the subsequent aquifer test. In this context, 'appropriate' means that during the pumping period of such an aquifer test the resulting drawdowns are substantial so that sufficiently accurate measurements can be made, but that the drawdown will not reach the top of the well screen before the end of the pumping period. The implicit assumption is that the drawdowns in the piezometers will then also be substantial. In the case of exploitation wells, the results of step-drawdown tests are used to determine the optimum production capacity and to analyse the well performance over time, to facilitate maintenance and rehabilitation. The latter analysis is done by repeating this type of test each year and by comparing the yearly results of the step-drawdown analyses.

This manual comprises 11 chapters. Chapters 2 to 5 are essential background reading. Chapter 2 summarises the basic concepts and definitions of terms relevant to the subject and the subsequent discussions. In Chapter 3, guidelines are presented on how to conduct an aquifer test, with special reference to the measurements, the duration, and the processing of the data. Chapters 4 and 5 present the theories of aquifer and step-drawdown tests and explain the procedures for analysing the data manually. We have done this to clarify how the computer analyses are actually performed in SATEM 2002.

Chapters 6 and 7 are indispensable for readers not familiar with previous versions of SATEM. Chapter 6 presents the features of the SATEM 2002 software package. It explains the installation procedure and discusses the three main modules: input, analysis, and output. Chapter 7 presents guidelines on how to perform the actual analyses for each of the four time-drawdown/recovery analysis methods of SATEM 2002; fictitious data are used to demonstrate the specific features of these methods.

Chapters 8, 9, and 10 present field data to show how the data can be analysed with the time-drawdown, distance-drawdown, and step-drawdown analysis methods of SATEM 2002, respectively. These three chapters assume that the user will follow the instructions in the manual while sitting at the computer. The user can opt to see how we personally analysed the data or to do the analyses himself. These three chapters can be read independently of each other. For instance, readers wishing to familiarise themselves with the analysis of step-drawdown data can go directly to Chapter 10.

Chapter 11 presents four case studies in which we have analysed field data combining the various analysis methods of SATEM 2002. It too is intended to be read while sitting at the computer. It is essential reading.

## 2 Basic concepts and definitions

This chapter summarises some basic concepts and definitions of terms relevant to the hydraulic properties of water-bearing layers and the discussions which follow.

### 2.1 Types of water-bearing layers

Water-bearing layers are classified according to their water-transmitting properties into aquifers, aquitards or aquicludes. With regard to the flow to pumped wells the following definitions are commonly used.

- An aquifer is a water-bearing layer in which the vertical flow component is so small with respect to the horizontal flow component that it can be neglected. The groundwater flow in an aquifer is assumed to be predominantly horizontal.
- An aquitard is a water-bearing layer in which the horizontal flow component is so small with respect to the vertical flow component that it can be neglected. The groundwater flow in an aquitard is assumed to be predominantly vertical.
- An aquiclude is a water-bearing layer in which both the horizontal and vertical flow components are so small that they can be neglected. The groundwater flow in an aquiclude is assumed to be zero.

Common aquifers are geological formations of unconsolidated sand and gravel, sandstone, limestone, and severely fractured volcanic and crystalline rocks. Examples of common aquitards are clays, shales, loam, and silt.

### 2.2 Aquifer types

The four types of aquifer distinguished (Figure 2.1) are: confined, unconfined, leaky and multi-layered.

A confined aquifer is a completely saturated aquifer bounded above and below by aquicludes. The pressure of the water in confined aquifers is usually higher than atmospheric pressure, which is why when a well is bored into the aquifer the water rises up the well tube, to a level higher than the aquifer (Figure 2.1.A). The piezometric level is the imaginary level to which the water

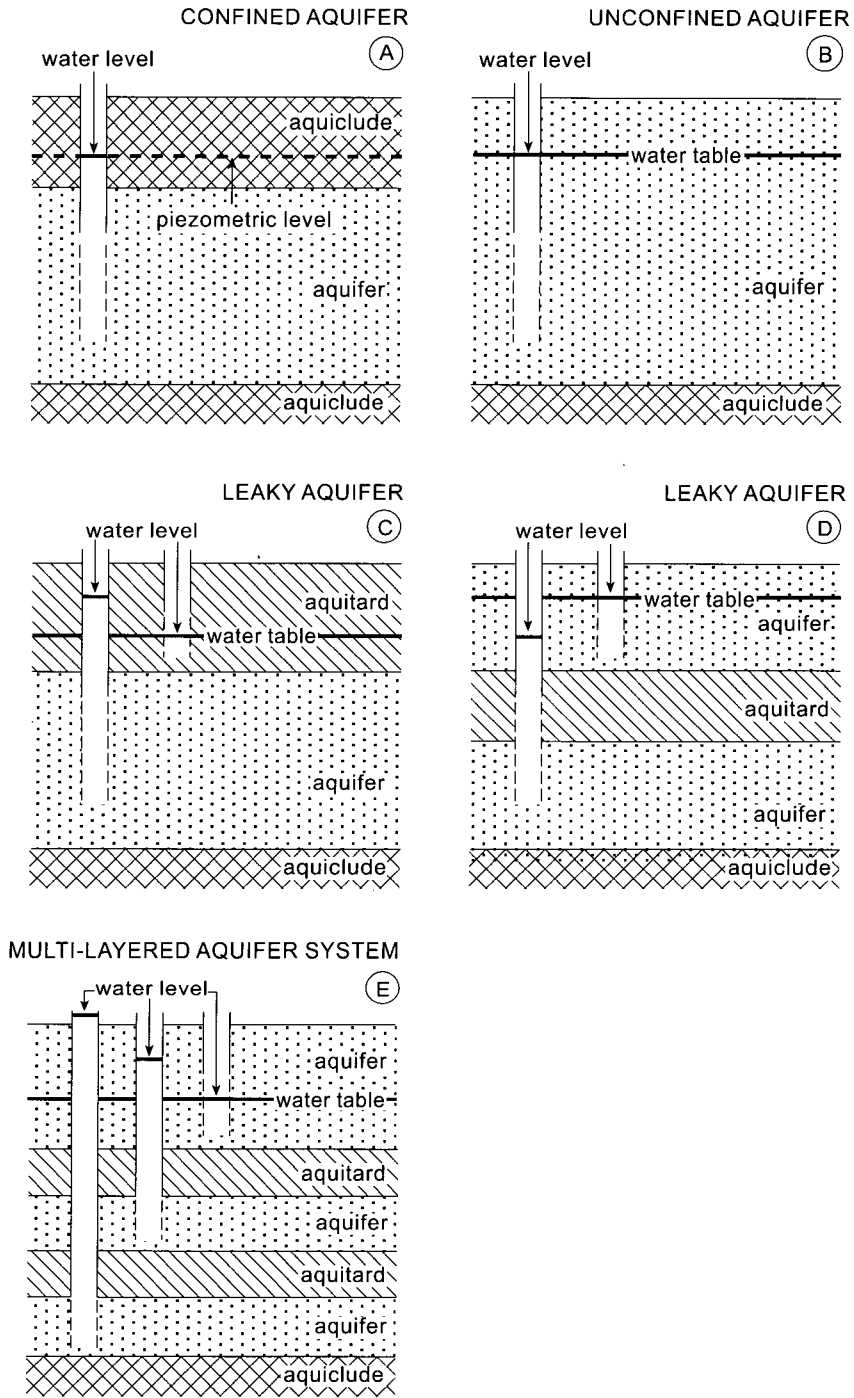


Figure 2.1 Types of aquifers

level will rise in wells penetrating the aquifer. If this level is above the ground surface, the well is a free-flowing or artesian well.

An unconfined aquifer is a partly saturated aquifer bounded below by an aquiclude and above by the free water table or phreatic surface (Figure 2.1.B). At the free water table, the groundwater is at atmospheric pressure. In general, the water level in a well penetrating an unconfined aquifer does not rise above the water table, except when there is vertical flow.

A leaky aquifer, also known as a semi-confined aquifer, is a completely saturated aquifer that is bounded below by an aquiclude and above by an aquitard. If the overlying aquitard extends to the land surface, it may be partly saturated (Figure 2.1.C), but if it is overlain by an unconfined aquifer that is bounded above by the water table (Figure 2.1.D), it will be fully saturated. If there is hydrological equilibrium, the piezometric level in a well tapping a leaky aquifer may coincide with the water table. In areas with upward or downward flow, in other words, in discharge or recharge areas, the piezometric level may rise above or fall below the water table.

A multi-layered aquifer is a succession of leaky aquifers sandwiched between aquitards (Figure 2.1.E). Systems of interbedded permeable and less permeable layers like this are very common in deep sedimentary basins.

### 2.3 Hydraulic head

Groundwater moves from levels of higher energy to levels of lower energy, so its energy level is essentially the result of elevation and pressure. The energy level of groundwater at a certain point in the water-bearing layer corresponds with the elevation – as measured from an arbitrary plane of reference – to which the groundwater will rise in a pipe that is open at the point in question (Figure 2.2). The length of the water column,  $h$ , represents this

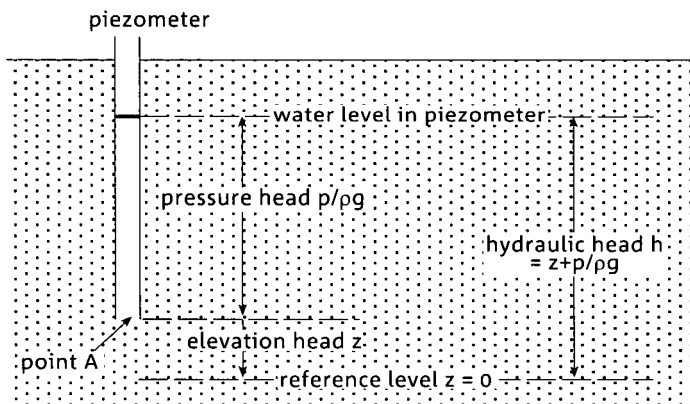


Figure 2.2 Hydraulic head

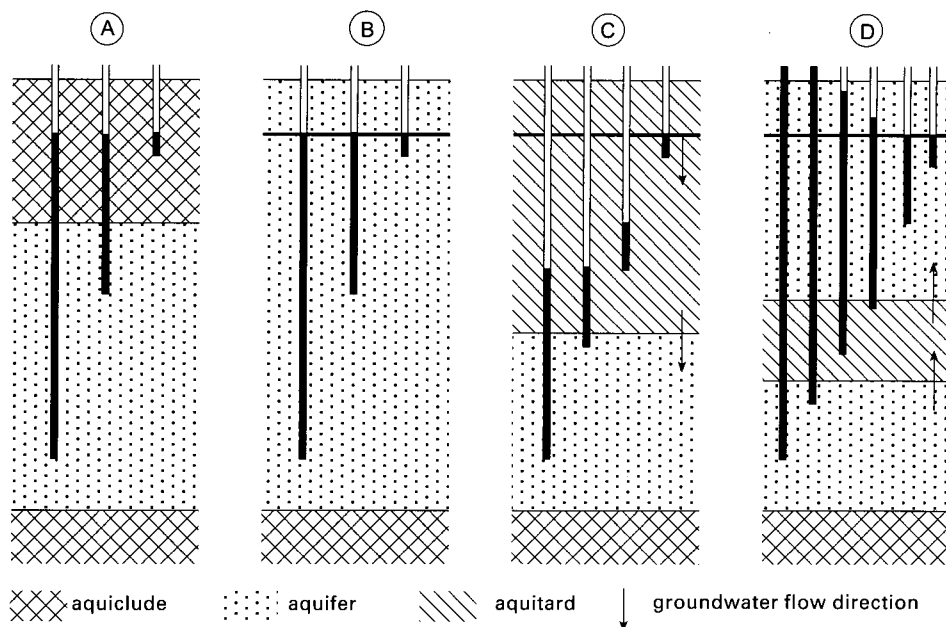


Figure 2.3 Examples of water levels observed in piezometers

energy level and is called the hydraulic head. A pipe driven or placed in the subsoil so that there is no leakage around it and all entrance of water into the pipe is through the open bottom, is called a piezometer. When the pipe has slots or perforations in its lower part (screen), it is called an observation well.

In aquifers, vertical flow components are usually lacking or of such minor importance that they can be neglected. Hence at any depth in an aquifer, the hydraulic head corresponds to the water table height; in other words, when measuring the water level it does not make any difference how far the piezometer penetrates the aquifer, as Figures 2.3.A to 2.3.D show.

In aquitards, the flow of groundwater is mainly vertical. When there is such a flow, the water level in a piezometer penetrating the aquitard is a function of the depth of penetration (Figures 2.3.C and 2.3.D).

In a confined or unconfined aquifer it is sufficient to install a single piezometer or observation well at a certain location, but in a leaky or multi-layered aquifer several piezometers penetrating to different depths should be installed at the same location.

## 2.4 Darcy's law

The fundamental equation describing the flow of groundwater was described by Darcy (1856). Darcy's law states that the rate of flow through a porous medium is proportional to the loss of head and inversely proportional to the



length of the flow path, or

$$v = K \frac{\Delta h}{\Delta l} = -Ki \quad (2.1)$$

where  $v$  is the specific discharge or Darcy velocity (m/d);  $K$  is the hydraulic conductivity (m/d);  $\Delta h$  is the head loss (m);  $\Delta l$  = length of flow path (m); and  $i$  is the hydraulic gradient (-).

Darcy's law can alternatively be written as

$$Q = -K \frac{\Delta h}{\Delta l} A = -KiA \quad (2.2)$$

where  $Q$  is the volume rate of flow ( $m^3/d$ ) and  $A$  is the cross-sectional area normal to flow direction ( $m^2$ ).

The hydraulic conductivity  $K$  is a parameter depending on the properties of the porous medium and of the fluid. It is the flow rate per unit cross-sectional area under influence of a unit gradient. The hydraulic conductivity  $K$  differs from the intrinsic permeability,  $k$ . The relation between these two parameters is

$$K = k \frac{\rho g}{\mu} \quad (2.3)$$

where  $k$  is the intrinsic permeability of the porous medium ( $m^2$ );  $\rho$  is the density of the fluid, i.e. the water ( $kg/m^3$ );  $g$  is the acceleration due to gravity ( $m/d^2$ ); and  $\mu$  is the dynamic viscosity of the fluid, i.e. water ( $kg/m.d$ ).

In using Darcy's law it is important to know the range of its validity. After all, Darcy (1856) conducted his experiments on sand samples in the laboratory. Darcy's law is valid for laminar flow, but it is not valid when the flow is turbulent, as may happen in cavernous limestone, or fractured basalt. If there is any doubt, the Reynolds number serves as a criterion to distinguish between laminar and turbulent flow. The Reynolds number is expressed as

$$N_R = \rho \frac{vd}{\mu} \quad (2.4)$$

where  $d$  is a representative length dimension of the porous medium, usually taken as a mean grain diameter or a mean pore diameter (m).

Several experiments have shown that Darcy's law is valid for  $N_R < 1$  and does not create severe errors up to  $N_R = 10$ . This value thus represents an upper limit to the validity of Darcy's law. It should not be considered as a unique limit, however, because turbulence arises gradually. At full turbulence, the head loss is not linear but is approximately the velocity squared. Fortunately, most groundwater flow occurs with  $N_R < 1$  so that Darcy's law applies. Only in exceptional situations, where the rock contains wide openings, or in the near vicinity of a pumped well, will the criterion of laminar flow remain unsatisfied and will Darcy's law then not be valid.

## 2.5 Anisotropy and heterogeneity

The well-flow equations presented in this manual are based on several assumptions, one of which is that aquifers and aquitards are homogeneous and isotropic. This means that the hydraulic conductivity is independent of where it is measured within the formation and also independent of the direction of measurement (Figure 2.4.A). The individual particles of geological formations are seldom spherical, so when deposited under water they tend to settle on their flat sides. Such a formation can still be homogeneous, but the hydraulic conductivity varies with the direction of measurement (Figure 2.4.B). In this particular case the hydraulic conductivity  $K_h$  measured in the horizontal plane is significantly greater than the hydraulic conductivity  $K_v$  measured in the vertical plane. This phenomenon is called anisotropy. In alluvial formations the  $K_h/K_v$  ratios normally range from 2 to 10, but values as high as 100 do occur.

The lithology of geological formations generally varies significantly in both horizontal and vertical planes. Consequently, the hydraulic conductivity now depends on the position within the formation. Such a formation is called heterogeneous. Figure 2.4.C is an example of layered heterogeneity. If the hydraulic conductivity of the individual layers also varies in the direction of

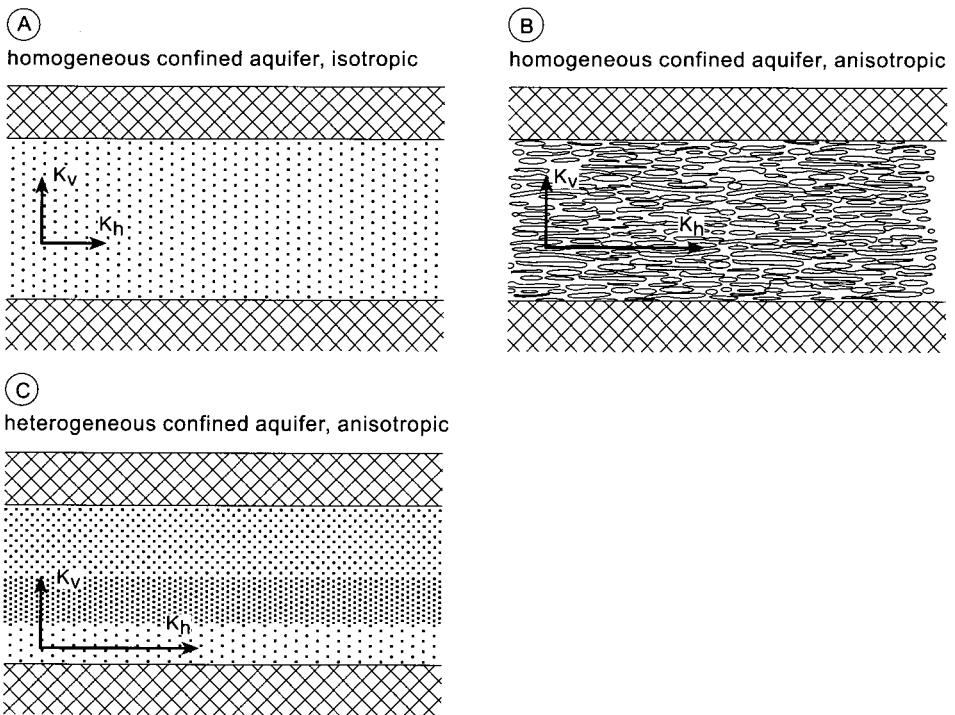


Figure 2.4 Homogeneous isotropic aquifer, homogeneous anisotropic aquifer, and heterogeneous anisotropic aquifer

measurement, the formation is, moreover, anisotropic. Heterogeneity appears in forms other than that shown in Figure 2.4.C: individual layers may pinch out, their grain size may vary in the horizontal plane, they may contain lenses of other grain sizes, or they may be discontinuous because of faulting.

## 2.6 Physical properties

This section summarises the physical properties and derived parameters of aquifers and aquitards which appear in the various equations that describe the flow to a pumped well.

### 2.6.1 Hydraulic conductivity (K)

The hydraulic conductivity is the proportionality constant in Darcy's law (Equation 2.1). Table 2.1 shows ranges of the hydraulic conductivities for aquifers consisting of different materials.

The hydraulic conductivity of a water-bearing layer is affected by the density and viscosity of the groundwater (Equation 2.3). The density of the water may vary with pressure, temperature and concentration of dissolved solids. For instance, saline water is denser than fresh water and will thus increase the hydraulic conductivity of a water-bearing layer. The viscosity is strongly influenced by the water temperature. The higher the temperature, the lower the viscosity of the water will be and the easier it will be for the water to move through the pores of a water-bearing layer, resulting in a higher value for hydraulic conductivity. Values of K are normally expressed for a temperature of 20°C.  $K_t$  values calculated for other temperatures (t) can be converted as follows

Table 2.1 Ranges of the hydraulic conductivity for different materials, in m/d (from Bouwer, 1978)

Geological classification	K
clay	$10^{-8} - 10^{-2}$
fine sand	1 - 5
medium sand	5 - 20
coarse sand	20 - 100
gravel	100 - 1000
sand and gravel mixes	5 - 100
clay, sand, gravel mixes (till)	$10^{-3} - 10^{-1}$
sandstone, carbonate rock	$10^{-3} - 10^0$
shale	$10^{-7}$
dense solid rock	$< 10^{-5}$
fractured or weathered rock (core samples)	almost 0 - $3 \cdot 10^2$
volcanic rock	almost 0 - $1 \cdot 10^3$

$$K_{20^\circ} = \frac{\mu_t}{\mu_{20^\circ}} K_t \quad (2.5)$$

The hydraulic conductivity values presented in Table 2.1 are valid for a temperature of 20°C.

### 2.6.2 Saturated thickness (H, D')

For confined aquifers, the saturated thickness is equal to the physical thickness of the aquifer between the aquicludes above and below it (see Figure 2.1.A). The same is true for the confined parts of a leaky aquifer bounded by an aquitard and an aquiclude (see Figures 2.1.C and 2.1.D). In both these cases, the saturated thickness is a constant over time.

For unconfined aquifers, the saturated thickness is equal to the difference between the free water table and the aquiclude (see Figure 2.1.B). Because the position of the water table changes over time, the saturated thickness of an unconfined aquifer is not constant over time. Whether constant or variable, the saturated thickness of an aquifer is denoted by the symbol H. It can range from several metres to hundreds or even thousands of metres.

For aquitards in leaky aquifers, the saturated thickness can be variable or constant. In Figure 2.1.C, the aquitard is partly saturated and has a free water table. Its saturated thickness depends upon the position of the water table. In Figure 2.1.D, the aquitard is bounded by two aquifers and is fully saturated. Its saturated thickness is physically determined and thus constant. The saturated thickness of an aquitard is denoted by the symbol D'. It may range from a few metres to tens of metres.

### 2.6.3 Transmissivity (KH or T)

The transmissivity is the product of the average hydraulic conductivity (K) and the saturated thickness of the aquifer (H). Consequently, the transmissivity is the rate of flow under a hydraulic gradient equal to unity through a cross-section of unit width over the whole saturated thickness of the water-bearing layer. It is expressed in m<sup>2</sup>/d. Its range can be derived from those of K and H.

### 2.6.4 Specific storage (S<sub>s</sub>) and storativity (S)

The specific storage S<sub>s</sub> of a saturated confined aquifer is the volume of water that a unit volume of aquifer releases from storage under a unit decline in head. This release of water under conditions of decreasing hydraulic head is brought about because the aquifer compacts under increasing effective stress

and because the water expands as a result of decreasing water pressure. The specific storage  $S_s$  depends on the elasticity of both the aquifer material and the water. For a certain location it can be regarded as a constant. Its order of magnitude is  $10^{-6}$ ; and it has the dimension of  $m^{-1}$ .

The storativity  $S$  of a saturated confined aquifer of thickness  $H$  is defined as the volume of water released from storage per unit surface area of the aquifer per unit decline in the component of hydraulic head normal to that surface. In a vertical column of unit area extending through the confined aquifer, the storativity  $S$  equals the volume of water released from the aquifer when the piezometric surface drops over a unit distance. Storativity is thus defined as

$$S = S_s H \tag{2.6}$$

The storativity of a saturated aquifer is a function of its thickness. Storativity is a dimensionless quantity, as it involves a volume of water per volume of aquifer. Its values in confined aquifers range from  $5 \times 10^{-5}$  to  $5 \times 10^{-3}$ .

### 2.6.5 Specific yield ( $S_y$ )

The specific yield is the volume of water that an unconfined aquifer releases from storage per unit surface area of aquifer per unit decline of the water table. In unconfined aquifers, the effects of the elasticity of the aquifer material and the water are negligible, except for a short time after pumping starts. Values for the specific yield are much higher than the storativities of confined aquifers. Table 2.2 shows ranges of the specific yield for different materials. Specific yield is sometimes called effective porosity, unconfined storativity, or drainable pore space. Small interstices do not contribute to the effective porosity, because the retention forces in them are greater than the weight of water. Hence, no groundwater will be released from these small interstices by gravity drainage.

Table 2.2 Ranges of the specific yield for different materials, in percentages (from Boonstra and de Ridder, 1981)

Geological classification	$S_y$
clay	1 - 18
fine sand, silt	1 - 46
medium and coarse sand	16 - 46
gravel	13 - 44
sandstone	2 - 41
siltstone	1 - 33
volcanic rock	2 - 47

### 2.6.6 Hydraulic resistance (c)

The hydraulic resistance characterises the resistance of an aquitard to vertical flow, either upward or downward. It is the ratio of the saturated thickness of the aquitard  $D'$  to its hydraulic conductivity for vertical flow  $K'$  and is thus defined as

$$c = D'/K' \quad (2.7)$$

The dimension of the hydraulic resistance is time and is, for example, expressed in days. It may range from a few days to thousands of days. Aquitards having c-values of 2000 to 2500 days or more, are regarded as acting as aquicludes, although theoretically an aquiclude has an infinitely high c-value.

### 2.6.7 Leakage factor (L)

The leakage factor, or characteristic length, is a measure of the spatial distribution of leakage through one or two aquitards into a leaky aquifer, or vice versa. It is defined as

$$L = \sqrt{KHc} \quad (2.8)$$

Large values of L originate from a high transmissivity of the aquifer and/or a high hydraulic resistance of the aquitard. In both cases the influence of leakage will be small and the area over which leakage takes place is large. The leakage factor is expressed in metres.

### 3 Performing an aquifer test

#### 3.1 General

An aquifer test is performed to ascertain one or more of the hydraulic properties of an aquifer. The principle of a single-well or aquifer test is that a well is pumped and the effect of this pumping on the aquifer's hydraulic head is measured in the well itself, and/or in a number of nearby piezometers or observation wells. The change in water level induced by the pumping is known as the drawdown. In the literature, aquifer tests based on the analysis of drawdowns during pumping, are commonly referred to as 'pumping tests'.

The aquifer properties can also be found from a recovery test. In such a test, a well that has been discharging for some time is shut down, and thereafter

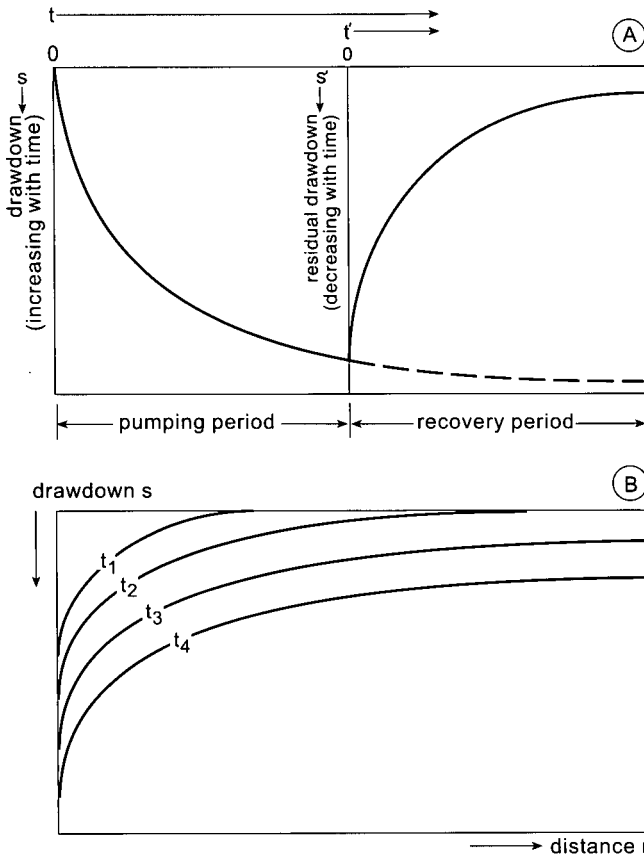


Figure 3.1 A: Time-drawdown relationship during a pumping test, followed by a recovery test  
B: Distance-drawdown relationships for increasing pumping times

the recovery of the aquifer's hydraulic head is measured in the well and/or in nearby piezometers. Figure 3.1.A gives an example of the time-drawdown relationship for the pumped well or a piezometer during a pumping test followed by a recovery test. Analyses based on time-drawdown and time-recovery relationships can be applied both to single-well test and aquifer test data.

With aquifer tests it is possible to perform the above-mentioned analyses for each piezometer separately and compare their results. In addition, use can also be made of the distance-drawdown relationship (see Figure 3.1.B). Analyses based on these relationships can only be applied to aquifer tests when drawdown data are available for two or more piezometers. Consequently, the results of aquifer tests will be more accurate than the results of single well tests. Moreover, they are representative of a larger volume of the aquifer.

How many piezometers should be employed depends not only on the amount of information desired and the required degree of accuracy, but also on the funds available for the test. It is always best to have several piezometers in various directions and at various distances from the pumped well. Although no fixed rule can be given, placing piezometers at distances of between 10 and 100 m from the well will usually give reliable data. For confined aquifers, these distances must be greater, say between 100 to 250 m or more, whereas for unconfined aquifers, the distances must be shorter, say between 10 to 30 m or less.

For information on the site selection, and the design and construction of the pumped well and the piezometers, see Boonstra (1999<sup>a</sup>), Driscoll (1986), Genetier (1984), Kruseman and de Ridder (1990), and the Groundwater Manual (1981).

## 3.2 Measurements

Ideally, an aquifer test should be performed under the natural conditions of a stable water table. This is not always possible, however. Water tables rise and fall in response to natural recharge and discharge of the groundwater reservoir (precipitation and evaporation), manmade recharge and discharge of the groundwater reservoir (irrigation losses and pumping from wells), changes in barometric pressure, and, in coastal aquifers, in response to tidal movements. Such short-term variations in the water table have an effect on the drawdown and recovery of the water table during testing. Hence, for some days prior to the actual test, the water levels in the well and the piezometers should be measured, say twice a day. For each observation point, a curve of time versus water level (a hydrograph) should be drawn. The trend and rate of water-level changes can be read from these curves. At the end of the test, i.e. after complete recovery, water-level readings should be continued at the obser-



Table 3.1 Recommended observation times to obtain an equidistant plotting position on a logarithmic time scale (10 observations per log cycle)

Time (sec)	Time (min)	Time (min)	Time (min)
60	10	100	1000
80	13	130	1300
100	16	160	1600
120	20	200	2000
150	25	250	2500
180	32	320	3200
240	40	400	4000
300	50	500	5000
380	65	650	6500
480	80	800	8000

vation points for one or two days. These data should be used to complete the hydrographs; the rate of water-level change during the test can then be determined and used to correct the drawdowns observed during the test itself (trend correction). For more information on this topic, see Kruseman and de Ridder (1990).

The water level must be measured many times during the course of a test. Because water levels fall rapidly during the first hour or two of the test, readings should initially be taken at short intervals, and these intervals should be gradually increased as pumping continues. Since the time is plotted on a logarithmic scale in the analysis procedures, it is recommended to have the same number of readings in each log cycle of time. Table 3.1 shows an example of the sequence of times for taking water-level measurements, based on ten readings in each log cycle and resulting in approximately equidistant plotting positions. For observation wells far from the well and for those in aquitards above or below the aquifer, the intervals in the first minutes of the pumping test can be disregarded.

After the pump has been shut down, the water levels in the well and the piezometers will start to rise. In the first hour they will rise rapidly, but as time goes on the rate of rise decreases. These rises can be measured in what is called a recovery test. If the discharge of the well was not constant throughout the pumping test, recovery-test data are more reliable than the drawdown data collected during pumping. Recovery-test data can thus be used as a check on the calculations that are based on the drawdown data. The time schedule for recovery measurements is the same as that for the drawdown measurements during the pumping period.

Water-level measurements can be taken in various ways, e.g. using the wetted-tape method, a mechanical sounder, an electric water-level indicator, a floating-level indicator or recorder, a pressure gauge, or a pressure logger. For detailed information on these devices, see Kruseman and de Ridder (1990) and Driscoll (1986). Water levels can be measured fairly accurately manually,

but then the instant of each reading should be recorded with a chronometer. Experience has shown that it is possible to measure the depth to water within two millimetres' accuracy. For piezometers close to the well, the wetted-tape method and the mechanical sounder cannot be used; the former because of the rapid water-level changes and the latter because of the noise of the pump. Although the pressure-gauge method is less accurate than the other methods (within 6 cm), it is the most practical method for measuring water levels in a pumped well. It should not be used for measuring water levels in observation wells.

Among the arrangements to be made for a pumping test is the control of the discharge rate. To avoid complicated calculations later, the discharge rate should preferably be kept constant throughout the test, by manipulating a valve in the discharge pipe. This gives more accurate control than changing the speed of the pump. During pumping tests, the discharge rate should be measured at least once every hour, and adjustments should be made to keep it constant. The discharge rate can be measured with various devices, such as a commercial water meter, a flume, a container, a weir, an orifice bucket, or with the jet-stream method. For detailed information on these devices, again see Kruseman and de Ridder (1990) and Bos (1989). The water delivered by the well should be prevented from returning to the aquifer. This can be done by conveying the water through a pipeline over a convenient distance, at least 300 m, depending on the location of the piezometers, and then discharging it into a canal or natural channel. The water should preferably be discharged away from the line of piezometers. The pumped water can also be conveyed through a shallow ditch, but to prevent leakage the ditch bottom should be sealed with clay or plastic sheeting.

### 3.3 Duration of a pumping test

It is difficult to say how long a pumping test should last, because the duration of pumping depends on the type of aquifer and the degree of accuracy desired in establishing its properties. It is inadvisable to economise on the pumping period, because the costs of running the pump for a few extra hours are low compared with the total costs of the test. Moreover, better and more reliable data are obtained if pumping continues until the cone of depression has stabilised and does not seem to be expanding further as pumping continues. At the beginning of the test, the cone develops quickly because the pumped water is initially derived from the aquifer storage immediately around the well. But, as pumping continues, the cone expands and deepens more slowly because, with each additional metre of horizontal expansion, a larger volume of stored water becomes available. This may often lead inexperienced observers to conclude that the cone has stabilised (i.e. that steady state has been reached). Inaccurate measurements of the drawdowns in the piezometers - drawdowns

that become smaller and smaller as pumping continues - can also lead to this wrong conclusion. In reality, the depression cone will continue to expand until the recharge of the aquifer, if any, equals the discharge.

The unsteady-state flow, also known as non-equilibrium flow, is time-dependent, i.e. the water level changes over time. During a pumping test, the unsteady-state flow condition occurs from the moment pumping starts until the steady state is reached. Theoretically, an infinite, horizontal, completely confined aquifer of constant thickness pumped at a constant rate, will always be in unsteady state, as such an aquifer is not recharged by an outside source.

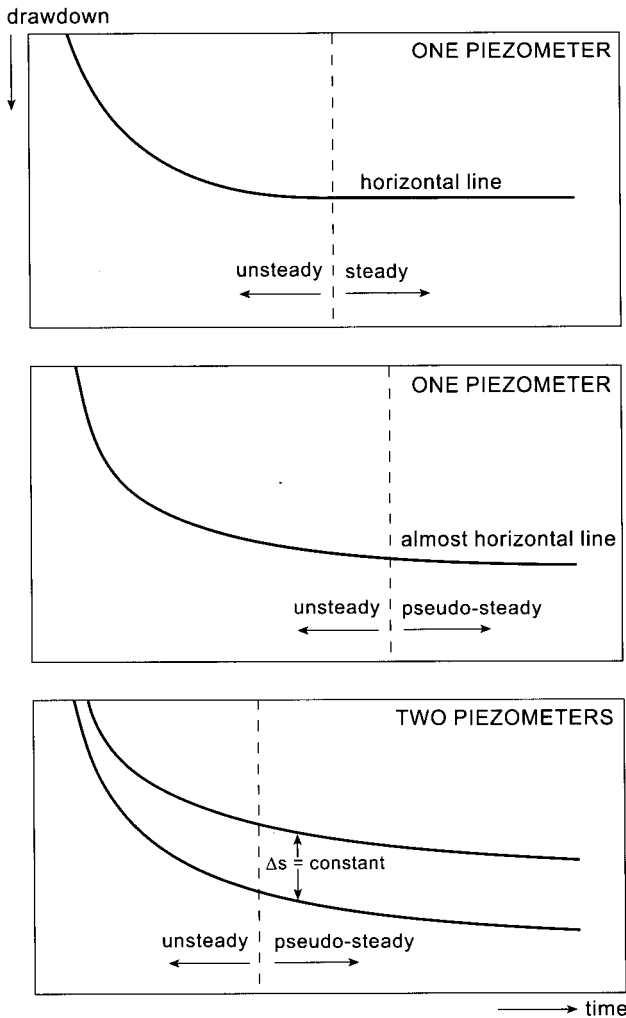


Figure 3.2 Time-drawdown plots showing the changes in drawdown during a pumping test and their interpretations

In practice, well flow is considered to be in unsteady state as long as the changes of the water level in the piezometers are measurable, or as long as the hydraulic gradient changes in a measurable way.

The steady-state flow, also known as equilibrium flow, is independent of time, i.e. the water level does not change over time. It occurs, for instance, when there is equilibrium between the discharge of a pumped well and the recharge of the pumped aquifer by an outside source. Such outside sources may be recharge from surface water of nearby rivers, canals, or lakes, or recharge from the groundwater of an unconfined aquifer with constant water table overlying an aquitard that in turn overlies a pumped leaky aquifer. Because real steady-state conditions seldom occur, in practice it is assumed that a steady-state condition is reached when the changes of the water level are negligibly small, or when the hydraulic gradient has become constant.

To establish whether unsteady or steady-state conditions prevail, the changes in head during the pumping test should be plotted. Figure 3.2 shows the different plots and their interpretations. In some wells, a steady state occurs a few hours after pumping starts; in others, it does not occur until after a few days or weeks. Kruseman and de Ridder (1990) suggest that under average conditions, steady-state flow is generally reached in leaky aquifers after 15 to 20 hours of pumping, and in a confined aquifer, after 24 hours. In an unconfined aquifer, the cone of depression expands more slowly, so a longer period of pumping is required: say, three days.

Preliminary plotting of drawdown data during the test will often show what is happening and may indicate whether or not the test should be continued. After some hours of pumping, sufficient time will become available in the field to draw the time-drawdown curves of each observation point. These graphs will be helpful in checking whether the test is running well and in deciding on the time that the pump can be shut down because steady or pseudo-steady state flow has been reached.

### 3.4 Reporting and filing the data

When the evaluation of the test data has been completed, a report should be written about the results. It is beyond the scope of this manual to specify the report's contents, but it should at least include the following items:

- a map, showing the location of the test site, the well and the piezometers;
- a lithological cross-section of the test site, based on the data obtained from the boreholes, and showing the depth of the well screen and the number, depth, and distances of the piezometers;
- tables of the field measurements made of the well discharge and the water levels in the well and the piezometers;
- hydrographs, illustrating the corrections applied to the observed data, if applicable;

- time-drawdown curves and distance-drawdown curves;
- the considerations that led to the selection of the analysis method used for the analysis;
- the calculations in an abbreviated form, including the values obtained for the aquifer properties and a discussion of their accuracy;
- recommendations for further investigations, if applicable;
- a summary of the main results.

A copy of the report should be kept on file for further reference and later studies. Samples of the different layers penetrated by the borings should be stored too, because they may be needed for other studies in a later phase of investigations. The basic field measurements of the test should be put on file as well. The conclusions drawn from the test may become obsolete in the light of new insights, but the hard facts carefully collected in the field remain facts and can always be re-evaluated.



## 4 Theory of aquifer test analysis

In this chapter, methods for evaluating aquifer test and single-well tests conducted in confined, leaky, and unconfined aquifers are presented. These methods have been incorporated in the SATEM 2002 software package.

The well-flow equations underlying the analysis methods were developed under the following common assumptions and conditions:

- The aquifer has a seemingly infinite areal extent;
- The aquifer is homogeneous, isotropic, and of uniform thickness over the area influenced by the test;
- Prior to pumping, the water table and/or the piezometric level is horizontal (or nearly so) over the area that will be influenced by the test;
- The aquifer is pumped at a constant-discharge rate;
- The water removed from storage is discharged instantaneously with decline of head.

Any additional assumptions and conditions are mentioned in the discussion of the individual methods. An analysis procedure is presented with each method, so that the method can be applied manually to verify the results from SATEM 2002.

### 4.1 Confined aquifers

Theis (1935) was the first to develop an equation for unsteady-state flow which introduced the time factor and the storativity. He noted that when a fully-penetrating well pumps an extensive confined aquifer at a constant rate, the influence of the discharge extends outward with time. The rate of decline of head, multiplied by the storativity and summed over the area of influence, equals the discharge.

The Theis equation, which was derived from the analogy between the flow of groundwater and the conduction of heat, is written as

$$s(r,t) = \frac{Q}{4\pi KH} \int_u^{\infty} \frac{e^{-y}}{y} dy = \frac{Q}{4\pi KH} W(u) \quad (4.1)$$

with

$$u = \frac{r^2 S}{4KHt} \quad (4.2)$$

where  $s(r,t)$  is the drawdown measured in a piezometer (m);  $r$  is the distance of the piezometer from the pumped well (m);  $t$  is the time since pumping started (d);  $Q$  is the constant well discharge ( $m^3/d$ );  $KH$  is the transmissivity

of the aquifer ( $m^2/d$ );  $W(u)$  is the Theis well function (-); and  $S$  is the storativity of the aquifer (-).

#### 4.1.1 Theis-Jacob's method

In Figure 4.1, the Theis well function  $W(u)$  is plotted against  $1/u$  on semi-log paper. This figure shows that, for large values of  $1/u$ , the Theis well function exhibits a straight-line segment. The Theis-Jacob method is based on this phenomenon. Cooper and Jacob (1946) showed that for the straight-line segment, Equation 4.1 can be approximated by

$$s(r,t) = \frac{2.3Q}{4\pi KH} \log \frac{2.25 KHt}{r^2 S} \quad (4.3)$$

with an error smaller than	1%	2%	5%	10%
for $1/u$ larger than	30	20	10	7

In most handbooks on this subject, the condition to use Equation 4.3 is taken as  $u < 0.01$ , i.e.  $1/u > 100$ . Our experience is that this condition can often be relaxed to  $1/u > 10$ ; the latter has been adopted in SATEM 2002.

The properties of a confined aquifer can be found by developing the time-drawdown relationship based on Equation 4.3. If the pumping time is sufficiently long, a plot of the drawdown  $s(r,t)$  observed in a particular piezometer at a distance  $r$  from the pumped well versus the logarithm of time  $t$ , will appear as a straight line. If the slope of the straight-line segment is expressed as the drawdown difference ( $\Delta s = s(r,t_2) - s(r,t_1)$ ) per log cycle of time ( $\log t_2 -$

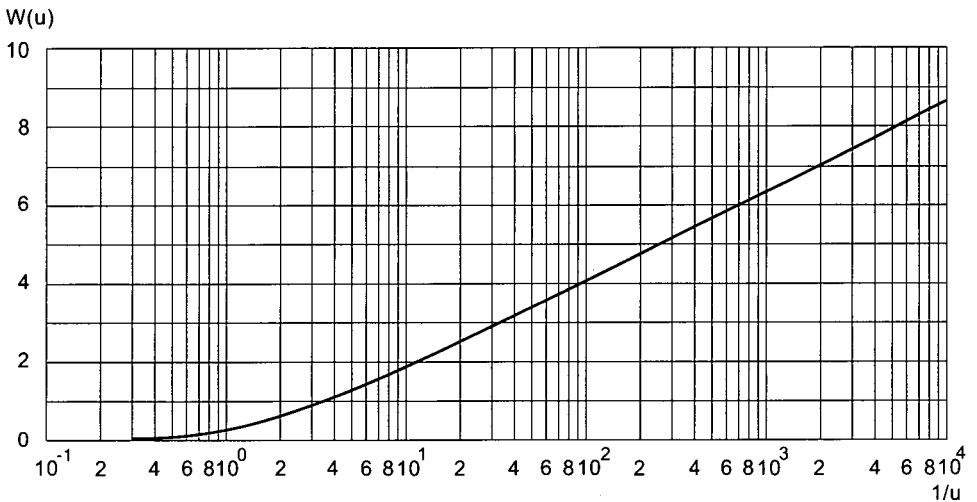


Figure 4.1 Theis well function  $W(u)$  plotted against  $1/u$  for fully penetrating wells in confined aquifers



$\log t_1 = 1$ ), rearranging Equation 4.3 gives

$$KH = \frac{2.3Q}{4\pi\Delta S} \quad (4.4)$$

If this line is extended until it intercepts the time-axis where  $s(r,t) = 0$ , the interception point has the co-ordinates  $s(r,t) = 0$  and  $t = t_0$ . Substituting these values into Equation 4.3, after rearrangement, gives

$$S = \frac{2.25KHt_0}{r^2} \quad (4.5)$$

The Theis-Jacob method is based on the assumptions listed at the beginning of this chapter and on the following conditions:

- The pumped well penetrates the entire thickness of the aquifer and thus receives water by horizontal flow;
- The pumping time is sufficiently long that a straight-line segment can be distinguished from a time-drawdown plot on semi-log paper.

*Procedure*

- For one of the piezometers, plot the drawdown values  $s(r,t)$  against the corresponding time  $t$ , on semi-log paper (with  $t$  on the logarithmic scale);
- Select a time range where the plots exhibit a straight line and draw a best fitting straight line through these plotted points;

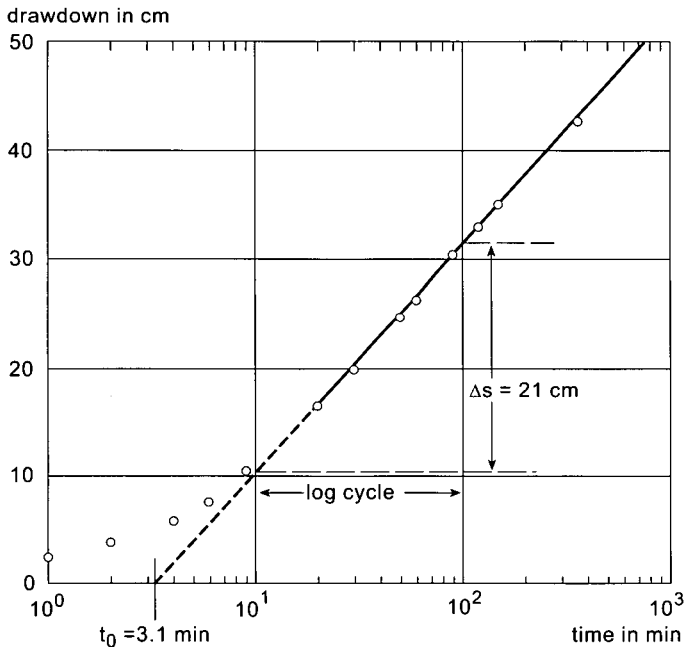


Figure 4.2 Time-drawdown data analysed with the Theis-Jacob method

- Determine the slope of the straight line, i.e. the drawdown difference  $\Delta s$  per log cycle of time;
- Substitute the values of  $Q$  and  $\Delta s$  into Equation 4.4 and solve for  $KH$ ;
- Extend the straight line until it intercepts the time axis where  $s(r,t) = 0$ , and read the value of  $t_0$ ;
- Substitute the values of  $KH$ ,  $t_0$ , and  $r$  into Equation 4.5 and solve for  $S$ ;
- Substitute the values of  $KH$ ,  $S$ , and  $r$  into Equation 4.2 together with  $1/u = 10$  and solve for  $t$ . This  $t$  value should be lower than the time range for which the straight-line segment was selected;
- If drawdown values are available for more than one piezometer, apply the above procedure to the other piezometers too. The resulting values for  $KH$  and  $S$  should agree closely.

This procedure is illustrated graphically in Figure 4.2.

#### 4.1.2 Thiem-Jacob's method

When a confined aquifer is pumped, the cone of depression will continue to deepen and expand, because theoretically these aquifers are not recharged by an outside source. Even at long pumping times, the water levels in the piezometers will never stabilise to a real steady state, therefore instead of steady state, the concept of pseudo-steady state is used for these types of aquifer. An aquifer is said to be in pseudo-steady state when the hydraulic gradient has become constant, i.e. when the time-drawdown curves of different piezometers are parallel (see Figure 4.3). This phenomenon occurs when the cone of depression finally deepens uniformly over the area influenced by the pumping.

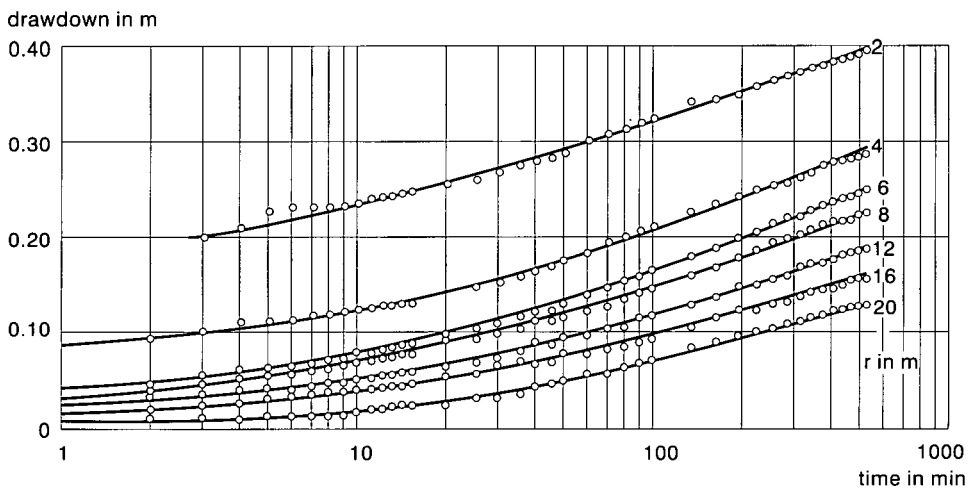


Figure 4.3 Time-drawdown curves of seven piezometers showing field data for an aquifer test in an unconfined aquifer

Using two or more piezometers, Thiem (1906) developed an equation for this situation, the Thiem-Dupuit equation, which can be written as

$$s(r_1, t)_m - s(r_2, t)_m = \frac{2.3Q}{2\pi KH} \log \frac{r_2}{r_1} \quad (4.6)$$

where  $s(r_1, t)_m$  and  $s(r_2, t)_m$  are the pseudo-steady state drawdowns of two piezometers. Equation 4.6 can also be derived by applying Equation 4.3 to two piezometers at distances  $r_1$  and  $r_2$  at large times and totalling the results.

The properties of a confined aquifer can be found by developing the distance-drawdown relationship based on Equation 4.6. That equation shows that the corresponding distance-drawdown plot will yield a straight line. If the slope of this straight line is expressed as the drawdown difference ( $\Delta s_m = s(r_1, t)_m - s(r_2, t)_m$ ) per log cycle of distance ( $\log r_2 - \log r_1 = 1$ ), rearranging Equation 4.6 gives

$$KH = \frac{2.3Q}{2\pi \Delta s_m} \quad (4.7)$$

Because in confined aquifers the cone of depression will continue to deepen and expand during the pseudo-steady state, the aquifer's storativity can also be estimated from the distance-drawdown plot. If the straight line is extended until it intercepts the distance-axis where  $s(r, t)_m = 0$ , the interception point has the co-ordinates  $s(r, t)_m = 0$  and  $r = r_0$ . Substituting these values into Equation 4.3, after rearrangement, gives

$$S = \frac{2.25KHt}{r_0^2} \quad (4.8)$$

The Thiem-Jacob method is based on the assumptions listed at the beginning of this chapter and on the following conditions:

- the pumped well penetrates the entire thickness of the aquifer and thus receives water by horizontal flow;
- the pumping time is sufficiently long for the flow system to have achieved a pseudo-steady state.

#### *Procedure*

- Plot the pseudo-steady-state drawdown value  $s(r, t)_m$  of each piezometer for a particular time against the distance  $r$  between the well and the piezometer, on semi-log paper (with  $r$  on logarithmic scale);
- Select a distance range where the plots exhibit a straight line and draw a best fitting straight line through these plotted points;
- Determine the slope of the straight line, i.e. the drawdown difference  $\Delta s_m$  per log cycle of distance;
- Substitute the values of  $Q$  and  $\Delta s_m$  into Equation 4.7 and solve for  $KH$ ;
- Extend the straight line until it intercepts the distance axis where  $s(r, t)_m = 0$ , and read the value of  $r_0$ ;

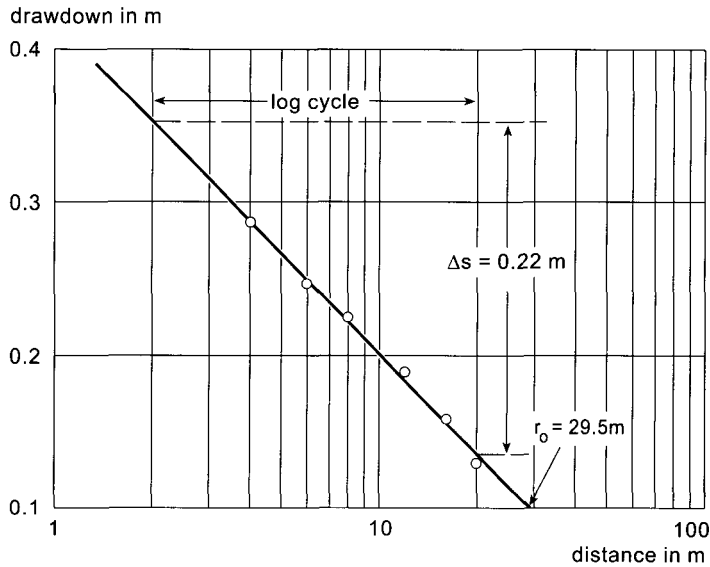


Figure 4.4 Distance-drawdown data analysed with the Thiem-Jacob method

- Substitute the values of  $KH$ ,  $r_o$ , and  $t$  into Equation 4.8 and solve for  $S$ ;
- Substitute the values of  $KH$ ,  $S$ , and  $t$  into Equation 4.2 together with  $1/u = 10$  and solve for  $r$ . This  $r$  value should be greater than the distance range for which the straight-line segment was selected;
- Repeat the above procedure for several large values of  $t$ . The resulting values for  $KH$  and  $S$  should agree closely.

This procedure is illustrated graphically in Figure 4.4.

## 4.2 Leaky aquifers

When a leaky aquifer is pumped (Figure 4.5), the piezometric level of the aquifer in the well is lowered. This lowering spreads radially outward as pumping continues, creating a difference in hydraulic head between the aquifer and the aquitard. Consequently, the groundwater in the aquitard will start moving vertically downward to join the water in the aquifer. The aquifer is thus partially recharged by downward percolation from the aquitard. As pumping continues, the percentage of the total discharge derived from this percolation increases. After a certain period of pumping, equilibrium will be established between the discharge rate of the pump and the recharge rate by vertical flow through the aquitard. This steady state will be maintained as long as the water table in the aquitard is kept constant.

According to Hantush and Jacob (1955), the drawdown due to pumping a

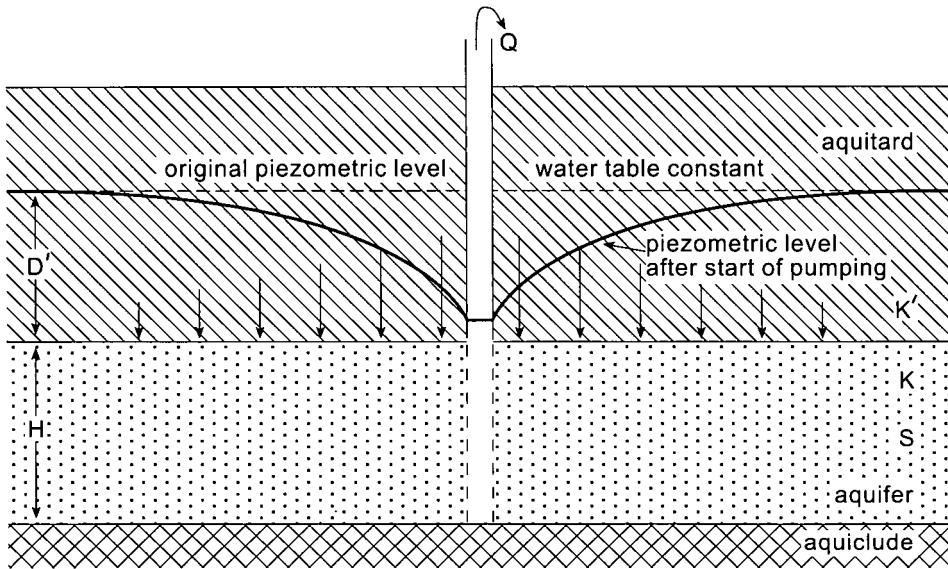


Figure 4.5 Schematic cross-section of a pumped leaky aquifer

leaky aquifer can be described by the following equation

$$s(r,t) = \frac{Q}{4\pi KH} \int_u^{\infty} \frac{1}{y} \exp\left(-y - \frac{r^2}{4L^2y}\right) dy = \frac{Q}{4\pi KH} W(u,r/L) \quad (4.9)$$

where  $W(u,r/L)$  is the Hantush well function (-),  $L (= \sqrt{KHc})$  is the leakage factor (m),  $c (= D'/K')$  is the hydraulic resistance of the aquitard (d),  $D'$  is the saturated thickness of the aquitard (m),  $K'$  is the vertical hydraulic conductivity of the aquitard (m/d); and the other symbols as defined earlier.

#### 4.2.1 Hantush's inflection-point method

Equation 4.9 has the same form as the Theis equation (Equation 4.1), but there are now two parameters in the integral:  $u$  and  $r/L$ . When the exponential term  $r^2/(4L^2y)$  approaches zero, Equation 4.9 approaches the Theis equation for large values of  $L$ . In Figure 4.6, the Hantush well function  $W(u,r/L)$  has been plotted versus  $1/u$  on semi-log paper for an arbitrary value of  $r/L$ . This figure shows that the Hantush well function exhibits an S-shaped curve and, for large values of  $1/u$ , a horizontal straight-line segment indicating steady-state flow. The Hantush inflection-point method was based on these phenomena. Hantush (1956) showed that for the inflection point ( $s_p, t_p$ ) the following relationships hold

a) The drawdown value  $s_p$  is given by

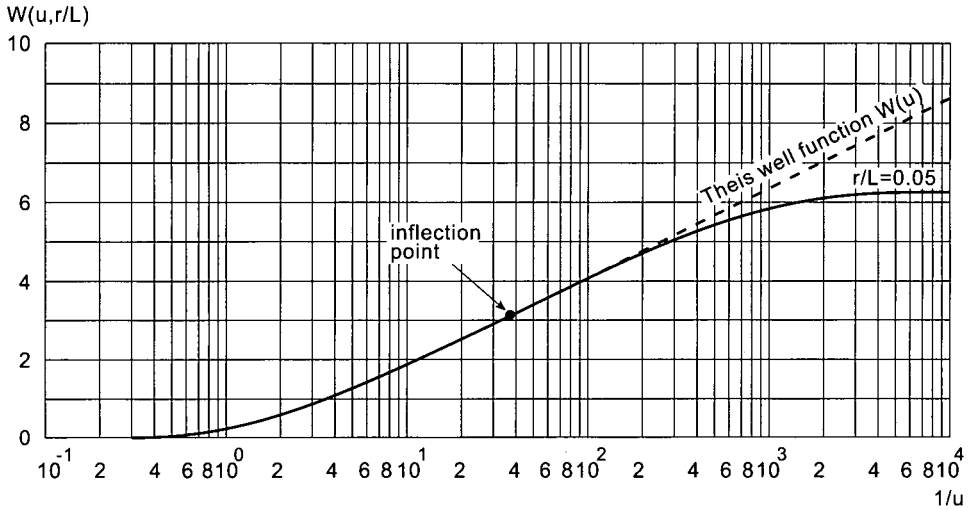


Figure 4.6 Hantush well function  $W(u, r/L)$  versus  $1/u$  for fully penetrating wells in leaky aquifers

$$s_p = 0.5 s_m \quad (4.10)$$

b) The  $u_p$  value is given by

$$u_p = \frac{r^2 S}{4KHt_p} = \frac{r}{2L} \quad (4.11)$$

c) The slope of the curve at the inflection point  $\Delta s_p$  per log cycle of time is given by

$$\Delta s_p = \frac{2.3Q}{4\pi KH} e^{-r/L} \quad (4.12)$$

d) At the inflection point, the relation between the drawdown and the slope of the curve is given by

$$2.3 \frac{s_p}{\Delta s_p} = e^{r/L} K_0(r/L) \quad (4.13)$$

where  $K_0(r/L)$  is the modified Bessel function of the second kind and of zero order (Hankel function). The Hantush inflection-point method is based on the assumptions listed at the beginning of this chapter and on the following conditions:

- The pumped well penetrates the entire thickness of the aquifer and thus receives water by horizontal flow;
- The phreatic level in the overlying aquitard remains constant, so leakage

through the aquitard takes place in proportion to the drawdown of the piezometric level;

- The pumping time is sufficiently long that the steady-state drawdown can be estimated from extrapolation of a time-drawdown curve on semi-log paper.

*Procedure*

- For one of the piezometers, plot the drawdown values  $s$  against the corresponding time  $t$ , on semi-log paper (with  $t$  on logarithmic scale);
- Draw the best fitting curve through the plotted points;
- From this plot determine the value of the steady-state drawdown  $s_m$ ;
- Substitute the value of  $s_m$  into Equation 4.10 and solve for  $s_p$ . The value of  $s_p$  on the curve locates the inflection point  $p$ ;
- Read the value of  $t_p$  at the inflection point from the time-axis;
- Determine the slope  $\Delta s_p$  of the curve at the inflection point. This can be closely approximated by reading the drawdown difference per log cycle of time over the straight portion of the curve on which the inflection point lies, or over the tangent to the curve at the inflection point;
- Substitute the values of  $s_p$  and  $\Delta s_p$  into Equation 4.13 and find  $r/L$  by interpolation from the table of the function  $e^{r/L} K_0(r/L)$  in Appendix A;
- Calculate  $L$  from this  $r/L$  value and the  $r$  value of the well;
- Substitute  $Q$ ,  $\Delta s_p$ , and  $r/L$  into Equation 4.12 and solve for  $KH$ ;
- Substitute  $r$ ,  $KH$ ,  $t_p$  and  $L$  into Equation 4.11 and solve for  $S$ ;
- Calculate  $c$  from the relation  $c = L^2/KH$ ;
- If drawdown values are available for more than one piezometer, apply the

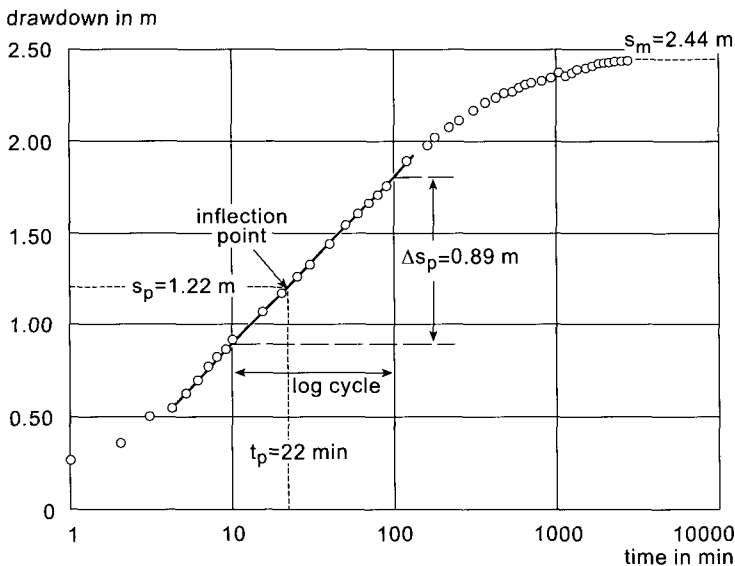


Figure 4.7 Time-drawdown data analysed with the Hantush inflection-point method

above procedure to the other piezometers too. The resulting values for KH, S, and c should agree closely.

This procedure is illustrated graphically in Figure 4.7.

#### 4.2.2 Hantush-Jacob's method

For the steady-state drawdown in a leaky aquifer, De Glee (1930, 1951) derived the following equation

$$s_m(r) = \frac{Q}{2\pi KH} K_0\left(\frac{r}{L}\right) \quad (4.14)$$

where  $s_m(r)$  is the steady-state, stabilised drawdown (m). Hantush (1956, 1964) noted that if  $L > 3H$ , Equation 4.14 can be approximated by

$$s_m(r) = \frac{2.3Q}{2\pi KH} \log \frac{1.12 L}{r} \quad (4.15)$$

with an error smaller than	1%	2%	5%	10%
for $r/L$ smaller than	0.16	0.22	0.33	0.45

In most handbooks on this subject, the condition to use Equation 4.15 is taken as  $r/L < 0.05$ . Our experience is that this condition can often be relaxed to  $r/L < 0.20$ ; the latter has been adopted in SATEM 2002.

It is important to note that the flow in a pumped leaky aquifer consists of a vertical component in the overlying aquitard and a horizontal component in the aquifer. In reality, the flow lines in the aquifer are not horizontal but curved, i.e. there are both vertical and horizontal flow components in the aquifer. The above equations can therefore only be used when the vertical-flow component in the aquifer is so small compared to the horizontal-flow component that it can be neglected. In practice, this condition is fulfilled if  $L > 3H$ .

The properties of a leaky aquifer can be found by developing the distance-drawdown relationship based on Equation 4.15. This equation shows that the corresponding distance-drawdown plot will yield a straight line. If the slope of this straight line is expressed as the drawdown difference ( $\Delta s_m = s_m(r_1) - s_m(r_2)$ ) per log cycle of distance ( $\log r_2 - \log r_1 = 1$ ), re-arranging Equation 4.15 gives

$$KH = \frac{2.3Q}{2\pi\Delta s_m} \quad (4.16)$$

If the straight line is extended until it intercepts the distance-axis where  $s_m(r) = 0$ , the interception point has the co-ordinates  $s_m(r) = 0$  and  $r = r_0$ .

Substituting these values into Equation 4.15 gives



$$\log \frac{1.12 L}{r_0} = 0 \text{ or } \frac{1.12 L}{r_0} = 1 \text{ or } L = \frac{r_0}{1.12} \quad (4.17)$$

The Hantush-Jacob method is based on the assumptions listed in the beginning of this chapter and on the following conditions:

- The pumped well penetrates the entire thickness of the aquifer and thus receives water by horizontal flow;
- The phreatic level remains constant so that leakage through the overlying aquitard takes place in proportion to the drawdown of the piezometric level;
- The pumping time is sufficiently long for the flow system to have achieved steady state.

*Procedure*

- Plot the steady-state drawdown values  $s_m(r)$  of each piezometer against the corresponding distance  $r$  on semi-log paper (with  $r$  on the logarithmic scale);
- Draw the best fitting straight line through the plotted points;
- Determine the slope of the straight line, i.e. the drawdown difference  $\Delta s_m$  per log cycle of distance;
- Substitute the values of  $Q$  and  $\Delta s_m$  into Equation 4.16 and solve for  $KH$ ;
- Extend the straight line until it intercepts the distance axis where  $s_m(r) = 0$ , and read the value of  $r_0$ ;
- Substitute this value into Equation 4.17 and solve for  $L$ ;
- Calculate  $c$  from the relationship  $c = L^2 / KH$ .

This procedure is illustrated graphically in Figure 4.8.

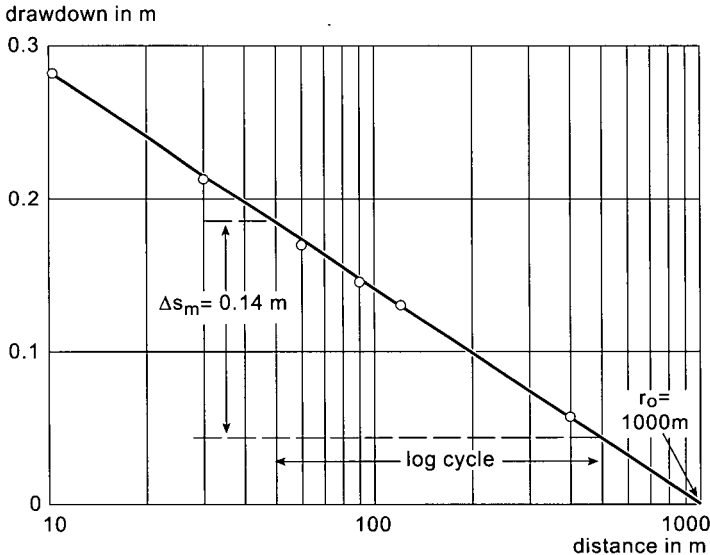


Figure 4.8 Distance-drawdown data analysed with the Hantush-Jacob method

### 4.3 Unconfined aquifers

Figure 4.9 shows a pumped unconfined aquifer underlain by an aquiclude. When unconfined and confined aquifers are pumped, the following basic differences emerge:

1. Pumping partly dewateres an unconfined aquifer, which decreases the thickness of the saturated part of the aquifer; when a confined aquifer is pumped the thickness remains constant.
2. The water produced by a well in an unconfined aquifer comes from the physical dewatering of the aquifer, whereas in a confined aquifer it comes from the expansion of the water in the aquifer in response to reduced water pressure, and from the compaction of the aquifer due to increased effective stresses.
3. The flow towards a well in an unconfined aquifer has clear vertical components near the pumped well, but there are no such vertical flow components in a confined aquifer, provided that the well is fully penetrating.

In an unconfined aquifer, the water levels in piezometers near the well often tend to decline at a slower rate than described by the Theis equation. Time-drawdown curves on semi-log paper therefore usually show a typical S shape: a relatively steep early-time segment, a flat intermediate segment, and a relatively steep segment again at later times, as depicted in Figure 4.10. Nowadays, the widely used explanation of this S-shaped time-drawdown curve is based on the concept of delayed yield. It is caused by a time lag between the early elastic response of the aquifer and the subsequent downward movement of the water table due to gravity drainage.

During the early stage of an aquifer test - which may last for only a few

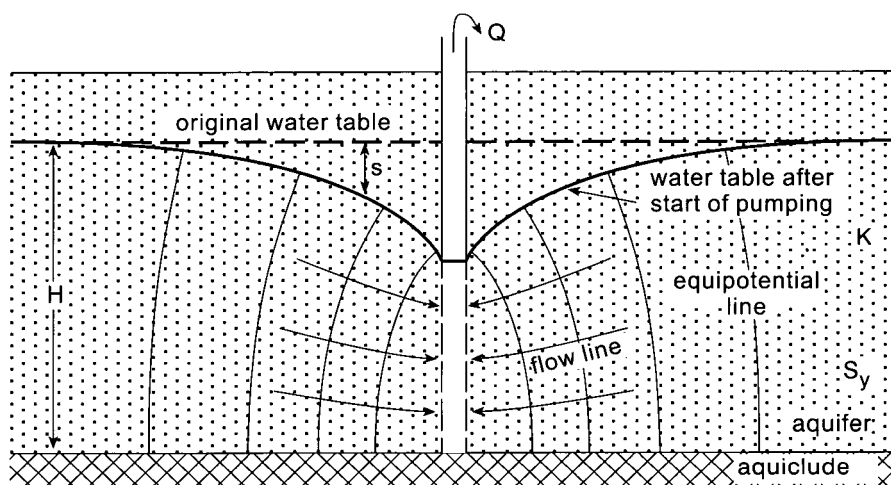


Figure 4.9 Schematic cross-section of a pumped unconfined aquifer

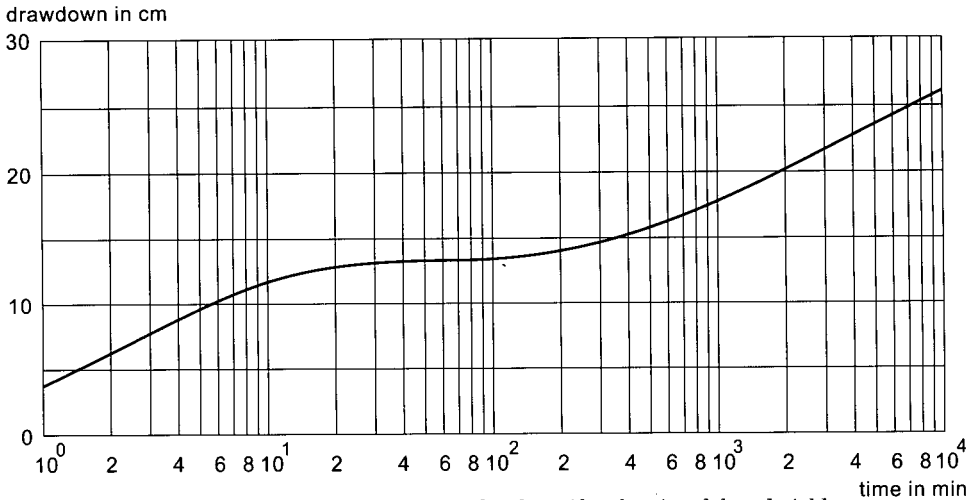


Figure 4.10 Time-drawdown plot in an unconfined aquifer showing delayed yield

minutes - the discharge of the pumped well is derived uniquely from the elastic storage within the aquifer. Hence the reaction of the unconfined aquifer immediately after the start of pumping is similar to the reaction of a confined aquifer as described by the Theis flow equation.

After the early stage, the water table starts to fall and the effect of the delayed yield becomes apparent. The influence of the delayed yield is comparable to that of leakage: the average drawdown slows down over time and no longer conforms to the Theis curve. The time-drawdown curve eventually approaches horizontality, though the time taken to achieve this varies from a few minutes to a few hours of pumping.

The late-time segment of the time-drawdown curve may start from several minutes to several days after the start of pumping. The declining water table can now keep pace with the increase in the average drawdown. The flow in the aquifer is essentially horizontal again and, as in the early pumping time, the time-drawdown curve approaches the Theis curve.

Jacob (1950) showed that if the drawdowns in an unconfined aquifer are small compared to the initial saturated thickness of the aquifer, the condition of horizontal flow towards the well is approximately satisfied, so that Equations 4.1 to 4.3 can also be applied to determine the aquifer properties. The only changes required are that the storativity  $S$  is replaced by the specific yield  $S_y$  of the unconfined aquifer, and that the transmissivity  $KH$  is defined as the transmissivity of the initial saturated thickness of the aquifer.

When the drawdowns in an unconfined aquifer are large compared with the aquifer's original saturated thickness, the observed drawdowns need to be corrected before this equation can be used. Jacob (1944) proposed the following correction

$$s_c(r,t) = s(r,t) - \frac{s^2(r,t)}{2H} \quad (4.18)$$

where  $s_c(r,t)$  is the corrected drawdown (m),  $s(r,t)$  is the observed drawdown (m), and  $H$  is the saturated aquifer thickness prior to pumping (m). This correction is only needed when the maximum drawdown at the end of the test is more than 5 per cent of the original saturated aquifer thickness.

The properties of an unconfined aquifer can be found by developing the time-drawdown relationship based on Equation 4.3. If the pumping time is sufficiently long, a plot of the drawdown  $s_c(r,t)$  observed in a particular piezometer at a distance  $r$  from the pumped well versus the logarithm of time  $t$ , will appear as a straight line as depicted in the right-hand side of Figure 4.10. Equations 4.4 and 4.5 can then be used to calculate the aquifer properties from this straight line.

In principle, the same procedure can be applied to the straight line as depicted in the left-hand side of Figure 4.10. Equations 4.4 and 4.5 can again be used to calculate the aquifer properties from that straight line, but the latter equation then yields an estimate of the elastic storativity within the aquifer instead of the aquifer's specific yield. Theoretically, both straight-line segments in Figure 4.10 should run parallel, i.e. both should yield the same value for the aquifer's transmissivity.

As with confined aquifers, in a pumped unconfined aquifer the cone of depression will continuously deepen and expand. For pseudo-steady-state conditions, Equation 4.6 can also be used to describe the drawdown behaviour in two piezometers in an unconfined aquifer, provided that the observed drawdowns are corrected according to Equation 4.18.

#### 4.4 Partially penetrating wells

When an aquifer is pumped by a partially penetrating well, the assumption that the well receives water exclusively from horizontal flow is no longer valid and therefore the previous equations cannot be used to describe the flow. Due to a contraction of flow lines, partial penetration causes the flow velocity in the immediate vicinity of the well to be faster than otherwise, leading to an extra loss of head. This effect is strongest at the well face, and decreases with increasing distance from the well. According to Hantush (1962) the drawdown due to pumping in a confined aquifer can be described by the following equation

$$s(r,t) = \frac{Q}{4\pi KH} [W(u) + f_s] \quad (4.19)$$

with

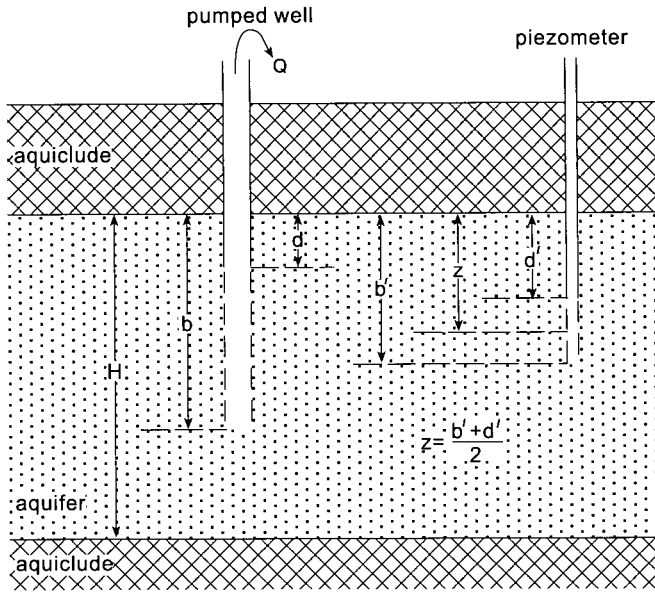


Figure 4.11 Schematic illustration of the parameters used for the analysis of partially penetrating wells

$$f_s = \frac{2H^2}{\pi^2(b-d)(b'-d')} \sum_{n=1}^{\infty} \left(\frac{1}{n^2}\right) W\left(u, \frac{n\pi r}{H}\right) \times \left[\sin\left(\frac{n\pi b}{H}\right) - \sin\left(\frac{n\pi d}{H}\right)\right] \left[\sin\left(\frac{n\pi b'}{H}\right) - \sin\left(\frac{n\pi d'}{H}\right)\right] \quad (4.20)$$

and

$$W\left(u, \frac{n\pi r}{H}\right) = \int_u^{\infty} \frac{1}{y} \exp\left(-y - \frac{n^2 \pi^2 r^2}{4H^2 y}\right) dy$$

where  $W(u, n\pi r/H)$  is the Hantush well function (-),  $b$  and  $b'$  are the penetration depths of the pumped well and the piezometer (m), and  $d$  and  $d'$  are the non-screened parts of the pumped well and the piezometer (m). The angles in Equation 4.20 are expressed in radians.

When the difference between  $b'$  and  $d'$  is small ( $b'-d' < 0.05 H$ ), Equation 4.20 can be replaced by

$$f_s = \frac{2H}{\pi^2(b-d)} \sum_{n=1}^{\infty} \left(\frac{1}{n}\right) W\left(u, \frac{n\pi r}{H}\right) \times \left[\sin\left(\frac{n\pi b}{H}\right) - \sin\left(\frac{n\pi d}{H}\right)\right] \left(\cos \frac{n\pi z}{H}\right) \quad (4.21)$$

where  $z = (b' + d')/2$  (m). Figure 4.11 illustrates some of the symbols used.

#### 4.4.1 Jacob-Hantush's method

In Figure 4.12 the expression  $W(u) + f_s$  has been plotted against  $1/u$  on semi-log paper. This figure shows that this expression exhibits a straight-line segment. It can be shown that this straight-line segment will develop under the following conditions

$$- 1/u > 10, \text{ i.e. } t > 2.5 r^2 S/KH \quad (4.22)$$

$$- f_s \text{ is constant, i.e. } t > H^2 S/2KH \quad (4.23)$$

If these conditions are fulfilled, Equations 4.20 and 4.21 reduce to

$$f_s = \frac{4H^2}{\pi^2(b-d)(b'-d')} \sum_{n=1}^{\infty} \left(\frac{1}{n^2}\right) K_0\left(u, \frac{n\pi r}{H}\right) \times \left[\sin\left(\frac{n\pi b}{H}\right) - \sin\left(\frac{n\pi d}{H}\right)\right] \left[\sin\left(\frac{n\pi b'}{H}\right) - \sin\left(\frac{n\pi d'}{H}\right)\right] \quad (4.24)$$

and

$$f_s = \frac{4H}{\pi(b-d)} \sum_{n=1}^{\infty} \left(\frac{1}{n}\right) K_0\left(\frac{n\pi r}{H}\right) \left[\sin\left(\frac{n\pi b}{H}\right) - \sin\left(\frac{n\pi d}{H}\right)\right] \left[\cos\left(\frac{n\pi z}{H}\right)\right] \quad (4.25)$$

In most handbooks on this subject, the condition to use Equations 4.24 and 4.25 is taken as  $u < 0.01$ , i.e.  $1/u > 100$ . Our experience is that this condition can often be relaxed to  $1/u > 10$ ; the latter has been adopted in SATEM 2002.

For a given set of parameters, Equations 4.24 and 4.25 yield constant

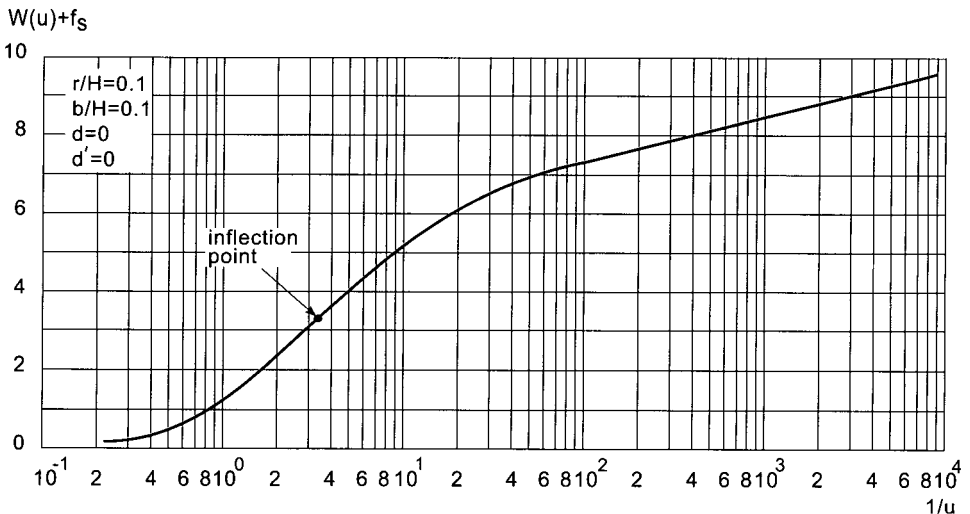


Figure 4.12 Hantush well function  $W(u) + f_s$  plotted against  $1/u$  for partially penetrating wells in confined aquifers

values. The Jacob-Hantush method was based on this phenomenon. Hantush (1962) showed that for the straight-line segment Equation 4.19 can be approximated by

$$s(r,t) = \frac{2.3Q}{4\pi KH} \log \frac{2.25 KHt}{r^2 S} e^{f_s} \quad (4.26)$$

The properties of a confined aquifer can be found by developing the time-drawdown relationship based on Equation 4.26. If the pumping time is sufficiently long, a plot of the drawdown  $s(r,t)$  observed in a particular piezometer at distance  $r$  from the pumped well versus the logarithm of time  $t$ , will appear as a straight line. If the slope of the straight-line segment is expressed as the drawdown difference ( $\Delta s = s(r,t_2) - s(r,t_1)$ ) per log cycle of time ( $\log t_2 - \log t_1 = 1$ ), rearranging Equation 4.26 gives

$$KH = \frac{2.3Q}{4\pi \Delta S} \quad (4.27)$$

If the straight line is extended until it intercepts the time-axis where  $s(r,t) = 0$ , the interception point has the co-ordinates  $s(r,t) = 0$  and  $t = t_0$ . Substituting these values into Equation 4.26 gives  $\log [2.25KHt_0 e^{f_s}/r^2 S] = 0$  or  $[2.25KHt_0 e^{f_s}/r^2 S] = 1$  or

$$S = \frac{2.25KHt_0}{r^2} e^{f_s} \quad (4.28)$$

The Jacob-Hantush method is based on the assumptions listed at the beginning of this chapter and on the following conditions:

- The pumped well partially penetrates the aquifer;
- The pumping time is long enough for a straight-line segment to be distinguished from a time-drawdown plot on semi-log paper.

#### *Procedure*

- For one of the observation wells or piezometers, plot the drawdown values  $s(r,t)$  against the corresponding time  $t$ , on semi-log paper (with  $t$  on the logarithmic scale);
- Select a time range where the plots exhibit a straight line and draw a best fitting straight line through these plotted points;
- Determine the slope of the straight line, i.e. the drawdown difference  $\Delta s$  per log cycle of time;
- Substitute the values of  $Q$  and  $\Delta s$  into Equation 4.27 and solve for  $KH$ ;
- Extend the straight line until it intercepts the time axis where  $s(r,t) = 0$ , and read the value of  $t_0$ ;
- Calculate  $f_s$  from Equation 4.24 or 4.25 as applicable; generally, a limited number of the series involved will be sufficient;
- Substitute the values of  $KH$ ,  $t_0$ ,  $f_s$ , and  $r$  into Equation 4.28 and solve for  $S$ ;
- Substitute the appropriate values into Equations 4.22 and 4.23 and solve

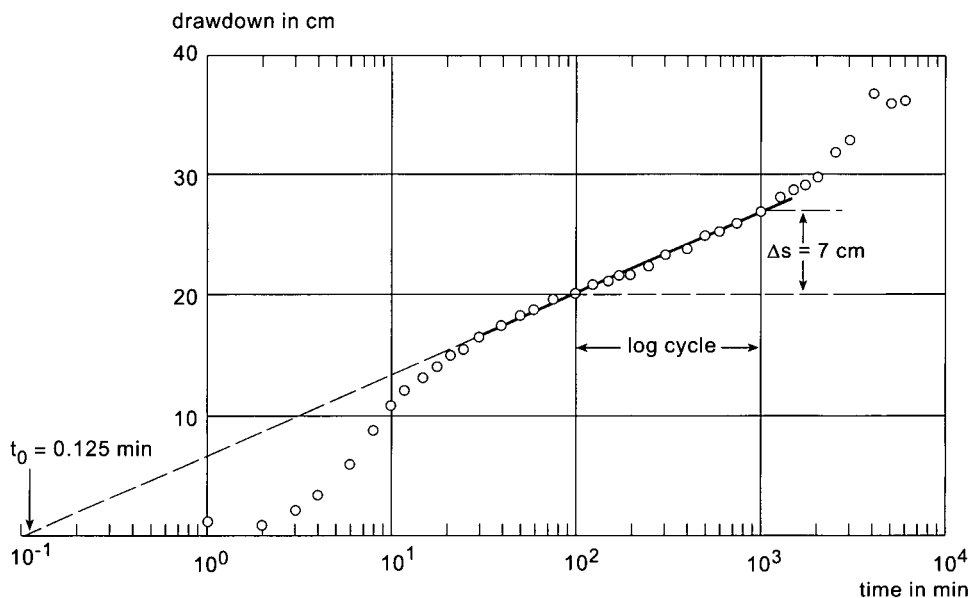


Figure 4.13 Time-drawdown data analysed with the Jacob-Hantush method

- for  $t$ . The largest  $t$  value should be smaller than the time range for which the straight-line segment was selected;
- If drawdown values are available for more than one observation well or piezometer, apply the above procedure to the other observation wells/piezometers also. The resulting values for  $KH$  and  $S$  should agree closely.

This procedure is illustrated graphically in Figure 4.13.

Equation 4.19 can also be applied to unconfined aquifers. It is then assumed that due to partial penetration the drawdowns will be small compared with the initial saturated thickness of the aquifer, i.e. no corrections using Equation 4.18 will be required. The only changes required are that the storativity  $S$  is replaced by the specific yield  $S_y$  of the unconfined aquifer, and that the transmissivity  $KH$  is defined as the transmissivity of the initial saturated thickness of the aquifer.

## 4.5 Recovery tests

After a well has been pumped for a certain period of time  $t_{\text{pump}}$  and is shut down, the water levels in the pumped well and in any piezometers present will stop falling and start to rise again to their original position (see Figure 4.14). This recovery of the water level can be measured as residual drawdown  $s'(r,t')$ , i.e. as the difference between the original water level prior to pumping and the



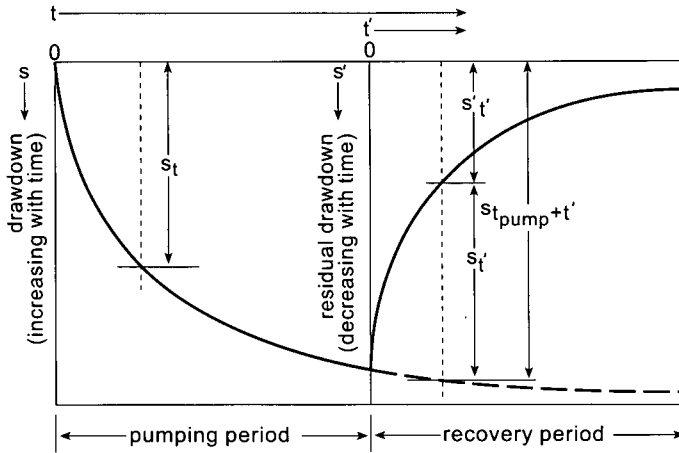


Figure 4.14 Time-drawdown behaviour during a pumping and recovery test

actual water level measured at a certain moment  $t'$  since pumping stopped.

This residual drawdown  $s'(r,t')$  is also equal to the difference between the drawdown caused by pumping the well with a discharge  $Q$  during the hypothetical time  $t_{\text{pump}} + t'$  and the recovery caused by injecting water at the same point at the same rate  $Q$  by a hypothetical injection well during time  $t'$

$$s'(r,t') = s(r,t_{\text{pump}}+t') - s(r,t') \quad (4.29)$$

Based on this principle, the recovery values  $s(r,t')$  can be calculated if the hypothetical drawdown values  $s(r,t_{\text{pump}}+t')$  can be estimated. This can be done if the drawdown data during pumping were analysed using one of the methods given in the previous sections. Theoretical values for  $s(r,t_{\text{pump}} + t')$  are calculated by back-substituting the obtained aquifer properties into the appropriate equations. Subtracting the observed residual-drawdown data  $s'(r,t')$  from these values yields the synthetic recovery values  $s(r,t')$ . An analysis based on the recovery data is identical to an analysis of drawdown data. So, any of the methods discussed in the previous sections can also be used to analyse the synthetic recovery data. This feature has been incorporated into SATEM 2002.

Instead of using synthetic recovery data, residual-drawdown data can be used directly in the analysis. The Theis recovery method is also based on the principle of Equation 4.29. Only the transmissivity value can be determined with this method.

#### 4.5.1 Theis's recovery method

According to Theis (1935) the residual drawdown  $s'(r,t')$  during the recovery period after a constant-rate pumping test is given by

$$s'(r,t') = \frac{Q}{4\pi KH} [W(u) - W(u')] \quad (4.30)$$

with

$$u = \frac{r^2 S}{4 KH t} \quad (4.31)$$

and

$$u' = \frac{r^2 S'}{4 KH t'} \quad (4.32)$$

where  $S'$  is the storativity during recovery (-);  $t = t_{\text{pump}} + t'$  is the time since pumping started (d); and  $t'$  is the time since pumping stopped (d).

In Figure 4.15 the expression  $W(u) - W(u')$  has been plotted against  $u'/u$  on semi-log paper. The figure shows that this expression exhibits a straight-line segment for small  $u'/u$  values. The Theis recovery method is based on this phenomenon. For the straight-line segment, Equation 4.30 can be approximated by

$$s'(r,t') = \frac{2.3Q}{4\pi KH} \log \frac{S't}{St'} \quad (4.33)$$

In most handbooks on this subject, the condition to use Equation 4.33 is taken as  $u' < 0.01$ . Our experience is that this condition can often be relaxed to  $u' < 0.1$ . The corresponding condition for the expression  $u'/u$  can then be refined as

$$\frac{u'}{u} = \frac{S't}{St'} < \frac{S'}{S} \left(1 + \frac{4KH t_{\text{pump}}}{10 r^2 S'}\right) \quad (4.34)$$

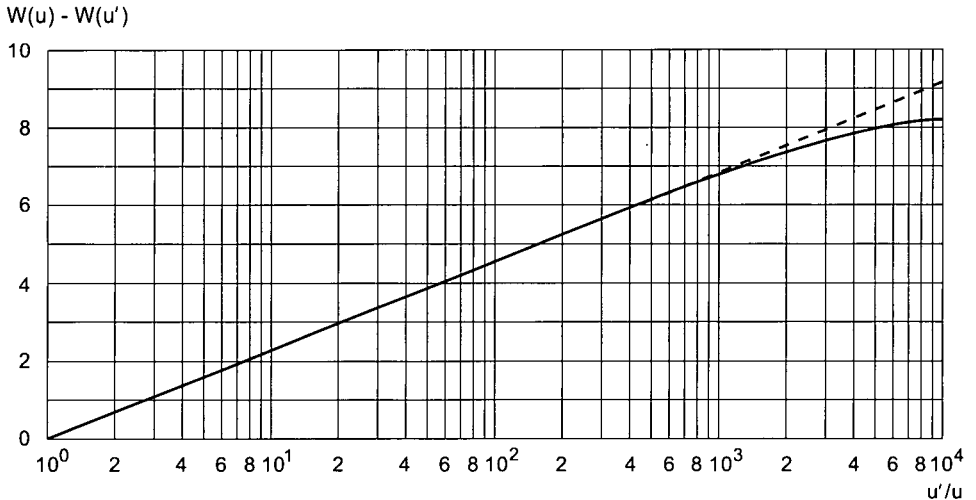


Figure 4.15 Theis recovery well function  $W(u) - W(u')$  versus  $u'/u$  for fully penetrating wells in confined aquifers

In SATEM 2002, Equation 4.34 has been adopted as the critical upper limit for  $u'/u$ .

The properties of a confined aquifer can be found by refining the time-ratio versus residual-drawdown relationship based on Equation 4.33. If the pumping and recovery times are sufficiently long, plotting the residual drawdown  $s'(r,t')$  observed in a particular piezometer at distance  $r$  from the pumped well against the logarithm of the time ratio  $t/t'$ , will yield a straight line. If the slope of the straight-line segment is expressed as the drawdown difference  $\Delta s' = s'(r,t/t_2') - s'(r,t/t_1')$  per log cycle of the time ratio ( $\log(t/t')_2 / \log(t/t')_1 = 1$ ), rearranging Equation 4.33 gives

$$KH = \frac{2.3Q}{4\pi\Delta s'} \quad (4.35)$$

If this line is extended until it intercepts the time-axis where  $s'(r,t/t') = 0$ , the interception point will have the co-ordinates  $s'(r,t/t') = 0$  and  $t/t' = (t/t')_0$ . Substituting these values into Equation 4.33, after rearrangement, gives

$$S' = S(t/t')_0 \quad (4.36)$$

The Theis recovery method is based on the assumptions listed at the beginning of this chapter and on the following conditions:

- The pumped well penetrates the entire thickness of the aquifer and thus receives water by horizontal flow;
- The pumping and recovery times are sufficiently long for a straight-line segment to be distinguished from a plot of time-ratio against residual drawdown on semi-log paper.

#### *Procedure*

- For one of the piezometers, plot the residual-drawdown values  $s'(r,t')$  against the corresponding time ratio  $t/t'$  on semi-log paper (with  $t/t'$  on the logarithmic scale);
- Select a time range where the plots exhibit a straight line and draw a best fitting straight line through these plotted points;
- Determine the slope of the straight line, i.e. the drawdown difference  $\Delta s'$  per log cycle of time ratio  $t/t'$ ;
- Substitute the values of  $Q$  and  $\Delta s'$  into Equation 4.35 and solve for  $KH$ ;
- Extend the straight line until it intercepts the time-ratio axis where  $s'(r,t/t') = 0$ , and read the value of  $(t/t')_0$ ;
- Substitute this value and the value of the storativity  $S$  obtained from analysing the drawdown data during the preceding pumping test into Equation 4.36 and solve for  $S'$ ;
- Substitute the values of  $S'$ ,  $S$ ,  $KH$ ,  $t_{\text{pump}}$  and  $r$  into Equation 4.34 and solve for  $t/t'$ . This  $t/t'$  value should be greater than the time-ratio range for which the straight-line segment was selected;

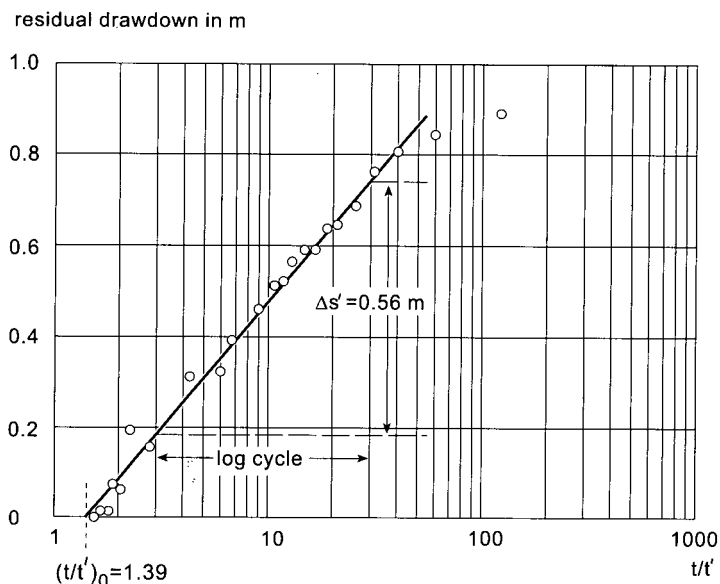


Figure 4.16 Time-residual-drawdown data analysed with the Theis recovery method

- If residual drawdown values are available for more than one piezometer, apply the above procedure to the other piezometers. The resulting values for  $KH$  and  $S'$  should agree closely.

This procedure is illustrated graphically in Figure 4.16.

Neuman (1975) showed that Equation 4.33 can also be used to describe the residual drawdown behaviour in unconfined aquifers, because its delayed water table response to pumping is fully reversible (no hysteresis effects). The only changes required are that the storativity  $S$  be replaced by the specific yield  $S_y$  of the unconfined aquifer, and that the transmissivity  $KH$  be defined as the transmissivity of the initial saturated thickness of the aquifer.

## 4.6 Single-well tests

A single-well test is a test in which no piezometers are used. Water-level changes during pumping and recovery are measured only in the well itself. The drawdown in a pumped well, however, is influenced by well losses (Chapter 5) and well-bore storage. In the hydraulics of well flow in the preceding sections, the well has been regarded as a line source or line sink, i.e. the well is assumed to have an infinitesimal radius so that the well-bore storage can be ignored. Well-bore storage is large when compared with the storage in an equal volume of aquifer material. In a single-well test, well-bore storage must be considered when analysing the drawdown data.

Papadopoulos and Cooper (1967) observed that the influence of well-bore

storage on the drawdown in a well decreases over time and becomes negligible at  $t > 25r_c^2/KH$ , where  $r_c$  is the radius of the unscreened part of the well. For a radius of a few decimetres and a transmissivity in the range of 100 to 1000 m<sup>2</sup>/d, the effect of the well-bore storage will thus become negligible after 1 to 10 minutes of pumping. So, the effect of discarding the early drawdown data from the pumped well is that the influence of any well-bore storage will no longer be reflected in the time-drawdown data of the pumped well.

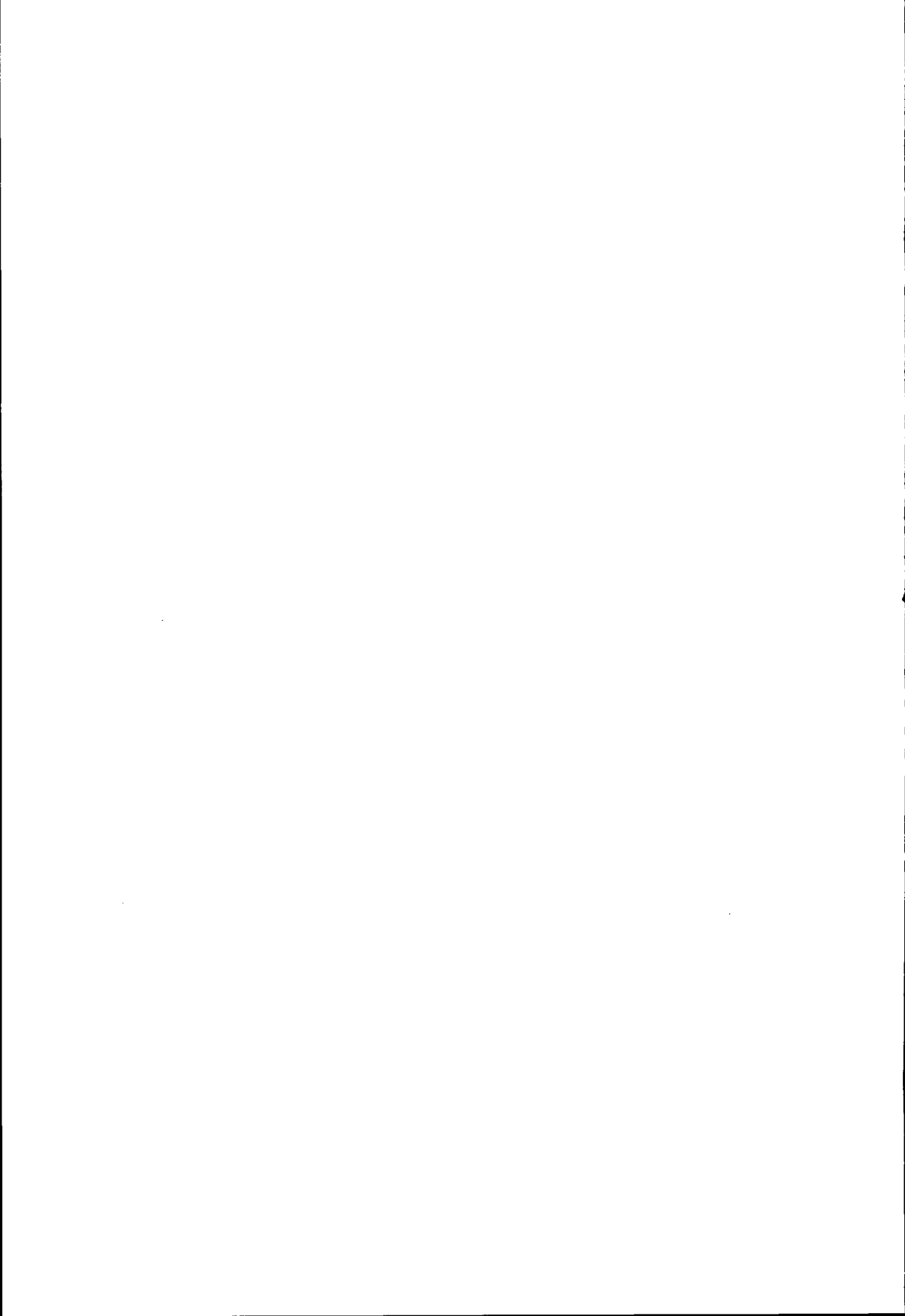
The late drawdown data are, however, still influenced by the well losses. These linear and non-linear well losses (see Chapter 5) have constant values over time, provided that the discharge rate is kept constant. This is one of the basic assumptions in the analysis methods presented in the foregoing sections, as was noted at the beginning of this chapter. This implies that the well losses will not affect the calculation of the transmissivity, because semi-log plots are used in all the preceding analysis methods.

So, with single-well tests, basically the same procedures to estimate the aquifer's transmissivity can be applied as with aquifer tests, provided that the early drawdown data are discarded from the analysis. However, the aquifer's storativity or specific yield cannot be estimated from single-well tests, for two reasons: (1) the straight line in the time-drawdown plot is located too high because of the well losses and (2) the  $r$ -value now represents the effective radius of the screened part of the well.

The non-linear well loss can be estimated if a step-drawdown test was conducted prior to the single-well test. The values of  $C$  and  $P$  (see Chapter 5) can then be estimated and the observed drawdowns can be corrected to eliminate the influence of the non-linear well loss. However, the influence of the linear well loss is still present in the corrected drawdowns. This loss can only be estimated from an aquifer test analysis, but with single-well tests no piezometers are used.

The effective radius of the screened part of the well can be calculated from the actual radius of the well and the so-called skin. This skin can only be calculated if the linear well loss is known. So, for a proper estimate of the effective radius, the result of an aquifer test is also required.

This means that when SATEM 2002 is used to analyse the data from a single-well test, the aquifer's storativity or specific yield value will not be estimated.



# 5 Theory of step-drawdown test analysis

In a step-drawdown test the well is initially pumped at a low constant rate until the drawdown within the well stabilises, i.e. until a steady state is reached. The pumping rate is then increased to a higher constant rate and the well is pumped until the drawdown stabilises once more (Figure 5.1). This process is repeated through at least three steps, which should be of equal duration (say, a few hours each).

## 5.1 Well and aquifer losses

The drawdown in a pumped well consists of two components: the aquifer losses and the well losses (Figure 5.2). Aquifer losses are the head losses that occur in the aquifer where the flow is laminar. They are time-dependent and vary linearly with the well discharge. The drawdown  $s_1$  corresponding to this linear aquifer loss can be expressed as

$$s_1 = B_{1(r_w,t)}Q \tag{5.1}$$

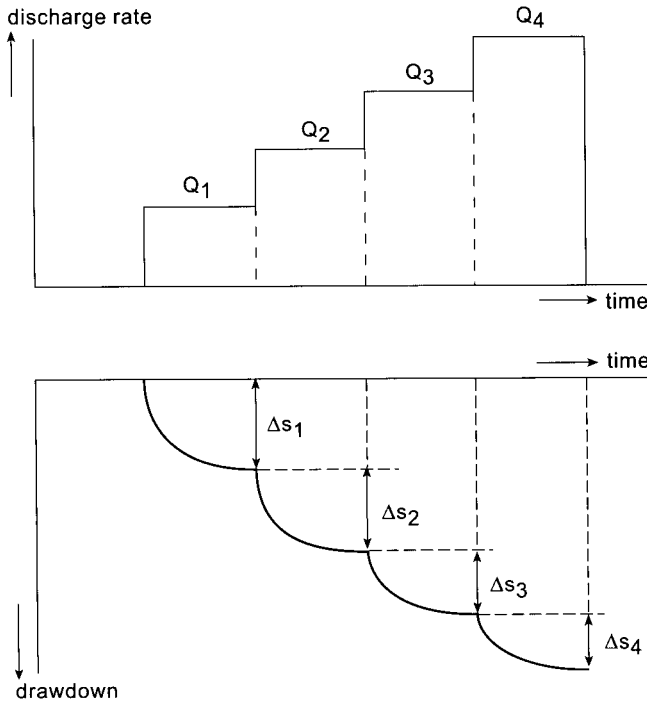


Figure 5.1 Principle of a step-drawdown test

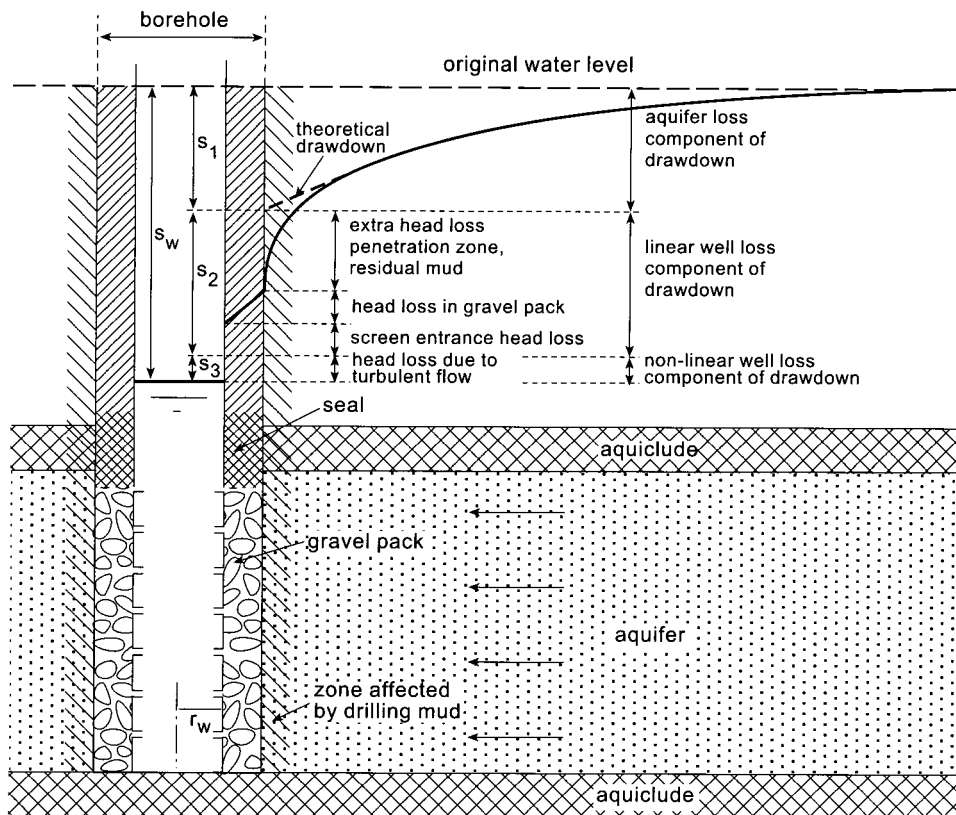


Figure 5.2 Various components of drawdown in a pumped well

where  $B_1$  is the linear aquifer loss coefficient in  $d/m^2$  and  $r_w$  is the effective radius of the well. This coefficient can be calculated from the well-flow equations presented in Chapter 4. For confined aquifers for example, it can be expressed using Equations 4.1 and 4.2 as

$$B_{1(r_w, t)} = \frac{W(u)}{4\pi KH}$$

where  $u = (r_w^2 S)/(4KHt)$ . From the results of aquifer-test analyses, the values for transmissivity  $KH$  and storativity  $S$  can be used to calculate  $B_1$  values as function of  $r_w$  and  $t$ .

Well losses are divided into linear and non-linear head losses. Linear well losses are caused by the aquifer being damaged during the drilling and completion of the well. They comprise, for example, head losses resulting from the aquifer material compacting during drilling; head losses resulting from the aquifer becoming plugged with drilling mud, which reduces the permeability near the bore hole; head losses in the gravel pack; and head losses in the



screen. The drawdown  $s_2$  corresponding to linear well losses can be expressed as

$$s_2 = B_2 Q \quad (5.2)$$

where  $B_2$  is the linear well loss coefficient in  $d/m^2$ . The non-linear well losses include the friction losses that occur inside the well screen and in the suction pipe where the flow is turbulent, and head losses that occur in the zone adjacent to the well where the flow is also usually turbulent. The drawdown  $s_3$  corresponding to these non-linear well losses can be expressed as

$$s_3 = C Q^P \quad (5.3)$$

where  $C$  is the non-linear well loss coefficient in  $d^P/m^{3P-1}$ , and  $P$  is an exponent. The general equation describing the drawdown in a pumped well as function of aquifer/well losses and discharge thus reads

$$s_w = s_1 + s_2 + s_3 = (B_1 + B_2) Q + C Q^P = B Q + C Q^P \quad (5.4)$$

Jacob (1947) used a constant value of 2 for the exponent  $P$ . According to Lennox (1966) the value of  $P$  can vary between 1.5 and 3.5. Our experience is that in fractured rock aquifers its value may even exceed 3.5. The value of  $P = 2$  as proposed by Jacob is, however, still widely accepted. The values of the three parameters  $B$ ,  $C$  and  $P$  in Equation 5.4 can be found from the analysis of step-drawdown tests. Note that  $B$  represents the contribution of the aquifer loss plus the linear well loss; their individual contributions can only be determined from a combination of step-drawdown and aquifer test analyses.

## 5.2 Well efficiency

The relationship between drawdown and discharge can be expressed as the specific capacity of a well,  $Q/s_w$ , which describes the productivity of both the aquifer and the well. The specific capacity decreases as pumping continues and also with increasing  $Q$ . The well efficiency,  $E_w$ , is defined as the ratio of the aquifer head loss to the total head losses; when expressed as a percentage it reads

$$E_w = \frac{100B_1 Q}{B Q + C Q^P} \quad (5.5)$$

The well efficiency according to Equation 5.5 can be assessed if the results of a step-drawdown and of an aquifer test are available. The former are needed for the values of  $B$ ,  $C$  and  $P$  and the latter for the value of  $B_1$ .

If only the results of a step-drawdown tests are available, the substitution of the  $B$  value into Equation 5.5 for the  $B_1$  value will overestimate the well efficiency, because  $B > B_1$ . For these cases, Driscoll (1986) introduced another parameter,  $L_p$ , being the ratio of the laminar head loss to the total head losses; when expressed as a percentage it reads

$$L_p = \frac{100BQ}{BQ + CQ^p} \quad (5.6)$$

Equation 5.6 can be used to analyse the well performance yearly, because step-drawdown tests are usually conducted as single-well tests, i.e. the drawdown is not observed in any piezometer. Note that Equation 5.6 is not representative for the well efficiency.

### 5.3 Diagnostic plots

The analysis of step-drawdown tests uses diagnostic plots in which values of  $s_w/Q$  versus  $Q$  are plotted on linear paper, with  $s_w$  representing the stabilised drawdown at the end of each step. Various configurations of diagnostic plots are possible:

- The points form a horizontal line; this implies that  $s_w/Q = B$ . Hence, there are no non-linear well losses ( $C = 0$ ). This situation is only encountered at

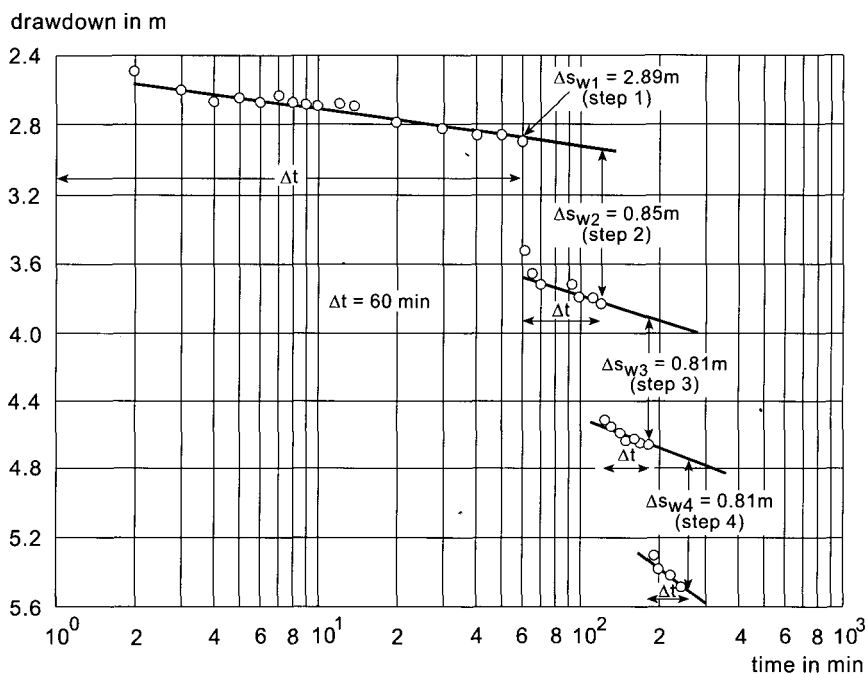


Figure 5.3 Time-drawdown plot of field data from a step-drawdown test

very low pumping rates. If the pumping rates are increased, the well will act differently.

- The points form a straight line under a slope; this means that  $P = 2$ . For this case, Jacob (1947) developed an analysis method to calculate B and C.
- The points form a curved line, i.e.  $P$  is unequal to 2. If the curve is concave,  $P > 2$ ; if it is convex,  $P < 2$ . For these cases, Rorabaugh (1953) developed an analysis method to calculate B, C and P.

Under field conditions, the condition that the  $s_w$  values used in these plots represent the stabilised drawdowns at the end of each step is not always met (see Figure 5.3). When this occurs, the observed drawdown values at the end of each step need to be corrected before a diagnostic plot can be made. This can be done using the following procedure as developed by Hantush-Bierschenk (Hantush 1964).

*Hantush-Bierschenk's procedure:*

- Plot the drawdown values of  $s_w(t)$  versus the corresponding time  $t$  on semi-log paper for all the steps (with  $t$  on the logarithmic scale);
- Select a time range in each step where the plots exhibit a straight line and draw the best-fitting straight line through these plotted points;
- Extrapolate the straight line to the end of the next step;
- Determine the increments of drawdown  $\Delta s_{w(i)}$  for each step by taking the difference between the observed drawdown at a fixed interval  $\Delta t$ , taken from the beginning of each step, and the corresponding drawdown on the straight line extrapolated from the preceding step;
- Determine the values of  $s_{w(n)}$  corresponding to the discharge  $Q_n$  from  $s_{w(n)} = \Delta s_{w(1)} + \Delta s_{w(2)} + \dots + \Delta s_{w(n)}$ , where  $n = 1, 2, \dots, N$  and  $N$  the number of steps.

It will be clear that for the drawdown at the end of the first step,  $\Delta s_{w(1)}$ , no correction can be made with this procedure, i.e. it may represent a non-stabilised drawdown.

## 5.4 Jacob's method

The values of B and C can be found directly from the diagnostic plot of  $s_w/Q$  against  $Q$ , when  $P = 2$ . Equation 5.4 then reads

$$s_w/Q = B + C Q \quad (5.7)$$

Equation 5.7 implies that a plot of  $s_w/Q$  versus  $Q$  on linear paper would yield a straight line under a slope (Figure 5.4). The slope of this straight line is equal to C, while the value of B can be found by extending the straight line until it intercepts the  $Q = 0$  axis.

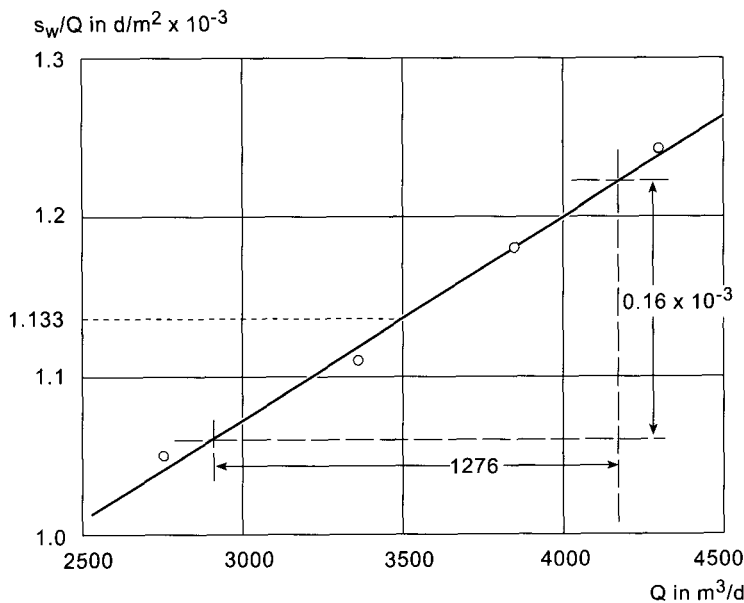


Figure 5.4 Diagnostic plot of  $s_w/Q$  versus  $Q$  of field data from a step-drawdown test analysed with the Jacob method

The Jacob method is applicable in any type of aquifer if the following assumptions and conditions are satisfied:

- The assumptions listed at the beginning of Chapter 4, with the exception of the fourth assumption, which is replaced by: the aquifer is pumped stepwise at increased discharge rates.

The following conditions are added:

- The pumped well penetrates the entire thickness of the aquifer and thus receives water by horizontal flow;
- The non-linear well losses are appreciable and vary according to the expression  $CQ^2$ .

#### Procedure

- Plot the drawdown values of  $s_w(t)$  versus the corresponding time  $t$  on semi-log paper ( $t$  on logarithmic scale);
- If the drawdowns at the end of each step did not stabilise, apply the Hantush-Bierschenk procedure and correct the values of  $s_{w(n)}$ ;
- On linear paper, plot the values of  $s_{w(n)}/Q_n$  versus the corresponding values of  $Q_n$ ;
- Fit a straight line through the plotted points;
- Determine the slope of the straight line  $\Delta(s_w/Q)/\Delta Q$ , which represents the value of  $C$ ;
- Extend the straight line until it intercepts the  $Q = 0$  axis. The  $s_w/Q$  value of the interception point represents the value of  $B$ .

## 5.5 Rorabaugh's method

The values of B, C, and P cannot be found directly from the diagnostic plot of  $s_w/Q$  versus Q itself, when P is unequal to 2. Equation 5.4 then reads

$$s_w/Q = B + CQ^{P-1} \tag{5.8}$$

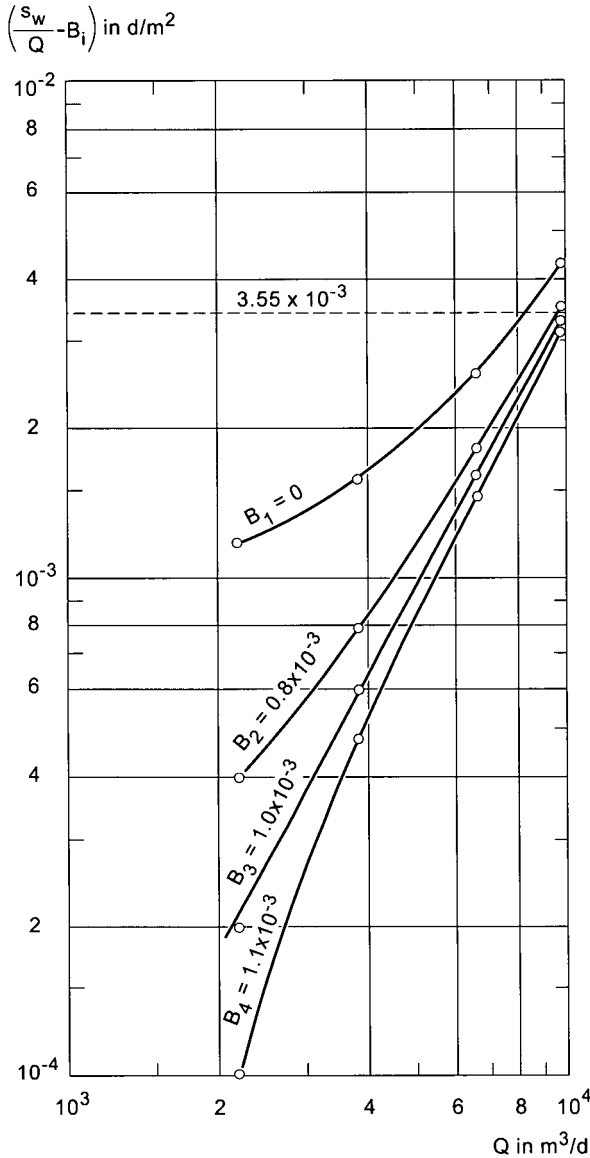


Figure 5.5 Log-log plot of  $[s_w/Q - B]$  versus Q of field data from a step-drawdown test analysed with the Rorabaugh method

Rearranging Equation 5.8 and taking the logarithms, it can also be written as

$$\log[s_w/Q - B] = \log C + (P-1)\log Q \quad (5.9)$$

Equation 5.9 implies that a plot of  $[s_w/Q - B]$  versus  $Q$  on log-log paper would yield a straight line under a slope. The slope of this straight line is equal to  $P-1$ , while the value of  $C$  can be found by extending the straight line until it intercepts the  $Q = 1$  axis.

The Rorabaugh method is applicable in any type of aquifer if the following assumptions and conditions are satisfied:

- The assumptions listed at the beginning of Chapter 4, with the exception of the fourth assumption, which is replaced by: the aquifer is pumped step-wise at increased discharge rates.

The following conditions are added:

- The pumped well penetrates the entire thickness of the aquifer and thus receives water by horizontal flow;
- The non-linear well losses are appreciable and vary according to the expression  $CQ^P$ .

#### *Procedure*

- Plot the drawdown values of  $s_w(t)$  versus the corresponding time  $t$  on semi-log paper (with  $t$  on the logarithmic scale);
- If the drawdowns at the end of each step did not stabilise, apply the Hantush-Bierschenk procedure and correct the values of  $s_{w(n)}$ ;
- On linear paper, plot the values of  $s_{w(n)}/Q_n$  versus the corresponding values of  $Q_n$ ;
- Fit a curved line through the plotted points;
- Extend the curved line smoothly until it intercepts the  $Q = 0$  axis. Take the interception point on this  $s_w/Q$  axis as initial estimate  $B_i$  of  $B$ ;
- Calculate  $[s_{w(n)}/Q_n - B_i]$  for each step;
- Plot the values of  $[s_{w(n)}/Q_n - B_i]$  versus  $Q_n$  on log-log paper. Repeat this part of the procedure for different values of  $B_i$ . The value of  $B_i$  that gives the straight line on the plot will be the correct value of  $B$ . Figure 5.5 shows that the data points are located on a straight line for a  $B$  value of  $1.0 \times 10^{-3}$ ;
- Calculate the slope of the straight line  $\log \Delta[(s_w/Q) - B] / \log \Delta Q$ . This equals  $(P-1)$ , from which  $P$  can be obtained;
- Extend the straight line until it intercepts the  $Q = 1$  axis. This value of  $[(s_w/Q) - B]$  represents the value of  $C$ .

## 6 SATEM 2002 software package

The SATEM 2002 software package can be used to (1) estimate aquifer properties of water-bearing layers from exploration wells and (2) determine the optimum production capacity of exploitation wells and analyse the well performance over time, to facilitate well maintenance and rehabilitation.

In the case of exploration wells, SATEM 2002 offers the user options for estimating the aquifer properties of water-bearing layers. This entails performing an aquifer test and analysing its data. Each piezometer yields one set of estimated aquifer properties when its drawdown data during pumping are analysed in a *time-drawdown analysis*. If the measurements continue after the pump has been shut down, a second set of estimated aquifer properties can be obtained for that piezometer if its residual-drawdown data during recovery are analysed in a *time-recovery analysis*. If there is more than one piezometer, separate estimates of the aquifer properties can be made for each piezometer and their values compared for their consistency. If there are more than two piezometers, a *distance-drawdown analysis* will give an additional estimate of the aquifer properties. This allows a closer check of the consistency of the resulting estimates of the aquifer properties.

In the case of exploitation wells, SATEM 2002 offers the user options for determining the optimum production capacity and analysing the well performance over time, to facilitate well maintenance and rehabilitation. The optimum production capacity is determined by performing a step-drawdown test and analysing its data; well performance is analysed by repeating this type of test annually and comparing the analysis results. A *step-drawdown analysis* will give estimates of the linear and non-linear well losses.

### 6.1 Installation procedure

To install SATEM 2002, insert the software in the appropriate drive and run `install.exe`. The installation will create a SATEM folder on the specified drive and folder, with the following four sub-folders:

- BGI, which contains files for internal use by SATEM 2002;
- SYNTETIC, which contains synthetic data that are used in Chapter 7 to illustrate the essentials of performing the various analyses with SATEM 2002;
- FEATURES, which contains other synthetic data, which are also used in Chapter 7 to illustrate the applicability of the presented time-drawdown analyses; and
- ILRIPU57, which contains field data that are used in Chapters 8-11 to further familiarise the user with all SATEM's analysis modules.

To run SATEM, use the Windows explorer to select the SATEM folder and run Satem.exe. SATEM starts by displaying an introductory screen, followed by its main menu. The main menu bar of SATEM contains four menu items: *Type of analysis*, *Input*, *Analysis*, and *Output*. Some of these items contain sub-menus. Usually, you choose the items on the main menu bar from left to right. If you want to start to analyse aquifer test data already stored in an existing file, for instance, you can go straight to *Analysis*.

## 6.2 Type of analysis

Type of analysis is the first item on the main menu bar. Once you select it, a dialogue form will appear on the screen. It contains the following four options:

Time-drawdown/recovery analysis
Time-residual-drawdown analysis
Distance-drawdown analysis
Step-drawdown analysis

Select an option by clicking on a radio button and then OK. To estimate the aquifer properties of water-bearing layers from exploration wells, select 'Time-drawdown/recovery analysis' or 'Time-residual-drawdown analysis'. If you have the drawdown data from the pumping period, either by themselves or in combination with the residual-drawdown data from the recovery period, select the first option. If you have only the residual-drawdown data - the drawdown data from the preceding pumping period are missing -, select the second option. If drawdown data from more than two piezometers are available, continue by selecting 'Distance-drawdown analysis'. You select 'Step-drawdown analysis' for determining the optimum production capacity and for analysing the well performance over time for the purpose of maintaining and rehabilitating exploitation wells.

Each type of these analyses has its own format for storing the data in a file and uses different analysis methods. So, which files you will see in the input/output menu and which analysis methods you can use in the actual analysis will depend on the type of analysis selected.

## 6.3 Input

Input is the second item on the main menu bar; its pull-down menu contains the following options:



New Satem file
Open existing file for editing

Once you select 'New Satem file', a main input dialogue form will appear on the screen. It contains the following options:

General test features
Features of data sets
Data set specific features
Units

Selecting one of the first three options and then OK will take you to a data entry form. A common feature in these forms is that ranges of acceptable values are displayed whenever you need to enter a specific value. If you enter a value outside the prescribed range, pressing <Enter> will not lead to acceptance. Either change the value so that it is within limits, or press <Esc> to retrieve the original value.

Another feature is that a warning screen pops up if you click the 'OK' button to leave any of the above three data entry forms but forgot to prescribe values in data fields that are essential for the analysis. This only happens when you use the option 'New Satem file'. You then have the possibility to rectify this. If you do not rectify this and you save the incomplete file under a particular name, a similar screen will appear when you try to open that file for analysis. The only remedy then is to return to the input menu, select that file in 'Open existing file for editing', and finish the required data entry.

Once you select 'Open existing file for editing', the Windows Open dialogue box will appear on the screen. You can change the drive and folder and select a certain file. You can also change the type of file, for instance, from 'time-drawdown/recovery analysis' to 'distance-drawdown analysis'. Once you have selected a particular file, the same main input dialogue form will then appear on the screen.

### 6.3.1 General test features

Under this heading you can enter general input data according to the type of analysis selected previously. Table 6.1 gives an overview of these input data specified for the three types of analysis.

Table 6.1 Overview of general input data for different types of analysis

Time-drawdown analysis	Distance-drawdown analysis	Step-drawdown analysis
Discharge of well	Discharge of well	Number of steps
Penetration depth well	Pumping time	Pumping time per step
Screened length well	Number of data sets	Type of data
Pumping time	Type of data	
Number of data sets	Type of aquifer	
Type of data		
Type of aquifer		

A data set is here defined as a series of data from a particular well. Data obtained during the pumping and subsequent recovery period in the same well counts as two data sets. For instance, if in the pumped well and in three observation wells the data on depth to the water table were obtained only during the pumping period, you should enter 4 as the number of data sets. If in a single-well test the data on depth to water table were recorded in the pumped well itself both during pumping and during the recovery period, you should enter 2.

Type of data can either be depth to water table or drawdown. The data observed in the field will always be depth to water table. In that case, you should also prescribe the initial depth to water table prior to pumping. In the case of time-drawdown and distance-drawdown data, this will appear in the option 'Data set specific features', but for step-drawdown data it will appear in the same menu.

The type of aquifer can be confined, leaky, or unconfined. If you select the unconfined type of aquifer, 'Thickness aquifer' appears as an additional data entry field on the screen. You need to prescribe a value for this, based on the water table prior to pumping, as it is used to correct the observed drawdown (Equation 4.18). If you don't have an estimate for the aquifer thickness, select 'confined' as type of aquifer.

### 6.3.2 Features of data sets

The form showing the features of the various data sets is identical for all the three types of tests. It contains the following input data:

Data set	Type of test	Number of data
1	pumping test	3
2	pumping test	3
3	pumping test	3
4	pumping test	3

The number of data sets in this screen depends on what you have specified under general test features. For time-drawdown analysis you can specify both 'Type of test' as well as 'Number of data', whereas for distance-drawdown and step-drawdown analysis you can only specify 'Number of data'.

With time-drawdown analysis you can use as 'Type of test' either 'pumping test' or 'recovery test'. The rule for using the option 'recovery test' is simple: you may only designate a data set as 'recovery test' if a preceding data set has been designated 'pumping test'. The reason for this is that the synthetic recovery values are calculated using the aquifer properties obtained from the preceding time-drawdown analysis (see Chapter 4, Section 5).

For 'Number of data' you specify the number of data pairs observed in the field, i.e. time and depth to water table data for time-drawdown and step-drawdown analysis, and distance and depth to water table data for distance-drawdown analysis. Either count exactly how many observations you have for each well, or make a rough estimate and use the special keys, as discussed in the next section.

### 6.3.3 Data set specific features

The data specific to each data set are displayed in the next form when selecting 'Data set specific features' on the main input dialogue form. If you selected the option 'New Satem file', you will see:

Set 1	Set 2	Set 3
r-value	= 0.00 m.	penetration depth = 0.00 m.
i.w.t. depth	= 0.00 cm.	screened length = 0.00 m.
Time (min)		w.t. depth (cm.)
0.00		0.00
0.00		0.00
0.00		0.00

(Note that i.w.t. = initial water table and w.t. = water table.)

All values are initially set to zero. If you selected an existing file through the option 'Open existing file for editing', this form displays the values you entered previously. Each data set has its own tab sheet, labelled Set 1, Set 2, etc. The number of tabs depends on the number of data sets. You can go from one data set to another one by clicking on the particular tab located at the top of the form. To add an additional data set, just click on the 'Append data set' button. The following message appears on the screen:

Would you like to copy the time values of data set 1 to the appended data set?

Clicking on the 'No' button, brings up a form similar to the previous one, but for the new appended data set. If the number of data sets was 6, clicking on the append button will generate a new tab sheet for data set 7, showing zeros only. If you had clicked on the 'Yes' button, the only difference would be that all displayed time values would equal those of data set 1. This is only recommended if the time interval for measuring depth to water table was the same time for all the observation wells.

To delete a particular data set, click on the particular tab of the data set that must be deleted and click on the 'Delete data set' button. You cannot delete a data set designated as 'pumping test' that is followed by a data set designated as 'recovery test'. In that case, you first need to go to the 'recovery test' data set and delete it, and then delete the data set designated as 'pumping test'.

To insert an additional data set, click on the particular tab of the data set to access the data set in front of which you wish to insert an additional data set and click on the 'Insert data set' button.

To add an additional data pair, click on the 'Append data pair' button: the cursor moves to the last line. To delete a particular data pair, click on that line and click on the 'Delete data pair' button. To insert an additional data pair, click on the line in front of which you wish to put the insertion, and click on the 'Insert data pair' button.

#### 6.3.4 Units

The default units in SATEM are  $m^3/d$  for the pumping rate, cm for the depth to water table observed in a well, m for well distance/depth and aquifer thickness, and min for the time. To use other units, select the 'Units' option in the main input dialogue form, click 'OK' and the following form will appear on the screen:

Pumping rate
Drawdown data
Well data
Time

For the pumping rate you can use  $m^3/d$ ,  $m^3/min$ ,  $l/s$ ,  $ft^3/s$ , or US gall/min. For the data on drawdown and depth to water table you can use cm, m, or ft. For

well distance, well depth, penetration depth, screen length, and aquifer thickness you can use either m or ft. For time since pumping started and total pumping time you can use either min or hours. This option to change units has been incorporated into SATEM to facilitate the data entry. It is usual to change the various units before you start entering data. If you use this option in an existing file, all input data will be converted to the new values. However, the aquifer properties resulting from the analysis are displayed in standard units, i.e. transmissivity in  $m^2/d$ , hydraulic resistance in d, aquifer thickness in m and hydraulic conductivity in m/d.

## 6.4 Analysis

Analysis is the third item on the main menu bar. Once you select it, the Windows Open dialogue box will appear on the screen. You can change the drive and folder and select a certain file. You can also change the type of file, for instance, from 'time-drawdown/recovery analysis' to 'distance-drawdown analysis'. Once you have selected a particular file, the method selection form will appear on the screen. It contains the complete list of analysis methods incorporated in SATEM:

Theis-Jacob's method
Hantush's inflection-point method
Jacob-Hantush's method
Theis's recovery method
Thiem-Jacob's method
Hantush-Jacob's method
Jacob's method
Rorabaugh's method

Which analysis methods you can actually select depends on which type of analysis you selected in the first item of the main menu bar or in the Windows Open dialogue box. These methods are shown in black, the others are greyed.

If you selected 'Time-drawdown/recovery analysis' and the file contains both drawdown and residual-drawdown data, you can choose between four analysis methods, whereas if the file contains only drawdown data, you can choose between three analysis methods. If you selected 'Time-residual-drawdown analysis', there is only one analysis method to be used. Table 6.2 gives an overview of the main features of these methods. The theory of these analysis

Table 6.2 Overview of the time-drawdown/recovery analysis methods

	Theis-Jacob's method	Hantush's inflection-point method	Jacob- Hantush's method	Theis's recovery method
aquifer test	+	+	+	+
single-well test	+	+	+	+
fully penetrating	+	+	+	+
partially penetrating	-	-	+	-
confined	+	+	+	+
leaky	-	+	-	-
unconfined	+	-	+	+
drawdown	+	+	+	-
recovery	+	+	+	-
residual	-	-	-	+

methods was discussed in Chapter 4, the synthetic data used to illustrate the essentials of doing the various analyses with SATEM are presented in Chapter 7, and field applications with examples are presented in Chapter 8.

If you selected 'Distance-drawdown analysis', you can choose between (1) Thieme-Jacob's method and (2) Hantush-Jacob's method. For confined and unconfined aquifers, you should select the first option, whereas for leaky aquifers you should select the second option. Both methods have in common that you need to have drawdown data from an aquifer test with more than 2 piezometers and the pumped well fully penetrates the aquifer. The theory underlying these analysis methods was discussed in Chapter 4 and field applications with examples are presented in Chapter 9.

If you selected 'Step-drawdown analysis', you can choose between (1) Jacob's method and (2) Rorabaugh's method. The method to select depends on the resulting diagnostic plot (see Chapter 10, Section 3). Both methods have in common that you need to have drawdown data from the fully penetrating pumped well. The theory underlying these analysis methods was discussed in Chapter 5 and field applications with examples are presented in Chapter 10.

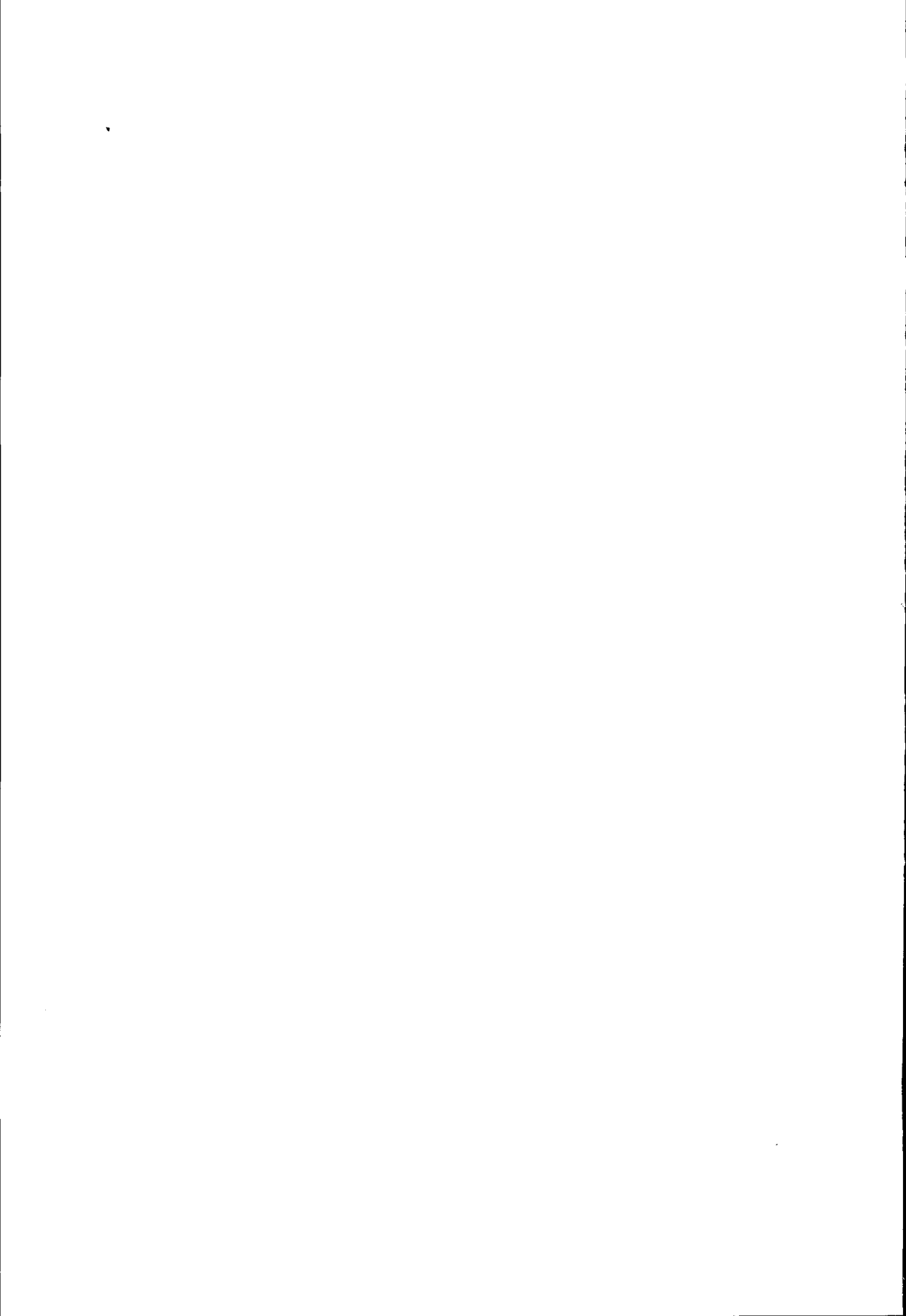
Once you have selected any of the above analysis methods, the actual analysis starts by showing you diagnostic plots of the field data plotted on semi-log paper. These are discussed in detail in Chapters 7 to 10.

The Windows Open dialogue box will not appear on the screen, if you prior to 'Analysis' saved a data file under 'Input'. In that case, the method selection form containing all the analysis methods will directly appear on the screen. Once you have selected a particular method, the actual analysis starts by showing you diagnostic plots of the field data stored in the file you just saved.

## 6.5 Output

Output is the fourth item on the main menu bar. Once you select it, the Windows Open dialogue box will appear on the screen. You can change the drive and folder and select a certain file. You can also change the type of file, for instance, from 'time-drawdown/recovery analysis' to 'distance-drawdown analysis'. Once you have selected a particular file, a short report file will appear on the screen. The first page always contains the general data. When you have analysed the data of that particular file, the first page continues with a table where values of the aquifer properties are presented for each well. The subsequent pages show the time-drawdown data or distance-drawdown data: one table per well.

To include the content of the file in any other Windows software, just click on the 'Copy to clipboard' button. To print the content of the file, click on the 'Print' button. The Windows Print dialogue box will appear on the screen.





## 7 Familiarising yourself with SATEM 2002

This chapter is for users with no previous experience of SATEM. Experienced users of SATEM may go directly to Chapter 8, where time-drawdown/recovery analysis methods are applied to field examples. Below, guidelines are given on performing the actual analyses for each of the four time-drawdown/recovery analysis methods of SATEM. Distance-drawdown and step-drawdown analyses, which are more straightforward than time-drawdown analyses, are discussed in Chapters 9 and 10, where they are applied directly to field examples.

To analyse time-drawdown data, use is made of diagnostic plots. Values of the unsteady-state drawdowns observed in a particular piezometer are plotted against the pumping time on semi-log paper. According to theory, the diagnostic plots, called time-drawdown plots, exhibit certain features that are specific to a particular analysis method. Below, fictitious data will be used to show you these features and to familiarise you with SATEM.

### 7.1 Using Theis-Jacob's method

This analysis method is based on the procedure described in Chapter 4, Section 1. The fictitious data set used here consists of the drawdown data during pumping and the residual-drawdown data during recovery of an observation well 100 m from the pumped well. These drawdowns, calculated using the aquifer properties  $KH = 200 \text{ m}^2/\text{d}$  and  $S = 0.0001$ , are stored in the 'Confined' file in the 'syntetic' folder.

Look at the data yourself. Select *Type of analysis* from the main menu bar of SATEM and select *Time-drawdown/recovery analysis*. Now, select *Input* from the main menu bar and use the option *Open existing file for editing*. Make sure that in the Window Open dialogue box the folder is `c:\Satem50\syntetic`. Select the file 'Confined' from the list of existing files. You are now in the data entry menu; select *Data set specific features*. For data set 1, you can see that the drawdown values increase over time. If you click on tab sheet Set 2, you switch to data set 2: as is to be expected, the residual-drawdown data now decrease with time. Next, select *Analysis* from the main menu bar of SATEM and select *Theis-Jacob's method* in the method selection form.

The first screen shows you the time-drawdown plot of the observation well at  $r = 100 \text{ m}$  distance. According to the Theis-Jacob method, the late-time drawdown data should exhibit a sloping straight line. On the basis of visual inspection you are requested to prescribe the range of time for which the data plot exhibits a straight-line segment. For the initial estimate of the lower limit, SATEM shows the time that the first observation was made; for the

Time-drawdown graph of well ( $r = 100$  m)

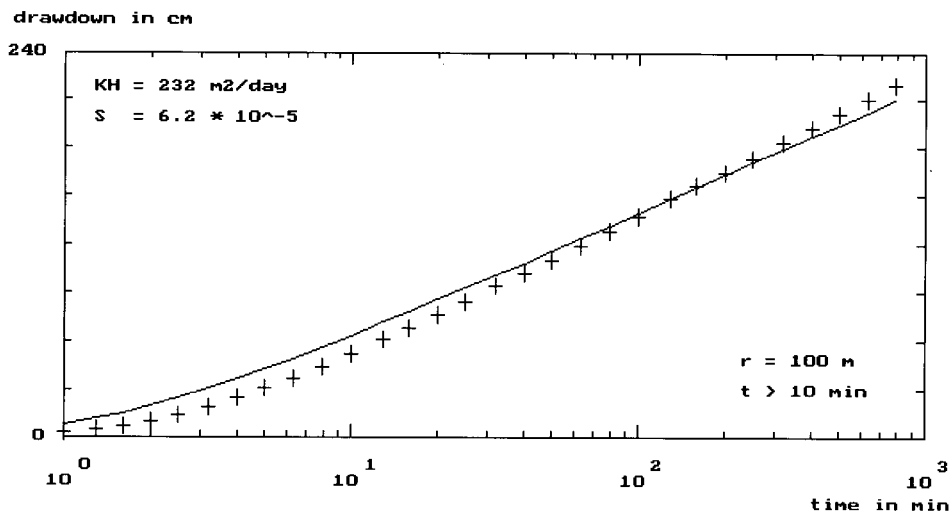


Figure 7.1 Mismatch of drawdown data with theoretical curve when the straight-line segment has been determined incorrectly

upper limit it uses the time that the last observation was made. Suppose you accept these initial estimates. SATEM then uses linear regression to calculate the best-fitting straight-line segment and takes into account only that part of the drawdown data within the prescribed time range. This straight-line segment is now displayed to show you how it is located with respect to your data points. Your choice now is to change the time range, if it is not satisfactory, or to continue. Although it is clear that the initial time range is not correct, let's suppose that you decide to continue. Press <Y> or <Enter>.

SATEM now calculates the aquifer properties according to the position of the selected straight-line segment. The transmissivity is calculated according to Equation 4.4 and the storativity according to Equation 4.5. In addition, SATEM calculates the time for which the  $1/u$  value is 10, substituting in Equation 4.2 the aquifer properties from the analysis and the distance from the pumped well. These values are displayed on the second screen, together with a line representing the calculated drawdowns (Figure 7.1). SATEM calculates these drawdowns according to Equations 4.1 and 4.2. Your choice now is to continue or to go back. From Figure 7.1 it is clear both from visual inspection and the indicated critical time value (10 min) that the match is not good. You are not satisfied, so press <N>.

You now change the lower limit from 1 to 10. The corresponding straight-line segment now proves more satisfactory and you continue. Figure 7.2 shows the new results of the analysis, together with the calculated drawdowns. The match is now much better, although the critical time value (15 min) exceeds the prescribed lower time limit (10 min). The change of critical time value is

Time-drawdown graph of well ( $r = 100 \text{ m}$ )

drawdown in cm

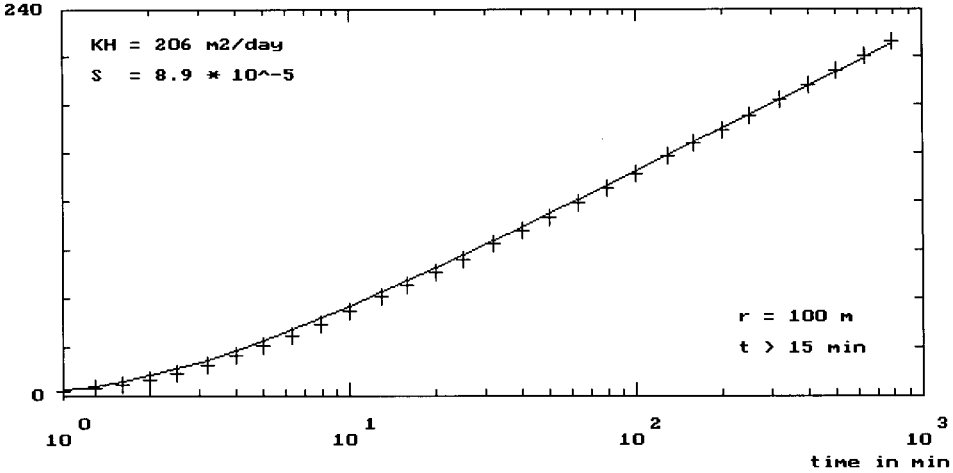


Figure 7.2 Near-perfect match of drawdown data with theoretical curve when only the data with  $t > 10 \text{ min}$  have been selected for determining the straight-line segment

due to the change in the transmissivity and storativity values. By returning once more and changing the lower time limit from 10 min to 16 min, you will see that the new values are almost identical to the ones shown in Figure 7.2. If you increase the lower limit even more, you will see that the resulting values of the aquifer properties increasingly approach the input values:  $KH = 200 \text{ m}^2/\text{d}$  and  $S = 0.0001$ . This is not so surprising, because the restriction that the value of  $1/u$  should be greater than 10 is only a relative indication (see Chapter 4, Section 1).

SATEM now repeats the above procedure for the next data set. In this case they are residual-drawdown data of the same well observed during recovery. For the analysis of residual-drawdown data the program converts them into synthetic recovery values. These recovery values are calculated as the difference between the hypothetical drawdown values if pumping continues and the observed residual-drawdown data. The aquifer properties found in the previous analysis are used for the calculation of these hypothetical drawdown values. So, the synthetic recovery values are influenced by the analysis of the drawdown data of the same well.

The first screen now shows you the time-drawdown plot of these time-recovery data. Back in Chapter 4, Section 5, it was shown that the analysis based on recovery data is identical to that of drawdown data. Changing the lower time limit from 1 to 16 will give almost identical results to the analysis of the drawdown data of this well.

The third and last screen gives you an overview of the results of your analysis:

Final results obtained with the Theis-Jacob method

r value well (m)	KH value (m <sup>2</sup> /d)	S value (-)
100	206	$8.9 \times 10^{-5}$
100	206	$8.9 \times 10^{-5}$

Results to be included in output file (Y/N) ?

The last question needs further explanation. If you press <Y>, then a table showing the aquifer properties of each well is included in the first page of the output file (see Chapter 6, Section 2.3). The values selected for the lower and upper time limits for determining the straight-line segment are stored in the file as well. This implies that when you analyse the data of this file again, you only need to press <Enter> repeatedly and you will see your previous analysis replayed on the screen.

If you press <N>, there will be no table in the first page of the output file (see Chapter 6, Section 5). The values you selected for the lower and upper time limits for determining the straight-line segment, are then not stored in the file. This implies that when you analyse the data of this file again, you need to go through all the steps again.

## 7.2 Using Hantush's inflection-point method

The method of analysis is based on the procedure described in Chapter 4, Section 2. The fictitious data set used here consists of drawdown data from an observation well 100 m from the pumped well and data from the pumped well itself. These drawdowns, calculated using the aquifer properties  $KH = 200 \text{ m}^2/\text{d}$ ,  $S = 0.0001$ , and  $c = 300 \text{ d}$ , are stored in the 'Leaky' file. Select this file from the list of existing files in the Windows Open dialogue box and select *Hantush's Inflection-Point method* in the method selection form.

The first screen shows you the time-drawdown plot of the observation well at  $r = 100 \text{ m}$  distance. According to the Hantush inflection-point method, the time-drawdown data should exhibit an S-shaped curve ending in a horizontal line indicating steady-state flow. On the basis of visual inspection you are requested to prescribe the steady-state drawdown (extrapolated). As initial estimate, SATEM shows the drawdown of the last observation. Let's suppose you decide not to change it, so press <Enter>. The level of the selected steady-state drawdown (dashed straight line) and the location of the inflection point (solid square) is now displayed on the screen. Again on the basis of visual inspection you are requested to prescribe the range of time for which the data

Time-drawdown graph of well ( $r = 100 \text{ m}$ )

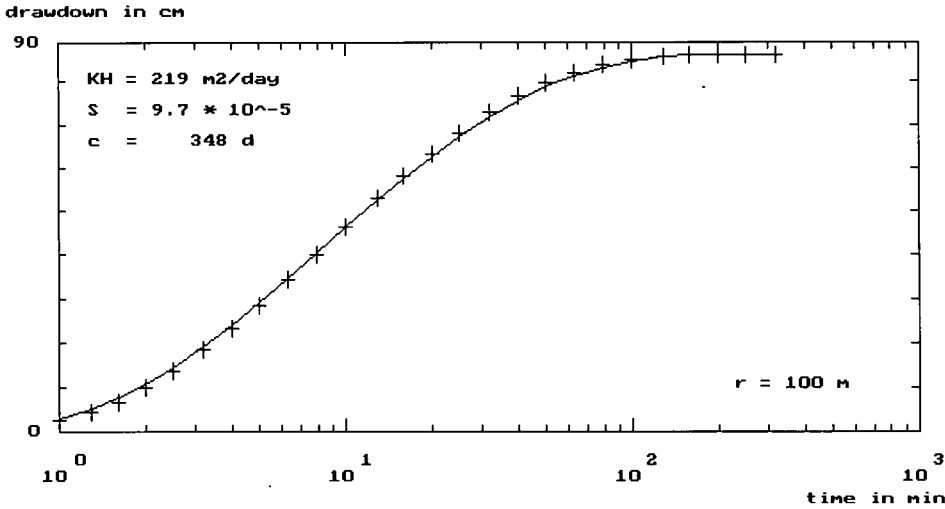


Figure 7.3 Reasonable match of drawdown data with theoretical curve for the observation well at distance 100 m

plot exhibits a straight-line segment around this inflection point. If no straight-line segment is present, the range of time to determine the tangent around the inflection point should be indicated. As initial estimate for the lower limit SATEM shows the time that the first observation was made, and for the upper limit it uses the time that the last observation was made. Suppose you change them as follows: lower limit = 4 min. and upper limit = 20 min. The screen now shows the new selected straight-line segment. The program calculates this straight-line segment using linear regression and takes into account only that part of the drawdown data within the prescribed time range. Your choice is to change the time range, if you are not satisfied, or to continue. Let's suppose you continue: press <Enter>.

SATEM now calculates the aquifer properties according to the location of the inflection point and the slope selected, substituting the appropriate values into Equations 4.10 to 4.13. These values are displayed on the second screen, together with a line representing the calculated drawdowns (Figure 7.3). SATEM calculates these drawdowns according to Equation 4.9.

Again there is the choice of continuing or going back. Although the match is satisfactory, the calculated aquifer properties differ some 10 per cent from those used to calculate the theoretical drawdowns. Let's suppose you are not satisfied; go back by pressing <N>.

When you change the lower limit from 4 to 7.5 min. and the upper limit from 20 to 10 min., the match is almost perfect and the aquifer properties obtained from the analysis are now almost identical to those used to calculate the theoretical drawdowns. The conclusion from this is that for the determi-

nation of the slope of the inflection point the smallest possible time range around the inflection point should be selected, provided that the plotted data show a smooth distribution.

SATEM now repeats the above procedure for the data on the next well. In this case they are drawdown data from the pumped well itself. SATEM again shows as initial estimate the drawdown of the last observation. Let's suppose you decide not to change it; press <Enter>. The level of the selected steady-state drawdown (dashed straight line) is now displayed on the screen, but not the location of the inflection point because that falls outside the plot. In these situations, which are typical for time-drawdown data of the pumped well itself, you are advised to take the first two or three observations as the time range for determining the slope. Let's suppose you take as the lower limit 1 min and as the upper limit 1.5 min. SATEM now determines internally the location of the inflection point by extrapolating the selected slope through the observation which was selected as the lower limit, until it intersects the horizontal line representing half the steady-state drawdown value. Figure 7.4 shows the results. The match is fairly good and the transmissivity value is close to the correct one. No values are given for the storativity of the tested aquifer or for the hydraulic resistance of the aquitard. The reason was explained in Chapter 4, Section 6.

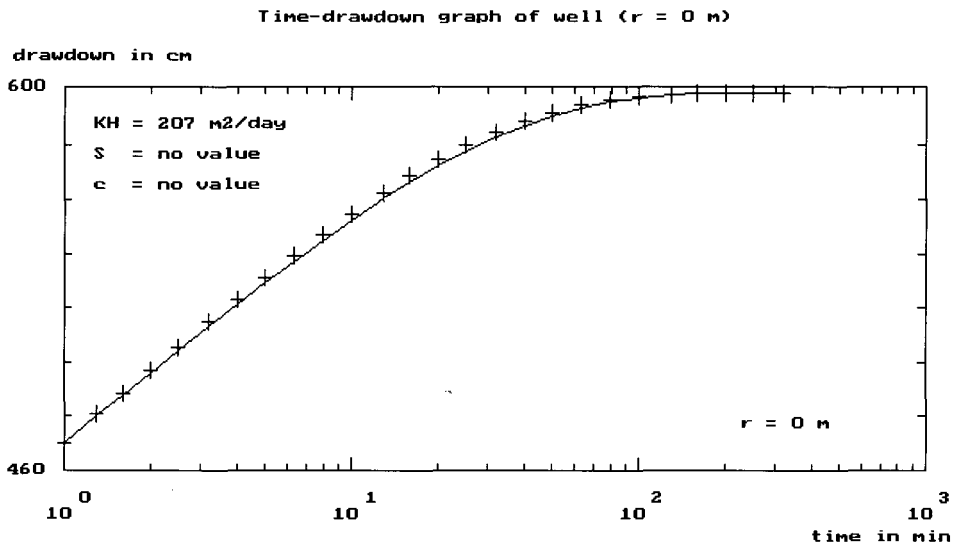


Figure 7.4 Match of drawdown data with theoretical curve for the pumped well itself

### 7.3 Using Jacob-Hantush's method

The method of analysis is based on the procedure described in Chapter 4, Section 4. The fictitious data set used here consists of drawdown data from an observation well 100 m from the pumped well, calculated using the aquifer properties  $K = 0.4$  m/d,  $H = 500$  m, and  $S = 0.0001$ . Both the pumped well and the observation well penetrated the aquifer to a depth of 100 m; the lower 50 m of these wells were screened. Apart from the partial penetration, the data set is identical to that used in the Theis-Jacob method. These data are stored in the 'Partial' file. Select this file from the list of existing files in the Windows Open dialogue box and select *Jacob-Hantush's method* in the method selection form.

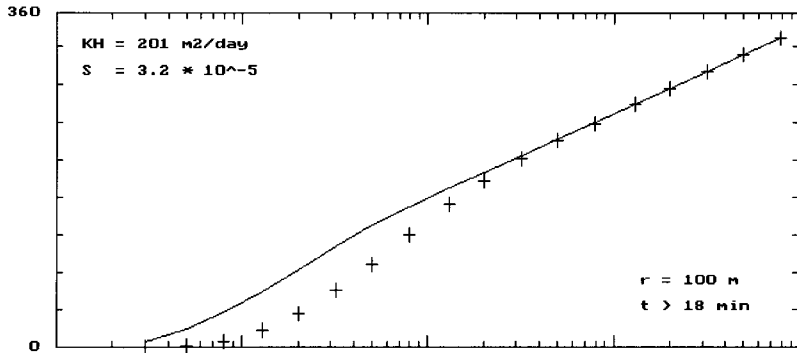
The first screen shows you the time-drawdown plot of the observation well at  $r = 100$  m distance. According to the Jacob-Hantush method, the late-time drawdown data should exhibit a sloping straight line, as was the case for the Theis-Jacob method. The difference between both time-drawdown plots is the shape of the early-time drawdowns. On the basis of visual inspection the range of time for which the data plot exhibits a straight-line segment must be prescribed. As initial estimate for the lower limit SATEM shows the time that the first observation was made, and for the upper limit it shows the time that the last observation was made. Let's suppose you change the lower limit from 0.32 to 100. Using linear regression, SATEM then calculates the straight-line segment and takes into account only the drawdown data within the prescribed time range. This straight-line segment is now displayed, to show you how it is located with respect to your data points.

The second screen shows you an arbitrary estimate of the aquifer thickness. Let's suppose you change it from 100 to 400 m. SATEM now calculates the aquifer properties according to the position of the selected straight-line segment. The transmissivity is calculated according to Equation 4.27 and the storativity according to Equation 4.28. In addition, SATEM calculates both the time for which the  $u$  value is 0.1, substituting the appropriate values into Equation 4.22, and the time for which the  $f_s$  value has reached a constant maximum value, substituting the appropriate values into Equation 4.23. The largest value of these two and the values of the aquifer properties are displayed on the third screen, together with a line representing the calculated drawdowns. SATEM calculates these drawdowns according to Equations 4.19 to 4.21. Figure 7.5.A shows this screen. Your choice is to continue or to go back. The match is clearly very poor in the early-time data, so you go back by pressing <N>. Do not change the time range describing the straight-line segment, because the match for the later-time data was good. Instead, change the thickness of the aquifer from 400 to 600 m. Figure 7.5.B shows that the match is again very poor for the early-time data, but now the calculated drawdowns lie below the observed drawdowns, instead of above as in Figure 7.5.A. The thickness of the aquifer apparently lies between 400 and 600 m. Now, change the

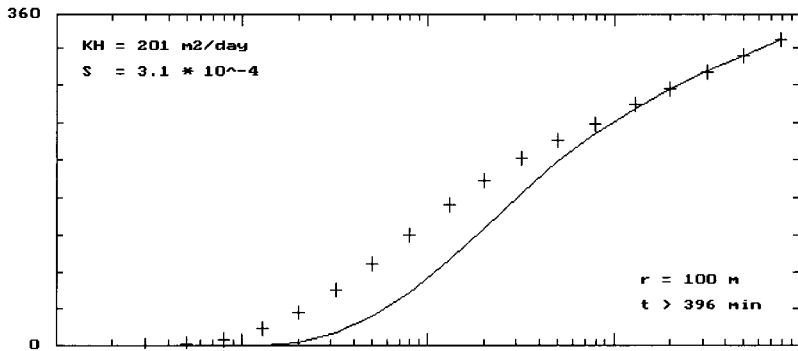
(A)

Time-drawdown graph of well ( $r = 100$  m)

drawdown in cm



(B)



(C)

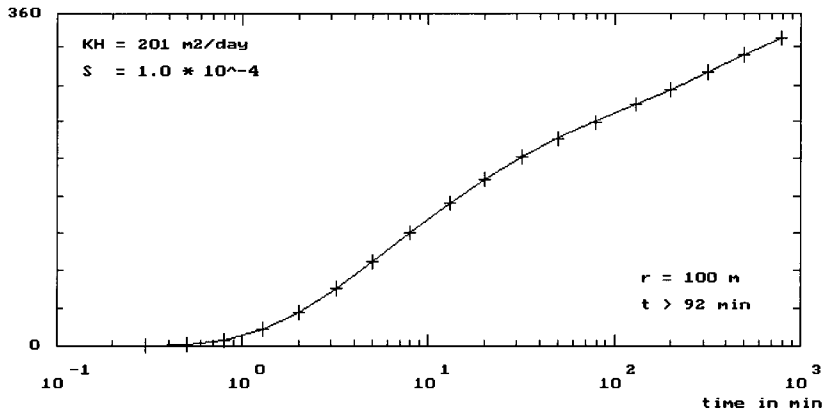


Figure 7.5 Matching drawdown data with theoretical curves

A: aquifer thickness 400 m

B: aquifer thickness 600 m

C: aquifer thickness 505 m



thickness of the aquifer from 600 to 505 m. Figure 7.5.C shows the results. The match is good and the critical time (92 min) is less than the lower limit you prescribed (100 min). The aquifer properties obtained from the analysis are now almost identical to those used to calculate the theoretical drawdowns.

So, with SATEM, the thickness of the aquifer can also be determined by trial and error. This was not mentioned in the procedure discussed in Chapter 4, Section 4 because of the very time-consuming manual calculations entailed.

## 7.4 Using Theis's recovery method

This method of analysis is based on the procedure described in Chapter 4, Section 5. The fictitious data set used here consists of residual-drawdown data during recovery of an observation well 100 m from the pumped well. These residual drawdowns, calculated using the aquifer properties  $KH = 200 \text{ m}^2/\text{d}$  and  $S = 0.0001$ , are stored in the 'Residual' file. Select Analysis from the main menu bar of SATEM. Make sure that in the Window Open dialogue box the file type is *Time-residual-drawdown*. Select the file 'Residual' from the list of existing files and select *Theis's recovery method* in the method selection form.

The first screen shows you a semi-log plot of the residual-drawdown data versus the time ratio  $t/t'$  of the observation well at  $r = 100 \text{ m}$  distance. According to the Theis recovery method, the late-time residual-drawdown data exhibit a sloping straight line. Note that late times in this respect mean small time ratios. On the basis of visual inspection, the range of time ratio for which the data plot exhibits a straight-line segment must be prescribed. As initial estimate for the lower limit SATEM shows the time ratio that the last observation was made, and for the upper limit it uses the time ratio that the first observation was made. Let's suppose you change the upper time-ratio limit from 791 to 10 min. SATEM calculates the straight-line segment using linear regression and takes into account only the drawdown data within the prescribed time range. This straight-line segment is now displayed to show you how it is located with respect to your data points. You can see that the extended straight-line intersects the time ratio axis at  $t/t' = 1$ . This implies that the storativity values during pumping and recovery are the same. Your choice is now to change the time range, if you are not satisfied, or to continue. Let's suppose you continue by pressing <Enter>. Next, you are asked to enter the value of the storativity as obtained from the analysis of the time-drawdown data from the preceding pumping test. Change it to 0.0001.

SATEM now calculates the aquifer properties according to the position of the straight-line segment selected. The transmissivity is calculated according to Equation 4.35 and the storativity according to Equation 4.36. In addition, SATEM calculates the time ratio for which the  $u'$  value is 0.1, substituting the

### Time-ratio-recovery graph of well (r = 100 m)

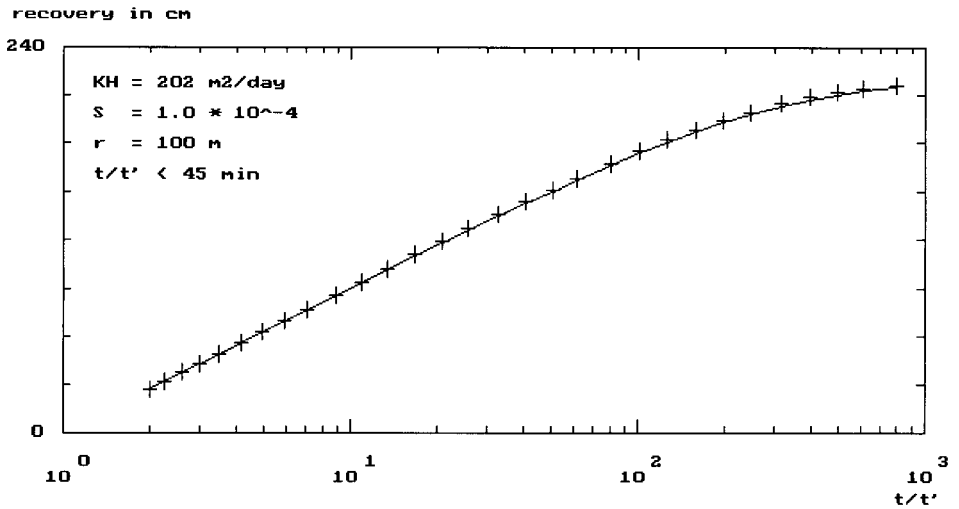


Figure 7.6 Match of residual-drawdown data with theoretical curve

appropriate values into Equation 4.34. These values are displayed on the second screen, together with a line representing the calculated drawdowns (Figure 7.6). SATEM calculates these drawdowns according to Equations 4.30 to 4.32. Once again you have the choice of continuing or going back. The match is good and the critical time ratio (45 min) is above the upper time ratio you prescribed (10 min). The aquifer properties obtained from the analysis are now almost identical to those used to calculate the theoretical drawdowns.

Note that if you do not have an estimate of the storativity obtained from the analysis of the time-drawdown data of the preceding pumping test you cannot use this method to obtain a value for the storativity from the analysis of the time and residual drawdown data. If you enter an arbitrary value for the former, you will also get an arbitrary value for the latter.

## 7.5 Applicability of time-drawdown methods

In the previous sections, fictitious data sets were used to demonstrate the basics of the various analysis procedures of SATEM. For each of the three time-drawdown analysis methods, sets of fictitious data files will be used below, to acquaint you with their procedures and to show you their applicability for obtaining reliable results from the analyses. In all the data files, the discharge rate from the pumped well is taken as 1000 m<sup>3</sup>/d and the data are stored in the folder c:\Satem50\features.

To obtain more data sets of values other than those we used, make them yourself using the auxiliary program SDG (Synthetic Data Generator). It is

stored on your computer in the same folder as SATEM. To start the program, type SDG and press <Enter>. The data entry procedure is the same as for SATEM.

### 7.5.1 Theis-Jacob's method

You can only apply the Theis-Jacob method if the time-drawdown plot exhibits a sloping straight line. When a fully penetrating well pumps a confined aquifer at a constant discharge rate, the time-drawdown plot starts with a curved line followed by a straight line under a slope. This straight line under a slope will continue infinitely in time, because it is assumed that no recharge will take place, i.e. the discharge from the pumped well is exclusively from the release of groundwater storage. The straight line starts approximately at  $1/u = 10$  for the Theis well function (see Figure 4.1). The corresponding time in a time-drawdown plot is related to the aquifer properties and the distance of the piezometer from the pumped well as follows (after rearranging Equation 4.2)

$$\frac{1}{u} = 10 = \frac{4KHt}{r^2S} \rightarrow t = \frac{2.5r^2S}{KH}$$

The  $t$  value thus varies with the distance of a piezometer from the pumped well and with the ratio of storativity to transmissivity. So, the greater the distance of the piezometer and/or the larger the ratio of aquifer properties, the later in time the straight line will develop in a time-drawdown plot. This phenomenon is illustrated with the following fictitious data.

For the properties of a confined aquifer, values of 100 and 1000  $m^2/d$  are used for the transmissivity, and of  $10^{-4}$  and  $10^{-3}$  for the storativity (see Chapter 2, Sections 6.3 and 6.4). For the piezometers, distances of 10 and 100 m from the pumped well are used (see Chapter 3, Section 1). The pumping period is taken as one day (see Chapter 3, Section 3). These parameters have

Table 7.1 Fictitious data files for a confined aquifer

File name	Distance from pumped well (m)	Aquifer transmissivity ( $m^2/d$ )	Aquifer storativity (-)	Values of $r^2S/KH$ (d)
Conf1	10	1000	$10^{-4}$	$10^{-5}$
Conf2	10	1000	$10^{-3}$	$10^{-4}$
Conf3	10	100	$10^{-4}$	$10^{-4}$
Conf4	10	100	$10^{-3}$	$10^{-3}$
Conf5	100	1000	$10^{-4}$	$10^{-3}$
Conf6	100	1000	$10^{-3}$	$10^{-2}$
Conf7	100	100	$10^{-4}$	$10^{-2}$
Conf8	100	100	$10^{-3}$	$10^{-1}$

been combined in eight sets of data files. Table 7.1 presents the data files for increasing values of  $r^2S/KH$ . When analysing the data of these files with SATEM you will observe the following features:

- For relatively small values of  $r^2S/KH$  (see time-drawdown plots of files 'Conf1' to 'Conf4'), the time-drawdown plots exhibit a straight line, but not the preceding curved line. It is unimportant whether this curved line is present, because the Theis-Jacob method is based solely on the presence of the sloping straight line.
- The preceding curved line becomes increasingly visible in the time-drawdown plots for increasing values of  $r^2S/KH$ . As a result, the part of the drawdown data showing a sloping straight line becomes shorter over time, as the pumping time was fixed to one day (see time-drawdown plots of files 'Conf5' to 'Conf8').
- For all eight data sets, the analysis results from SATEM give more or less the same values for transmissivity and storativity as were used as input values to SDG. The difference in storativity values is greater than that in transmissivity values; this phenomenon is implicit to the analysis procedure.
- For all eight data sets, the matches between calculated and observed drawdown values are good, except for the data set of file 'Conf8'.

From this, you can conclude that an analysis of time-drawdown data of a confined aquifer with the Theis-Jacob method is usually possible and accurate with a pumping time of one day and using piezometers at a distance ranging from 10 to 100 m from the pumped well. Only for a relatively large ratio of storativity to transmissivity may it be necessary to pump longer than one day to have a better match and thus more representative values for the aquifer properties. In other words, using SDG and SATEM, you have verified the statements we made in Chapter 3, Sections 1 and 3.

You may also apply the Theis-Jacob method to unconfined aquifers, as was discussed in Chapter 4, Section 3. For the aquifer properties, values of 100 and 1000  $m^2/d$  are again used for the transmissivity, but for the specific yield, values of  $10^{-2}$  and  $10^{-1}$  are now used (see Chapter 2, Sections 6.3 and 6.5). Values for the specific yield (unconfined aquifer) are two orders of magnitude greater than those of the storativity (confined aquifers). For the piezometers, distances of 10 and 30 m from the pumped well are used (see Chapter 3, Section 1). The pumping period is taken as three days (see Chapter 3, Section 3). These parameters have been combined in eight sets of data files. Table 7.2 presents the data files for increasing values of  $r^2S/KH$ .

When analysing the data of these files with SATEM you will observe the following features:

- For relatively small values of  $r^2S/KH$  (see time-drawdown plot of file 'Unconf1'), the time-drawdown plots exhibit a straight line, but not the preceding curved line. It is unimportant whether this curved line is present,

Table 7.2 Fictitious data files for an unconfined aquifer

File name	Distance from pumped well (m)	Aquifer transmissivity (m <sup>2</sup> /d)	Aquifer storativity (-)	Values of r <sup>2</sup> S/KH (d)
Unconf1	10	1000	10 <sup>-2</sup>	1 × 10 <sup>-3</sup>
Unconf2	30	1000	10 <sup>-2</sup>	9 × 10 <sup>-3</sup>
Unconf3	10	1000	10 <sup>-1</sup>	1 × 10 <sup>-2</sup>
Unconf4	10	100	10 <sup>-2</sup>	1 × 10 <sup>-2</sup>
Unconf5	30	1000	10 <sup>-1</sup>	9 × 10 <sup>-2</sup>
Unconf6	30	100	10 <sup>-2</sup>	9 × 10 <sup>-2</sup>
Unconf7	10	100	10 <sup>-1</sup>	1 × 10 <sup>-1</sup>
Unconf8	30	100	10 <sup>-1</sup>	9 × 10 <sup>-1</sup>

because the Theis-Jacob method is based solely on the presence of the sloping straight line.

- The preceding curved line becomes increasingly visible in the time-drawdown plots for increasing values of r<sup>2</sup>S/KH. As a result, the part of the drawdown data showing a sloping straight line becomes shorter over time, as the pumping time was fixed at three days (see time-drawdown plots of files 'Unconf2' to 'Unconf8').
- For all eight data sets, the analysis results from SATEM give more or less the same values for transmissivity and specific yield as were used as input values to SDG. The difference in specific yield values is again greater than that in transmissivity values.
- For all eight data sets, the matches between calculated and observed drawdown values are good, except for the data set of file 'Unconf8'.

From this, you can conclude that an analysis of time-drawdown data of an unconfined aquifer with the Theis-Jacob method is usually possible and accurate with a pumping time of three days and using piezometers at a distance ranging from 10 to 30 m from the pumped well. Only for a relatively large ratio of specific yield and transmissivity may it be necessary to pump longer than three days to have a better match and thus more representative values of the aquifer properties.

### 7.5.2 Hantush's inflection-point method

You can apply the Hantush inflection-point method if your time-drawdown plot exhibits both a horizontal straight line indicating steady state conditions, and an inflection point. When a fully penetrating well pumps a leaky aquifer at a constant discharge rate, the time-drawdown plot starts with a curved line, followed by an inflection point, a second curved line, and a horizontal straight line, as was depicted in Figure 4.6. The first part resembles the behaviour of a confined aquifer, but as pumping continues, the recharge from

the aquitard to the aquifer increases in value, resulting in a flattening of the time-drawdown shape. When this recharge finally equals the discharge from the pumped well, steady state is reached, resulting in a horizontal straight line. In the case of leaky aquifers, the shape of the theoretical time-drawdown curve depends not only on the  $1/u$  value, but also on the  $r/L$  value (Equation 4.9). The influence of these values on time-drawdown plots is illustrated with the following fictitious data.

For the aquifer properties, the same values are used as in Table 7.1, whereas for the aquitard properties, values of 500 and 1500 d are used for the hydraulic resistance (see Chapter 2, Section 6.6). For the piezometers, distances of 10 and 100 m from the pumped well are again used. The pumping period is taken as 1 day. These parameters have been combined in eight sets of data files. Table 7.3 presents these data files in two sets of increasing values of  $r^2 S/KH$  for different values of aquitard hydraulic resistance.

When analysing the data of these files with SATEM you will observe the following features:

- For a relatively low value of the hydraulic resistance (see time-drawdown plots of files 'Leaky1' to 'Leaky4'), all the time-drawdown plots exhibit a curved line followed by a horizontal straight line indicating steady state conditions. The location of the inflection point depends on the value of  $r^2 S/KH$ : the higher its value, the later in time it is located. For a low value of  $r^2 S/KH$  (see time-drawdown plot of file 'Leaky1'), the inflection point is located outside the plot. A reliable analysis is still possible if it is assumed that the first recorded data represent the slope of the inflection point located somewhere on the left-hand side of the plot.
- For a relatively high value of the hydraulic resistance (see time-drawdown plots of files 'Leaky5' to 'Leaky8'), all the time-drawdown plots exhibit two curved lines with the inflection point in between, but not a horizontal straight line indicating steady state conditions. Reliable analyses are still possible by estimating the steady-state drawdown in a trial-and-error procedure by matching the observed data on the second curved line with the

Table 7.3 Fictitious data files for a leaky aquifer

File name	Distance from pumped well (m)	Aquifer transmissivity ( $m^2/d$ )	Aquifer storativity (-)	Hydraulic resistance (d)	Values of $r^2 S/KH$	Values of $r/L$
Leaky	10	1000	$10^{-4}$	500	$10^{-5}$	0.01
Leaky2	10	100	$10^{-4}$	500	$10^{-4}$	0.04
Leaky3	100	1000	$10^{-4}$	500	$10^{-3}$	0.14
Leaky4	100	100	$10^{-4}$	500	$10^{-2}$	0.45
Leaky5	10	1000	$10^{-3}$	1500	$10^{-4}$	0.01
Leaky6	10	100	$10^{-3}$	1500	$10^{-3}$	0.03
Leaky7	100	1000	$10^{-3}$	1500	$10^{-2}$	0.08
Leaky8	100	100	$10^{-3}$	1500	$10^{-1}$	0.26

theoretical curve. Note that the resulting value of the hydraulic resistance is sensitive to the extrapolated value of the steady-state drawdown you select in the trial-and-error procedure.

- For all eight data sets, the analysis results from SATEM give more or less the same values for transmissivity, storativity, and hydraulic resistance as were used as input values to SDG. The difference in hydraulic resistance values is greater than the difference in storativity values which, in turn, is greater than that in transmissivity values; this phenomenon is implicit to the analysis procedure.
- For all eight data sets, the matches between calculated and observed drawdown values are good.

From this, you can conclude that an analysis of time-drawdown data of a leaky aquifer with the Hantush inflection-point method is usually possible and accurate with a pumping time of one day and using piezometers in the range from 10 to 100 m from the pumped well. Only for a high value of the hydraulic resistance may it be necessary to pump longer than one day to have steady-state drawdowns in the time-drawdown plot.

### 7.5.3 Jacob-Hantush's method

You can apply the Jacob-Hantush method if your time-drawdown plot exhibits both the second curved-line segment and the straight line under a slope. When a partially penetrating well pumps a confined or unconfined aquifer at a constant discharge rate, the time-drawdown plot starts with two curved-line segments with an inflection point in between and followed by a straight line under a slope, as was depicted in Figure 4.12. This straight line under a slope will continue infinitely in time, because it is assumed that no recharge will take place, i.e. the discharge from the pumped well is exclusively from the release of groundwater storage. The shape of the theoretical time-drawdown curve depends not only on the  $1/u$  value, but also on the value of the component  $f_s$ . For given penetration ratios of the pumped well and the piezometer,  $f_s$  only varies with the distance of the piezometer from the pumped well, as you can see from Equations 4.24 or 4.25. It can be shown that for piezometers at increasing distances from the pumped well the value of  $f_s$  decreases, resulting in a straight-line segment running parallel to the one depicted in Figure 4.12, but at a lower position. With distances in the order of magnitude of the aquifer thickness, the inflection point can no longer be determined on the basis of visual inspection. For even greater distances, the value of  $f_s$  approaches zero, resulting in a time-drawdown plot of a fully penetrating well like that depicted in Figure 4.1.

The influence of  $1/u$  and  $f_s$  values on time-drawdown plots is illustrated with the following fictitious data. For the properties of an unconfined aquifer,

Table 7.4 Fictitious data files for an unconfined aquifer (partial penetration)

File name	Distance from pumped well (m)	Aquifer transmissivity ( $m^2/d$ )	Aquifer storativity (-)	Aquifer thickness (m)	Values of $r^2S/KH$ (d)
Partpen1	3	100	$10^{-2}$	100	$9.0 \times 10^{-4}$
Partpen2	10	100	$10^{-2}$	100	$1.0 \times 10^{-2}$
Partpen3	30	100	$10^{-2}$	100	$9.0 \times 10^{-2}$
Partpen4	50	100	$10^{-2}$	100	$2.5 \times 10^{-1}$

a value of  $100 m^2/d$  is used for the transmissivity, a value of  $10^{-2}$  for the specific yield, and 100 m for the aquifer thickness. For the piezometers, distances of 3, 10, 30, and 50 m from the pumped well are used. The pumped well and the piezometer both penetrated the aquifer for the first 30 m; the former was fully screened and the latter not screened. The pumping period is taken as three days. In other words, all the parameters are constant, except the distance of the piezometer. Table 7.4 presents the four data files for increasing distances, i.e. increasing values of  $r^2S/KH$ .

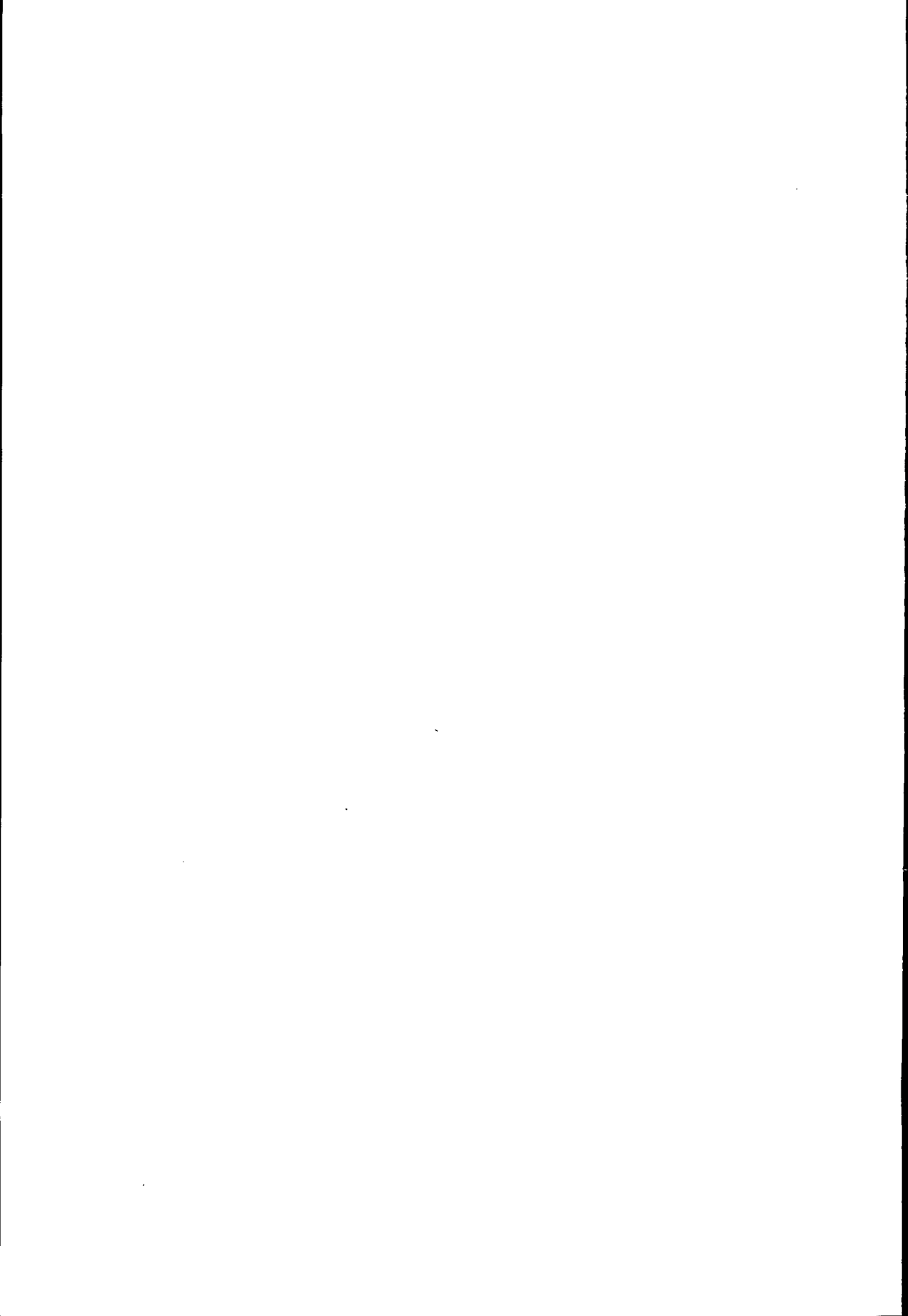
When analysing the data of these files with SATEM you will observe the following features:

- For a relatively small value of  $r^2S/KH$  (see time-drawdown plot of file 'Partpen1'), the time-drawdown plot exhibits the second curved-line segment followed by a straight-line segment under a slope. The aquifer thickness is estimated in a trial-and-error procedure, by matching the observed data located on the preceding curved line with the theoretical curve. It is important that this curved line is present, because the resulting value of the specific yield is sensitive to the value of the aquifer thickness selected in the trial-and-error procedure.
- For a larger value of  $r^2S/KH$  (see time-drawdown plot of file 'Partpen2'), the time-drawdown plot also exhibits the first curved-line segment and the inflection point in the plot. The time-drawdown plot now exhibits the typical shape depicted in Figure 4.12.
- For even larger values of  $r^2S/KH$  (see time-drawdown plots of files 'Partpen3' and 'Partpen4'), the time-drawdown plots still exhibit this typical shape, but the effect of partial penetration diminishes (value of  $f_s$  decreases).
- For all four data sets, the analysis results from SATEM give more or less the same values for transmissivity, aquifer thickness, and specific yield as were used as input values to SDG. With less pronounced effects of partial penetration it gradually becomes more difficult to assess the aquifer thickness and, with that, the specific yield value.
- For all four data sets, the matches between calculated and observed drawdown values are good, except for the data set of 'Partpen4'.

From this, you can conclude that an analysis of time-drawdown data of an



unconfined aquifer with the Jacob-Hantush method is only possible and accurate if the effect of partial penetration is clearly visible in the time-drawdown plot. This will only occur for a limited range of distances for piezometers fairly close to the pumped well.



## 8 Time-drawdown analyses

One of the most important steps in the time-drawdown analysis of aquifer test data is to identify the method most appropriate for your data. To be able to do this, the geology of the test site must be properly known. Well logs may indicate which type of aquifer you are dealing with, i.e. whether it can be regarded as confined, leaky, or unconfined. You may obtain similar information from the results of aquifer tests conducted previously in the same region. Usually, you also have some indication of whether your pumped well can be regarded as a fully penetrating or partially penetrating well. In addition, you can also use the specific features of the diagnostic plots to identify the method most suitable for your data (see Chapter 7).

Below, field data will be used to show how data on time and drawdown and on time and residual drawdown can be analysed with SATEM's time-drawdown/recovery analysis methods. When the pumped well fully penetrates the tested aquifer, the Theis-Jacob method can be applied in the case of confined and unconfined aquifers, while the Hantush inflection-point method can be applied in the case of leaky aquifers. If the pumped well only partially penetrates the tested aquifer, the Jacob-Hantush method can be applied in the case of confined and unconfined aquifers. Finally, if the drawdown has also been observed during the recovery period, Theis's recovery method can be applied in the case of confined and unconfined aquifers and, in certain cases, also in the case of leaky aquifers. An overview of the main features of these four methods was presented in Table 6.2.

### 8.1 Using Theis-Jacob's method

The way the Theis-Jacob method for aquifer tests in confined aquifers is used in SATEM will be illustrated using the time-drawdown data in Kruseman and de Ridder (1990). These data are stored in the 'Korendyk' file. Select Analysis from the main menu bar of SATEM. Make sure that in the Window Open dialogue box the folder is c:\Satem50\ilripu57 and the file type is *Time-drawdown/recovery*. Select the file 'Korendyk' from the list of existing files and select *Theis-Jacob's method* in the method selection form.

The first screen shows you the time-drawdown plot of the first piezometer 30 m from the pumped well. The initial time limits selected for the straight-line segment were 1 and 10 min. The second screen (Figure 8.1) shows that only the observed drawdown data up to 10 min can be matched with the theoretical drawdown data based on the displayed aquifer properties, but that the late-time drawdowns deviate from the theoretical values. In the plot of Figure 8.1, the  $t$  value gives you information on which data points may be

Time-drawdown graph of well ( $r = 30 \text{ m}$ )

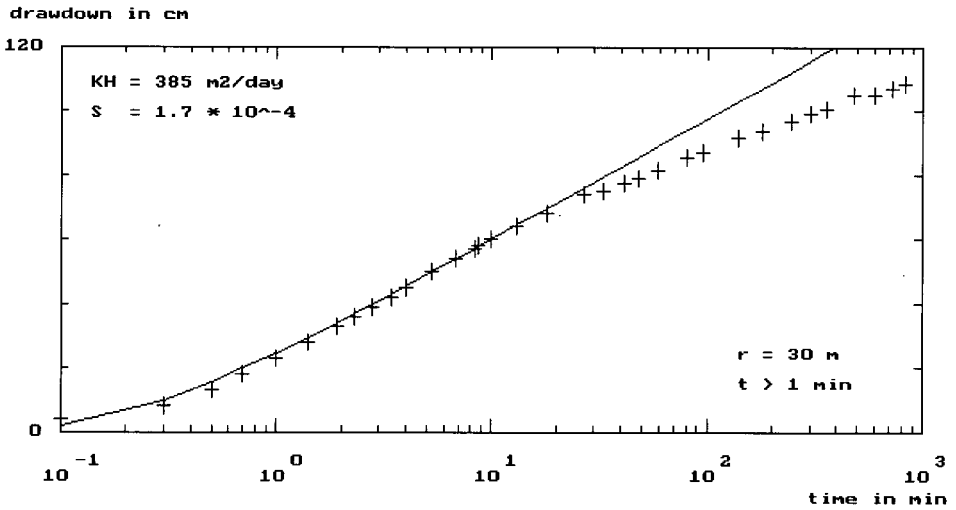


Figure 8.1 Time-drawdown analysis of the drawdown data for the piezometer at distance 30 m

used for the analysis. Interpret this value as follows: for all  $t$  values greater than 1 min the corresponding  $1/u$  values are greater than 10 (Equation 4.2). The lower time limit selected for delineating the straight-line segment was taken as 1 min, so the condition that  $1/u$  should be larger than 10 has been met for all the data points in the selected time range.

The second screen gives you the information you need for deciding whether you are satisfied with your analysis (yes or no). Since the match is not satisfactory, press 'N' and prescribe the time limits of 10 to 830 min for the straight-line segment. The analysis now results in a transmissivity of 580  $\text{m}^2/\text{d}$  and a storativity of  $3.2 \times 10^{-5}$ . You will see that the match between observed and calculated drawdowns is now good for the late-time drawdown data, but that the early-time drawdowns deviate from the theoretical ones. In other words, no match can be found for the whole range of time-drawdown data. A distance-drawdown analysis was also performed for the same test site (see Chapter 9, Section 1). Its results indicate that the values of the aquifer properties based on the first selected time range for the straight-line segment (1-10 min) are closer to the results of the distance-drawdown analysis. Therefore, the values depicted in Figure 8.1 are adopted as final values for this time-drawdown analysis.

*Aquifer test in unconfined aquifer*

The way the Theis-Jacob method for unconfined aquifers is used in SATEM will be illustrated using time-drawdown data from an aquifer test conducted in the eastern part of The Netherlands. Here, the Miocene clay is overlain by sandy deposits constituting an unconfined aquifer only about 6.5 m thick. The

well was pumped at a constant rate of  $167 \text{ m}^3/\text{d}$  for 520 min. The water table was observed in ten piezometers at distances ranging from 2 to 60 m from the pumped well. These data are stored in the 'Eiber' file. Select this file from the list of existing files and select again *Theis-Jacob's method* in the method selection form.

Repeatedly pressing <Enter> calls up the time-drawdown graphs of the various wells one by one on your screen, together with the selections already made. Figure 8.2 shows the second screen with the analysis results for the first piezometer 2 m from the pumped well. Note that the displayed drawdown values have already been corrected by SATEM (Equation 4.18). The time limits selected for the straight-line segment were 30 and 520 min. This figure shows that for most of the data points the match between observed and calculated drawdowns is rather good, except for the early drawdowns. You will usually encounter this phenomenon when analysing time-drawdown data from an unconfined aquifer showing delayed yield. As discussed in Chapter 4, Section 3, when analysing the data from an unconfined aquifer with delayed yield the Theis-Jacob method can either be applied to the early-time drawdown data (left-hand side of Figure 4.10) or to the late-time drawdown data (right-hand side of Figure 4.10). The data points in Figure 8.2 correspond to the right-hand side of Figure 4.10. So, when judging the match between observed and theoretical drawdown data you need to discard the early-time drawdown data.

For the piezometers at distances of 4, 6, and 8 m from the pumped well, time limits for delineating the straight-line segment were taken as 30 and 520 min. For the other piezometers the time limits were taken as 100 and 520 min.

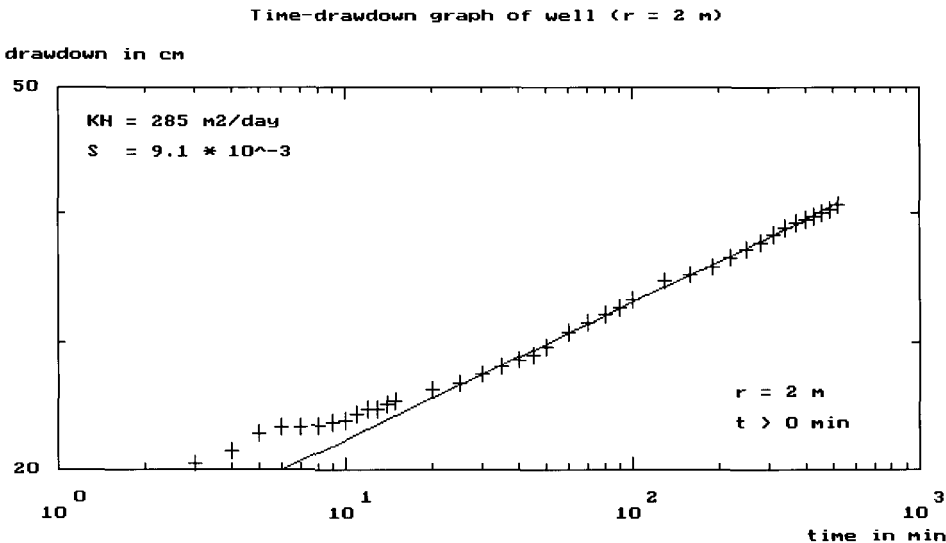


Figure 8.2 Time-drawdown analysis of the drawdown data for the piezometer at distance 2 m

Table 8.1 Hydraulic properties of the unconfined aquifer at Eiber, calculated with the Theis-Jacob method

Distance to pumped well (m)	Transmissivity (m <sup>2</sup> /d)	Storativity (-)
2	285	$9.1 \times 10^{-3}$
4	265	$3.7 \times 10^{-2}$
6	261	$4.1 \times 10^{-2}$
8	281	$2.8 \times 10^{-2}$
10	275	$3.2 \times 10^{-2}$
12	300	$2.2 \times 10^{-2}$
16	329	$1.9 \times 10^{-2}$
20	367	$2.0 \times 10^{-2}$
40	628	$2.5 \times 10^{-2}$
60	779	$5.0 \times 10^{-2}$

min, except for the piezometer 60 m from the pumped well, where 300 and 520 min were selected.

The third and last screen gives you an overview of the results of your analysis obtained from the time-drawdown data of the various piezometers. Table 8.1 shows that the first six time-drawdown analyses produced reasonably consistent results for the aquifer transmissivity. This value starts to increase steadily when the analyses of the piezometers at greater distances are considered. This phenomenon can be explained as follows. For time-drawdown data of piezometers at increasing distances from the pumped wells, it will take longer to meet the limiting condition that  $1/u$  is sufficiently large. This is reflected in the various  $t$  values as displayed in the second screens of this test. For the analyses of the piezometers up to a distance of 20 m, the displayed  $t$  values are lower than the lower time limits selected for delineating the straight-line segments. For the last two piezometers, they were actually higher than the selected lower limits. So you should give less weight to the analysis results of the piezometers at greater distances. Using the criterion that  $1/u$  should be larger than 10, you should discard the analysis results from the last two piezometers.

A distance-drawdown analysis was performed for the same test site. In that test, too, the data from the piezometers at distances of 40 and 60 m were discarded from the analysis because they deviated from the distance-drawdown behaviour of the other piezometers (see Chapter 9, Section 1).

#### *Single-well test in confined aquifer*

The way the Theis-Jacob method for single-well tests in confined aquifers is used in SATEM will be illustrated using the time-drawdown data in Kruseman and de Ridder (1990). These data are from the first step of a step-drawdown test (see Chapter 10, Section 1) and are stored in the 'Clark' file. Select this file from the list of existing files and select once more *Theis-Jacob's method* in the method selection form.

Time-drawdown graph of well ( $r = 0$  m)

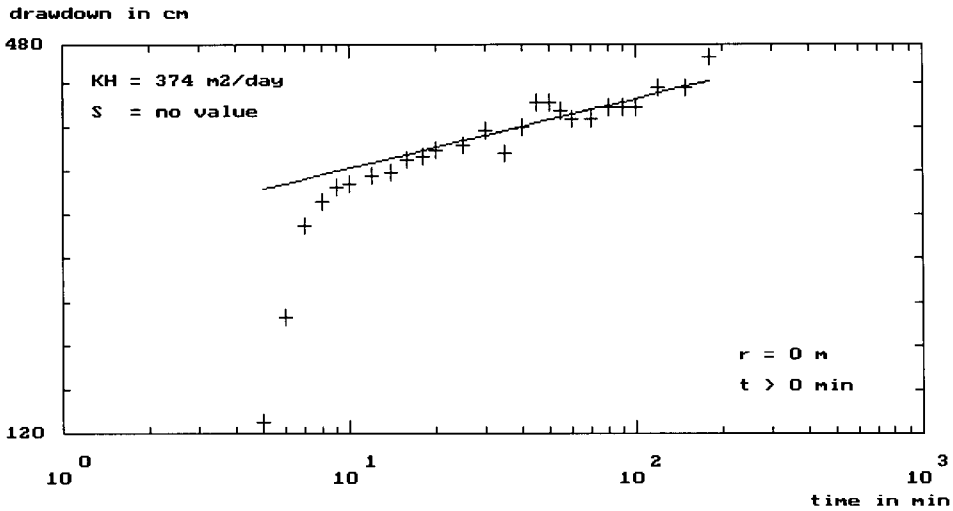


Figure 8.3 Time-drawdown analysis of the drawdown data in the pumped well itself

Repeatedly pressing <Enter> brings up the time-drawdown graph of the pumped well on your screen, together with the selections already made. Figure 8.3 shows the second screen of the analysis results of this single-well test. The time limits selected for the straight-line segment were 20 and 150 min. This figure shows that for most of the data points the match between observed and theoretical drawdowns is rather good, except for the early drawdowns. This is because in the Theis-Jacob method no allowance has been made for well-bore storage. So, when you apply this method to drawdown data of the pumped well, you should discard the early-time drawdown data when judging the match between observed and theoretical drawdown data.

In the case of single-well-test data no estimate of the aquifer storativity is provided, as explained in Chapter 4, Section 6.

## 8.2 Using Hantush's inflection-point method

The way Hantush's inflection-point method for leaky aquifers is used in SATEM will be illustrated using the time-drawdown data in Kruseman and de Ridder (1990). These data are stored in the 'Dalem' file. Select this file from the list of existing files and select *Hantush's inflection-point method* in the method selection form.

The first screen shows you the time-drawdown plot of the first piezometer 30 m from the pumped well. This screen shows you that the drawdown data did not reach a steady state. Most of the drawdown data are actually located on a sloping straight line. Only the last three drawdown data show a tendency

for stabilisation. This means that you need to find the extrapolated steady-state drawdown in a trial-and-error procedure. A value of 25 cm for the extrapolated steady-state drawdown and a time range from 40 to 70 min for the slope of the tangent around the inflection point gave the best match between observed and theoretical drawdowns. Figure 8.4 shows that the observed drawdown data can be matched with the theoretical drawdown data based on the displayed aquifer properties.

Next, SATEM shows you the time-drawdown plot of the second piezometer 60 m from the pumped well, and the procedure described above is repeated. A value of 19 cm for the extrapolated steady-state drawdown and a time range from 30 to 300 min for the slope of the tangent around the inflection point gave the best match between observed and theoretical drawdowns for this second piezometer. SATEM next shows you the time-drawdown plot of the third piezometer 90 m from the pumped well, and the procedure is repeated. A value of 16 cm for the extrapolated steady-state drawdown and a time range from 35 to 300 min for the slope of the tangent around the inflection point gave the best match between observed and theoretical drawdowns for this third piezometer. Finally, SATEM shows you the time-drawdown plot of the fourth piezometer at a distance of 120 m from the pumped well, and the same procedure is repeated as described above. A value of 15 cm for the extrapolated steady-state drawdown and a time range from 36 to 300 min for the slope of the tangent around the inflection point gave the best match between observed and theoretical drawdowns for this fourth and final piezometer.

The third and last screen gives you an overview of the results of your analysis obtained from the time-drawdown data of the various piezometers. Table

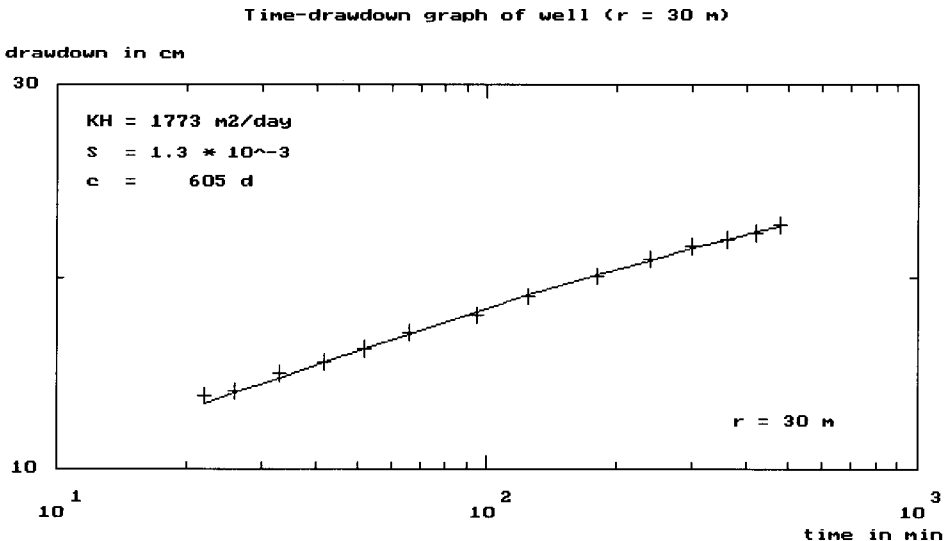


Figure 8.4 Time-drawdown analysis of the drawdown data for the piezometer at distance 30 m



Table 8.2 Hydraulic properties of the leaky aquifer at Dalem, calculated with the Hantush inflection-point method

Distance to pumped well (m)	Transmissivity (m <sup>2</sup> /d)	Storativity (-)	Hydraulic resistance (d)
30	1773	$1.3 \times 10^{-3}$	605
60	1884	$1.9 \times 10^{-3}$	552
90	1731	$1.7 \times 10^{-3}$	353
120	1728	$1.6 \times 10^{-3}$	464

8.2 summarises the results. The four time-drawdown analyses produce reasonably consistent results for the various aquifer properties. The values for aquifer transmissivity are the most consistent, followed by those for aquifer storativity, whereas the values for the hydraulic resistance of the aquitard are the most variable.

The analysis of the above aquifer test data is rather complicated because the pumping time was not sufficiently long, i.e. steady-state conditions did not prevail at the end of the test. Because you had to estimate the extrapolated steady-state drawdowns by trial and error, a straightforward analysis was no longer possible. For instance, a value of 27 cm for the extrapolated steady-state drawdown and a time range from 22 to 70 min for the slope of the tangent around the inflection point also give a good match between observed and theoretical drawdowns of the first piezometer.

When pumping time is sufficiently long, the Hantush inflection-point method can be applied more straightforwardly, as will be shown in Chapter 11, Section 3.

#### *Single-well test in leaky aquifer*

The way the Hantush inflection-point method for single-well tests in leaky aquifers is used in SATEM will be illustrated using time-drawdown data for the pumped well from an aquifer test that will be discussed in detail in Chapter 11, Section 3. They are stored in the 'Kuwpw' file. Select this file from the list of existing files and select again *Hantush's inflection-point method* in the method selection form.

Repeatedly pressing <Enter> brings up the time-drawdown graph of the pumped well on your screen, together with the selections already made. Figure 8.5 shows the second screen of the analysis results of this single-well test. This figure shows that at the end of the pumping time the drawdowns reached a steady state, one of the characteristic features of the time-drawdown behaviour of a pumped leaky aquifer. The steady-state drawdown was selected as 779.2 cm. The corresponding inflection point has a value of 389.6 cm (Equation 4.10). Its value is lower than the first observed drawdown, so this point was not visible in the first screen. Because the early drawdown data will be influenced by well-bore storage, the time limits selected for the straight-line segment were 10 and 100 min. Figure 8.5 shows that for most of the data points the match between observed and theoretical drawdowns is

Time-drawdown graph of well ( $r = 0$  m)

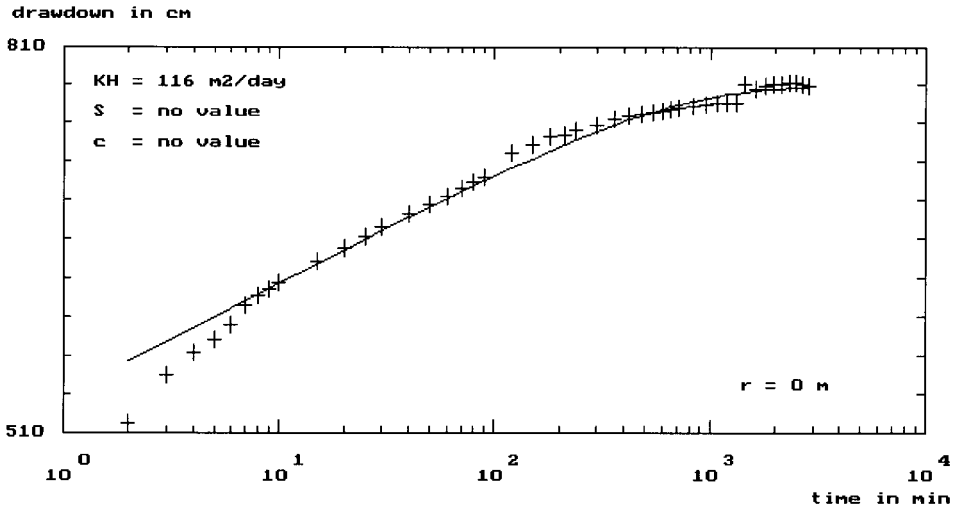


Figure 8.5 Time-drawdown analysis of the drawdown data in the pumped well itself

rather good, except for the early drawdowns. This is because in the Hantush inflection-point method no allowance has been made for well-bore storage. So, when you apply this method to drawdown data for the pumped well, you should discard the early-time drawdown data when judging the match between observed and theoretical drawdown data.

In the case of single-well-test data, no estimates of the aquifer storativity and aquitard hydraulic resistance are provided, as explained in Chapter 4, Section 6.

### 8.3 Using Jacob-Hantush's method

The way the Jacob-Hantush method for partially penetrating wells in unconfined aquifers is used in SATEM will be illustrated using the time-drawdown data in Kruseman and de Ridder (1990). These data are stored in the 'Janpur' file. Select this file from the list of existing files and select *Jacob-Hantush's method* in the method selection form.

The first screen shows you the time-drawdown plot of the first piezometer 15 m from the pumped well. The time limits selected for the straight-line segment were 100 and 1000 min. The second screen asks you to indicate an estimate of the aquifer thickness. In the case of partially-penetrating wells you usually have no information on this aquifer property. In SATEM, however, you will find its value from the analysis itself, by a trial-and-error procedure. So, take 100 m as an initial estimate.

The third screen shows you the values of the aquifer properties, together with a line representing the theoretical drawdowns; these were calculated by

substituting the values of transmissivity and storativity as found from the analysis in Equation 4.19. The match between theoretical and observed drawdowns is influenced by two factors. The time range you selected for delineating the straight line segment influences the match of the late drawdowns, whereas the actual value of the aquifer thickness influences the match with the early drawdowns. So, adopting an arbitrary value for the aquifer thickness in the second screen will usually result in a poor match with the early drawdowns. You therefore need to keep changing the value until you have found the best match. The aquifer thickness is changed as follows: if the early theoretical drawdowns are located above the observed ones, you increase the aquifer thickness value, and vice versa. An aquifer thickness of 512 m gave the best match between observed and theoretical drawdowns during the early stages of pumping. Figure 8.6 shows that except for the last few points, the observed drawdown can be matched with the theoretical drawdown data based on the displayed aquifer properties.

Next, SATEM shows you the time-drawdown plot of the second piezometer 31 m from the pumped well, and the procedure described above is repeated. The time limits selected for the straight-line segment were again 100 and 1000 min, but this time the aquifer thickness of 415 m produced the best match. Finally, SATEM shows you the time-drawdown plot of the third piezometer 92 m from the pumped well, and the procedure is repeated. The time limits selected for the straight-line segment were once again 100 and 1000 min, but now the aquifer thickness of 470 m produced the best match.

The fourth and last screen gives you an overview of the results of your analysis obtained from the time-drawdown data of the various piezometers.

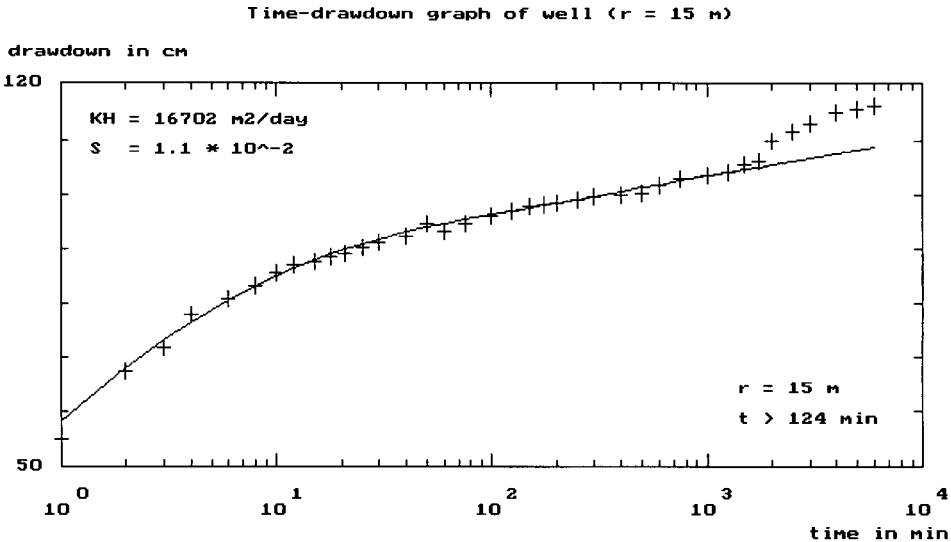


Figure 8.6 Time-drawdown analysis of the drawdown data for the piezometer at distance 15 m

Table 8.3 Hydraulic properties of the unconfined aquifer at Janpur, calculated with the Jacob-Hantush method

Distance to pumped well (m)	Hydraulic conductivity (m/d)	Aquifer thickness (m)	Specific yield (-)
15	32.6	512	$1.1 \times 10^{-2}$
31	34.0	415	$1.5 \times 10^{-2}$
92	35.9	470	$1.8 \times 10^{-2}$

Table 8.3 summarises the results. The values for hydraulic conductivity are the most consistent, followed by those of the aquifer thickness, whereas the values of the specific yield are the most variable.

In Kruseman and de Ridder (1990) the same data were analysed with the Theis-Hantush method; in that method time-drawdown data are plotted on log-log paper and matched with type curves. That analysis yielded basically the same value for the hydraulic conductivity as depicted in Table 8.3, but a very different value for the aquifer thickness: about 1150 m. Boonstra (1992) has shown that using the Theis-Hantush method will lead to a serious overestimate of the thickness of the tested aquifer. This illustrates that many professionals believe that the analysis methods based on semi-log plots are often superior to those based on log-log plots. The only additional requirement for applying the former is that the pumping time should be sufficiently long.

Note that the Jacob-Hantush method is the only method in which the analysis yields separate estimates of the hydraulic conductivity and aquifer thickness; all other analysis methods only yield their algebraic product, being the transmissivity of the tested aquifer.

## 8.4 Using Theis's recovery method

The way the Theis recovery method for confined aquifers is used in SATEM will be illustrated using data on time and residual drawdown from an aquifer test which will be discussed in detail in Chapter 11, Section 2. The data observed in the piezometer 90 m from the pumped well are stored in the 'Umhilrec' file. Select Analysis from the main menu bar of SATEM. Make sure that in the Window Open dialogue box the file type is *Time-residual-drawdown*. Select the file 'Umhilrec' from the list of existing files and select *Theis's recovery method* in the method selection form.

The first screen shows you the plot of time ratio against residual drawdown for the piezometer 90 m from the pumped well. The time-ratio limits selected for the straight-line segment were 4.7 and 80. Next, you are asked to enter the value of the aquifer storativity as obtained from the analysis of the time-drawdown data of the preceding pumping test. This value has been assessed as  $3.2 \times 10^{-4}$  (see Chapter 11, Section 2).

The second screen (Figure 8.7) shows that only the observed residual-draw-

Time-ratio-recovery graph of well (r = 90 m)

recovery in cm

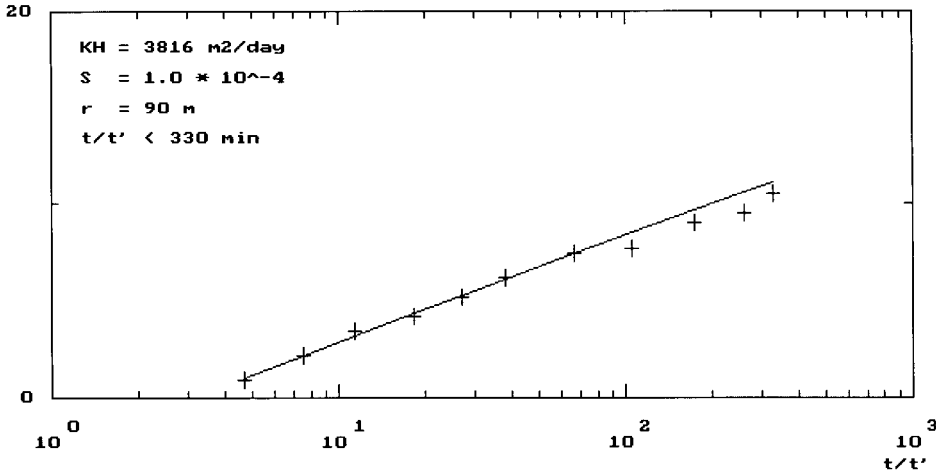


Figure 8.7 Analysis of time ratio versus residual drawdown for the residual drawdown data from the piezometer at distance 90 m

down data up to a  $t/t'$  value of 80 can be matched with the theoretical residual-drawdown data. The  $t/t'$  value shown in this screen is calculated on the basis of Equation 4.34 in which the critical  $u'$  value has been taken as 0.1. You should interpret this value as follows: for all  $t/t'$  values less than 330 the corresponding  $1/u'$  values are greater than 10. The upper time-ratio range selected for delineating the straight-line segment has been taken as 80, so the condition that  $1/u'$  should be larger than 10 has been met for all the data points in the selected time-ratio range.

*Aquifer test in leaky aquifer*

Although the Theis recovery method was developed for confined and unconfined aquifers, it is now applied to a leaky aquifer. For this purpose, data on time and residual drawdown will be used from an aquifer test which will be discussed in detail in Chapter 11, Section 3. The data observed in the piezometer 20 m from the pumped well are stored in the 'Kuwrec' file. Select this file from the list of existing files and select again *Theis's recovery method* in the method selection form.

Repeatedly pressing <Enter> brings up the graph of time ratio plotted against residual drawdown for the piezometer on your screen, together with the selections already made. Figure 8.8 shows the second screen of the analysis results for the piezometer 20 m from the pumped well. The time-ratio limits selected for the straight-line segment were 100 and 1000 and the value of the aquifer storativity as obtained from the analysis of the time-drawdown data of the preceding pumping test has been assessed as  $4.7 \times 10^{-4}$  (See Chapter 11, Section 3). This figure shows that for most of the data points the

Time-ratio-recovery graph of well ( $r = 20$  m)

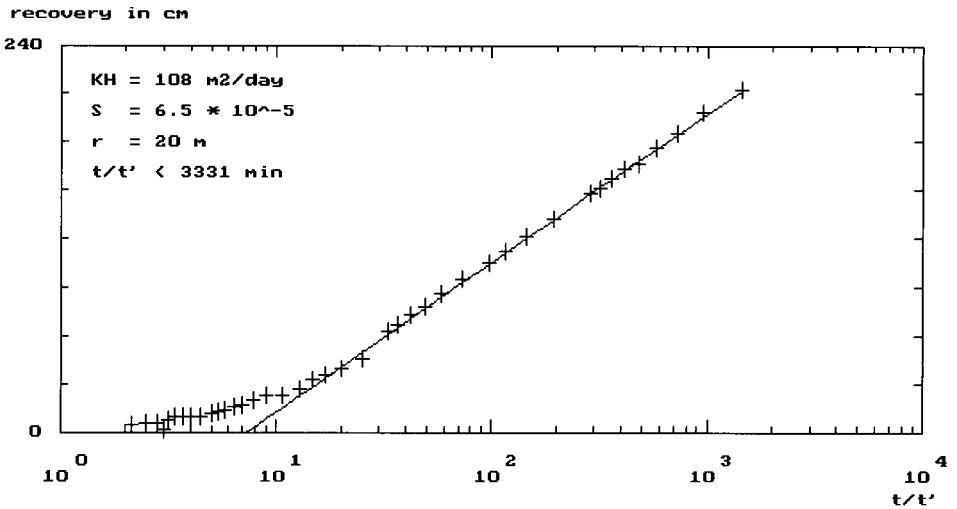


Figure 8.8 Analysis of time ratio versus residual drawdown for the residual drawdown data from the piezometer at distance 20 m

match between observed and theoretical drawdowns is fairly good, except for the residual drawdowns with small  $t/t'$  values. This is because in the Theis recovery method no allowance has been made for the recharge from aquitard to aquifer, ultimately resulting in steady-state conditions for leaky aquifers.

So, when you apply the Theis recovery method to residual-drawdown data of a leaky aquifer, you should discard the late-time residual-drawdown data (i.e. the data with small  $t/t'$  values) when judging the match between observed and theoretical residual-drawdown data. In these cases, the transmissivity will be overestimated (compare Equations 4.4 and 4.12) and the storativity underestimated, because the  $(t/t')_0$  value is greater than one. The Theis recovery method can thus only be used for leaky aquifers if the value of  $r/L$  is small.

## 8.5 Guidelines

For the analysis of time-drawdown data you can use any of the analysis methods presented in the first three sections of this chapter. It is up to you to judge which of these methods gives the most consistent results for your data.

For drawdown data observed in piezometers during the pumping period, the best way is always to start with the Theis-Jacob method. SATEM will show you the specific features of the various time-drawdown plots. These features may help you in selecting the most appropriate method. If the late-time drawdowns form a straight line under a slope, this generally indicates that you are testing a confined or unconfined aquifer, so you may apply the Theis-Jacob method to estimate the aquifer properties. If the late-time drawdowns

form a horizontal straight line (steady-state condition) or show a tendency towards stabilisation, this generally indicates that you are testing a leaky aquifer. To estimate the aquifer properties you should then switch from the Theis-Jacob method to the Hantush inflection-point method. If the observed early-time drawdown data are located below the extended straight-line under a slope, this generally indicates that the pumped well partially penetrates the tested aquifer. To estimate the aquifer properties you should then switch from the Theis-Jacob method to the Jacob-Hantush method.

For residual-drawdown data observed in piezometers during the recovery period, you have only one option: to apply Theis's recovery method. This method was developed for confined and unconfined aquifers. You may also apply it to residual-drawdown data on a leaky aquifer from piezometers relatively close to the pumped well (small  $r/L$  values).

Under field conditions an almost perfect match tends to be the exception rather than the rule. This implies that when the result of an analysis produces a match which is not perfect, this does not automatically mean that the analysis has been performed incorrectly. Remember that all the analysis methods presented in this manual are based on highly simplified representations of the natural aquifer. No real aquifers conform fully to these assumed geological or hydrological conditions. It is actually remarkable that these methods often produce good results.

With this in mind, deviations between theoretical drawdown curves and field data could very well stem from the fact that one or more of the general assumptions and conditions mentioned at the beginning of Chapter 4 is not met in the field. To help you distinguish between these kinds of deviations and deviations which stem from the fact that the selected method is not the correct one for your field data, the most common departures from the theoretical curves are now discussed.

#### *Delayed yield*

In unconfined aquifers there will often be a time lag between the early elastic response of the aquifer and the subsequent fall of the water table due to gravity drainage. In such instances, the general assumption that water removed from storage is discharged instantaneously with decline of head is not met. Figure 8.2 showed the result of an analysis based on field data of a piezometer in an unconfined aquifer, matched with the corresponding theoretical data. For unconfined aquifers showing delayed yield, early time-drawdowns should be discarded when using the Theis-Jacob method in SATEM to judge the goodness of fit between the field data and the theoretical curve.

#### *Well-bore storage*

When, contrary to the assumption in all the methods presented above, the well-bore storage cannot be ignored, the opposite phenomenon takes place.

Usually, this assumption is not violated when dealing with piezometers. When analysing drawdown data from the pumped well itself, well-bore storage may, however, affect the early drawdowns. These early drawdowns then also reflect the withdrawal of water stored in the casing. Figures 8.3 and 8.5 showed the results of an analysis based on field data from the pumped well, matched with the corresponding theoretical data. For the pumped well, the early time-drawdowns should be discarded when judging the goodness of fit between the field data and the theoretical curve using any of the analysis methods presented in the first three sections of this chapter.

#### *Steepening of late-time slope*

All real aquifers are limited by geological or hydrological boundaries. If, however, at the end of the pumping period, no such boundaries have been encountered within the cone of depression, it is said that the aquifer has a seemingly infinite areal extent. When the cone of depression intersects an impervious boundary (e.g. a fault or an impermeable valley wall), it can expand no further in that direction. To maintain the yield of the well the cone must expand and deepen more rapidly at the fault or valley wall.

All the methods presented in this manual also assume that the tested aquifer is homogeneous within the area influenced by the pumping. This condition is never fully met; whether these variations will cause deviations from the theoretical time-drawdown curves depends on the variations in hydraulic conductivity. If the hydraulic conductivity decreases in one direction, the slope of the time-drawdown curve will steepen when the cone of depression spreads into these finer sediments. The typical shape resulting from this phenomenon resembles that of an impervious boundary. Where two wells are close to each other, well interference will bring about a similar phenomenon.

Figure 8.6 showed the results of an analysis based on field data from a piezometer in an unconfined aquifer, matched with the most appropriate Hantush curve for partially penetrating wells. In this case, the late time-drawdowns should be discarded when judging the goodness of fit between the field data and the theoretical curve.

#### *Flattening of late-time slope*

An opposite effect is encountered when the cone of depression intersects an open water body. If the open water body is hydraulically connected to the aquifer, the aquifer recharges at an increasing rate as the cone of depression spreads with time. This results in a flattening of the slope of the time-drawdown curve at later times. The phenomenon resembles the recharge that occurs in a leaky aquifer.

The same phenomenon occurs if hydraulic conductivity and/or aquifer thickness increases in one direction. Figure 8.1 showed the results of an analysis based on field data from a piezometer in a confined aquifer, matched with the corresponding Theis curve. In this case too, the late-time drawdowns



should be discarded when judging the goodness of fit between the field data and the theoretical curve.

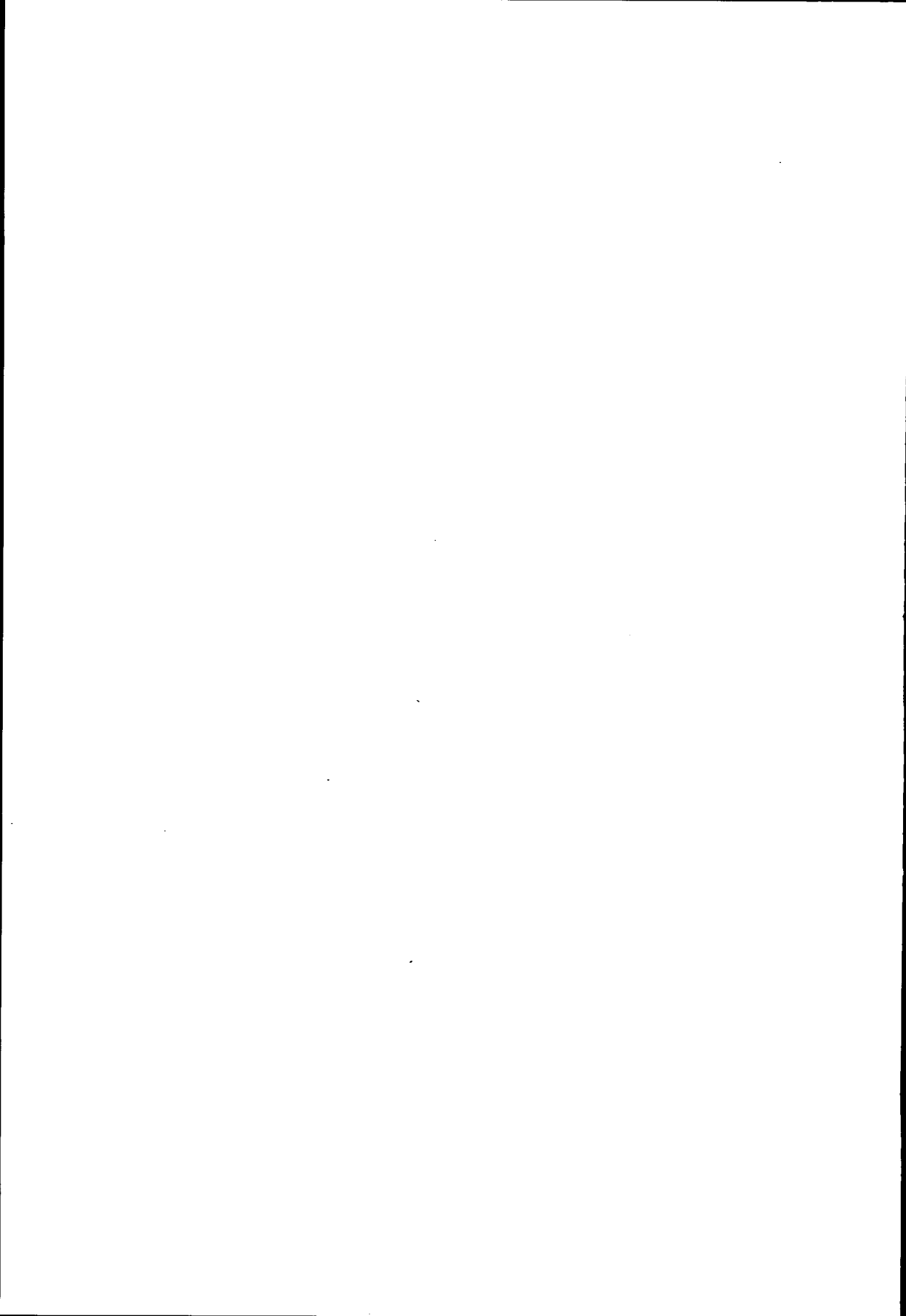
#### *Pumped-well drawdown data*

Due to linear and non-linear well losses, the water levels inside the pumped well itself are generally lower than those directly outside the well screen. This implies that drawdown data from the pumped well cannot be used for analysis unless corrected. Because the slope of the straight-line segment in the time-drawdown data when plotted on semi-log paper is not affected by these well losses, transmissivity values can still be determined accurately by using the uncorrected data. Storativity and hydraulic resistance values, however, are then not correct. This, together with the facts that the effective radius ( $r_w$ ) of the pumped well is difficult to determine under field conditions and that the storativity and hydraulic resistance values are highly sensitive when  $r_w$  is not correctly determined, are the reasons why values of these aquifer properties are not presented in SATEM.

#### *Conclusions*

A number of reasons why time-drawdown data may depart from theoretical curves have been discussed. It will be clear that different phenomena can cause approximately the same anomalies. Without proper knowledge of the geology of the test site a correct analysis is then impossible. But in general it can also be stated that knowledge of the geology of the test site is vital in analysing aquifer test and single-well data. Because this knowledge is often fragmentary, the assessment of the values of the aquifer properties often remains an art. This is one of the main reasons why it is strongly recommended to continue to monitor the water table behaviour during the recovery period. This allows a second estimate of the aquifer's transmissivity to be made, which can then be compared with the one found during the pumping period. Even with single-well tests, this second estimate is possible. With SATEM, even a third estimate of the transmissivity and a second estimate of the specific yield or storativity is then possible. These features will be discussed in detail in Chapter 11, Sections 2 and 3.

Finally, a few remarks on the difference between aquifer tests and single-well tests. The results of aquifer tests are more reliable and more accurate than those of single-well tests. Another advantage is that aquifer tests allow estimates to be made of both the aquifer's transmissivity and its specific yield or storativity, which is not possible with single-well tests. Further, if more than one piezometer is drilled in an aquifer test, separate estimates of the aquifer properties can be made for each piezometer, allowing the various estimates to be compared. Moreover, you can obtain yet another estimate of the aquifer properties by using not only the time-drawdown relationship, but also the distance-drawdown relationships. These features will be discussed in Chapter 11, Section 1.



## 9 Distance-drawdown analyses

Distance-drawdown analyses are performed to obtain independent estimates of the aquifer properties in addition to the estimates obtained from the time-drawdown analyses of each piezometer separately. This allows the consistency of the resulting aquifer properties to be checked.

The analysis of distance-drawdown data uses diagnostic plots called distance-drawdown plots, in which values of the steady-state (or pseudo-steady state) drawdowns observed in at least two piezometers are plotted on semi-log paper. In theory, for all three aquifer systems, such a plot should exhibit a straight-line segment that is the basis for the actual analysis. Because a straight line can be drawn through any two points, a distance-drawdown analysis only makes sense if you have data from more than two piezometers at different distances from the pumped well.

Below, field data will be used to show how distance-drawdown data can be analysed with the Thiem-Jacob method for confined and unconfined aquifers and with the Hantush-Jacob method for leaky aquifers. Both analysis methods require that the pumped well fully penetrates the tested aquifer.

### 9.1 Using Thiem-Jacob's method

The way the Thiem-Jacob method for confined aquifers is used in SATEM will be illustrated using the distance-drawdown data in Kruseman and de Ridder (1990), which are stored in the 'Korendyk' file. Select Analysis from the main menu bar of SATEM. Make sure that in the Window Open dialogue box the folder is c:\Satem50\ilripu57 and the file type is *Distance-drawdown*. Select the file 'Korendyk' from the list of existing files and select *Thiem-Jacob's method* in the method selection form.

The first screen shows you the distance-drawdown plot. According to the Thiem method, these data should exhibit a straight line. On the basis of visual inspection, you now indicate which part of the plotted data exhibit such a straight line. You do this by giving numerical values for the lower and upper distance limits. SATEM then uses linear regression to calculate the best-fitting straight line through the selected points. This straight line is now displayed to show you how it is located with respect to your data points. If you are not satisfied with the match, press 'N' and SATEM again displays the distance-drawdown plot. Note that the lower and upper distance limits displayed are updated each time you change a limit. Distance limits of 0.8 and 90 m have been selected for the straight-line segment.

Once you press <Enter>, SATEM performs the actual analysis. The aquifer properties can be calculated from this straight line: the transmissivity is

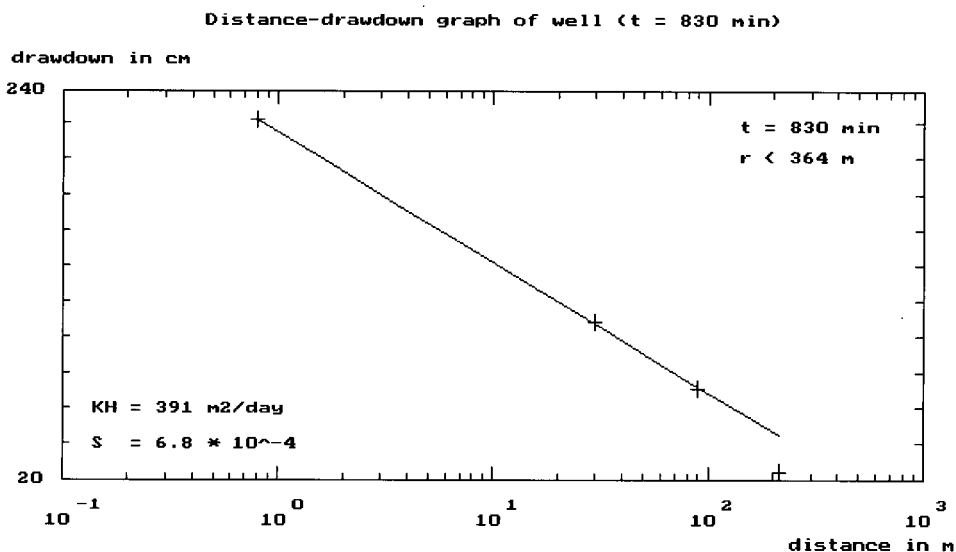


Figure 9.1 Distance-drawdown analysis for a confined aquifer ('Korendijk') using the Thiem-Jacob method

based on its slope and the storativity is based on its intercept with the x-axis ( $s = 0$ ). The former is calculated using the Thiem method (Equation 4.7) and the latter using the Jacob method (Equation 4.8).

The second screen shows you these values, together with a line representing the theoretical drawdowns; these have been calculated by substituting the values for transmissivity and storativity found from the analysis in the Theis equation. Figure 9.1 shows the theoretical drawdowns based on a transmissivity value of  $391 \text{ m}^2/\text{d}$  and a storativity value of  $6.8 \times 10^{-4}$ . In this plot, two more parameters are displayed. The  $t$  value gives you information about which time you have selected the distance drawdown data, whereas the  $r$  value gives you information about which data points may be used for the analysis. As was discussed in Chapter 4, the application of the Thiem-Jacob method is only valid when the  $u$  value is sufficiently small. The  $r$  value shown in this screen has been calculated based on Equation 4.2 in which the transmissivity, storativity and time values have been substituted and where the critical  $u$  value has been taken as 0.1. You should interpret this value as follows: for all  $r$  values less than 364 m the corresponding  $u$  values are smaller than 0.1.

The second screen gives you all the information on which you should decide whether you are satisfied with your analysis (yes or no). If you are not satisfied, press 'N' and SATEM again displays the distance-drawdown plot, where you can select different lower and upper limits and re-analyse your data. Figure 9.1 shows that the observed drawdown data can be matched with the theoretical drawdown data based on the displayed aquifer properties and that the three data points have  $u$  values less than 0.1. If you are satisfied, this implies that you have discarded the drawdown value at the piezometer at a

distance of 215 m from your analysis. To see the results of including this draw-down data in your analysis, go back and prescribe the full range for the straight-line segment. The analysis now results in a transmissivity of 365 m<sup>2</sup>/d and a storativity of  $1.3 \times 10^{-4}$ . You will see that the match between observed and calculated drawdowns is now less good, although the aquifer properties have not changed considerably. It is up to you to decide which of the two analyses produces the most consistent results. Both sets of aquifer properties correspond more or less equally well to the results of the time-drawdown analysis of the first piezometer (see Chapter 8, Section 1).

The third and last screen gives you an overview of the results of your analysis. In the case of confined aquifers, no steady state will ever occur. The concept of pseudo-steady state is used instead. This implies that you can select late distance-drawdown data for various times and compare their results for consistency.

### Unconfined aquifer

The way the Thiem-Jacob method for unconfined aquifers is used in SATEM will be illustrated using the distance-drawdown data in Boonstra and de Ridder (1994). The time-drawdown data of this test were analysed in Chapter 8, Section 1. The corresponding distance-drawdown data are stored in the 'Eiber' file. Select this file from the list of files and select again *Thiem-Jacob's method* in the method selection form.

Figure 9.2 shows the second screen of this analysis. Note that the displayed drawdown values have already been corrected by SATEM (Equation 4.18). Distance limits of 4 and 20 m have been selected for the straight-line segment.

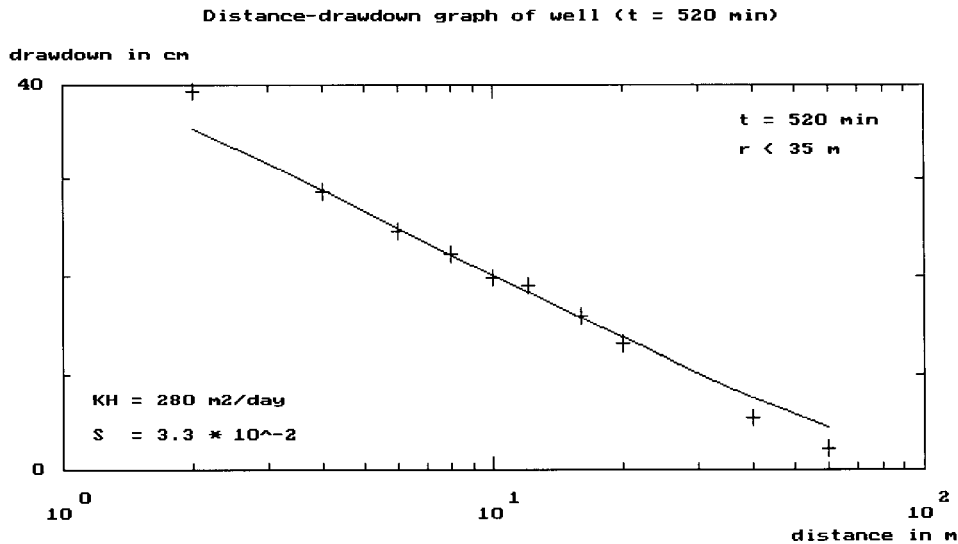


Figure 9.2 Distance-drawdown analysis for an unconfined aquifer ('Eiber') using the Thiem-Jacob method

The figure shows that for most of the data points the match between observed and calculated drawdowns is excellent. The drawdown data from the piezometers at distances of 40 and 60 m have been discarded because their  $u$  values are larger than 0.1 ( $r > 35$  m). The resulting transmissivity and specific yield values correspond very well with those obtained from the time-drawdown analyses of the piezometers separately (Table 8.1). In these tests too, the data from the piezometers at distances of 40 and 60 m have also been discarded from the analysis. It is not known why the drawdown data from the piezometer at 2 m distance deviates from the straight line.

## 9.2 Using Hantush-Jacob's method

The way the Hantush-Jacob method is used in SATEM will be illustrated using the distance-drawdown data in Kruseman and de Ridder (1990), which are stored in the 'Dalem' file. Select this file from the list of existing files and select *Hantush-Jacob's method* in the method selection form.

The first screen shows you the distance-drawdown plot. According to the Hantush-Jacob method, these data should also exhibit a straight line. On the basis of visual inspection, you again indicate which part of the plotted data exhibit such a straight line. SATEM then uses linear regression to calculate the best-fitting straight line through the selected points. The straight line is now displayed to show you how it is located with respect to your data points. The distance limits selected for the straight-line segment are the full range (10 and 400 m). Once you press <Enter>, SATEM performs the actual analysis. The aquifer properties can be calculated from this straight line: the transmissivity is based on its slope and the hydraulic resistance on its intercept with the x-axis ( $s = 0$ ). The former is calculated using Equation 4.16 and the latter using Equation 4.17 and the expression  $c = L^2/KH$ .

The second screen shows you these values, together with a line representing the theoretical drawdowns; these have been calculated by substituting the values of transmissivity and hydraulic resistance as found from the analysis in De Glee's equation (Equation 4.14). Figure 9.3 shows the theoretical drawdowns based on a transmissivity value of 2025 m<sup>2</sup>/d and a hydraulic resistance value of 447 d. In this plot, two more parameters are displayed. The  $t$  value gives you information about the time you have selected the distance drawdown data, whereas the  $r$  value gives you information about which data points may be used for the analysis. As was discussed in Chapter 4, the application of the Hantush-Jacob method is only valid if the  $r/L$  value is sufficiently small. In SATEM,  $r/L = 0.2$  has been adopted as critical threshold value. This means that for this test the  $r$  value should be lower than 190 m. This would imply that the drawdown value of the piezometer at distance 400 m should be eliminated from the analysis. Figure 9.3, however, shows that this point too lies on the straight line, so in this case this condition is not restrictive. This

Distance-drawdown graph of well ( $t = 480 \text{ min}$ )

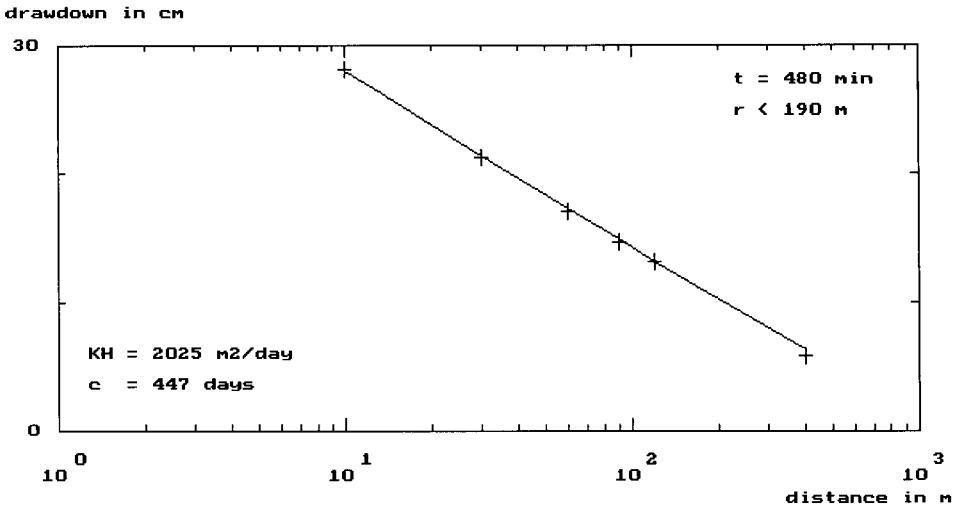


Figure 9.3 Distance-drawdown analysis for a leaky aquifer ('Dalem') using the Hantush-Jacob method

can also be confirmed numerically by going back to the first screen and eliminating this point from the straight-line calculation. The resulting aquifer properties are then  $2017 \text{ m}^2/\text{d}$  for the transmissivity and  $437 \text{ d}$  for the hydraulic resistance, i.e. almost the same values as with the last point included in the analysis.

The third and final screen gives you an overview of the results of your analysis. The above transmissivity and hydraulic resistance values correspond fairly well with those found from the time-drawdown analyses based on the individual piezometers (see Table 8.2).

### 9.3 Guidelines

Which of the two presented distance-drawdown analyses you should select depends upon the results of the time-drawdown analysis you made earlier. If the latter indicate that the tested aquifer can be regarded either as confined or as unconfined, you should select the Thiem-Jacob method. If the results of the time-drawdown analysis indicated a leaky aquifer, you should select the Hantush-Jacob method.

When you analyse distance-drawdown data from a confined or unconfined aquifer with the Hantush-Jacob method, the distance-drawdown analysis will, in any case, yield a hydraulic resistance value for the aquitard. This is inherent to the analysis method itself, but in the case of a confined or unconfined aquifer it has no physical meaning. You can check this for yourself by analysing the Eiber data with the Hantush-Jacob method. The analysis will

again yield a transmissivity value of  $280 \text{ m}^2/\text{d}$ , but the hydraulic resistance value of the aquitard is calculated as 20 d. This is a small value, indicating that the aquitard is virtually absent.

The following consideration is important when selecting data points for the determination of the best fitting straight-line segment. Theoretically, for infinitely long pumping times, the drawdown behaviour of all piezometers will first exhibit unsteady-state conditions, followed by steady-state conditions in leaky aquifers and pseudo-steady-state conditions in confined or unconfined aquifers. Because the pumping period is limited in time, this implies that the drawdown behaviour of piezometers further away from the pumped well may not yet have achieved steady state, even though the piezometers closer to the well have already reached steady (or pseudo-steady) state.

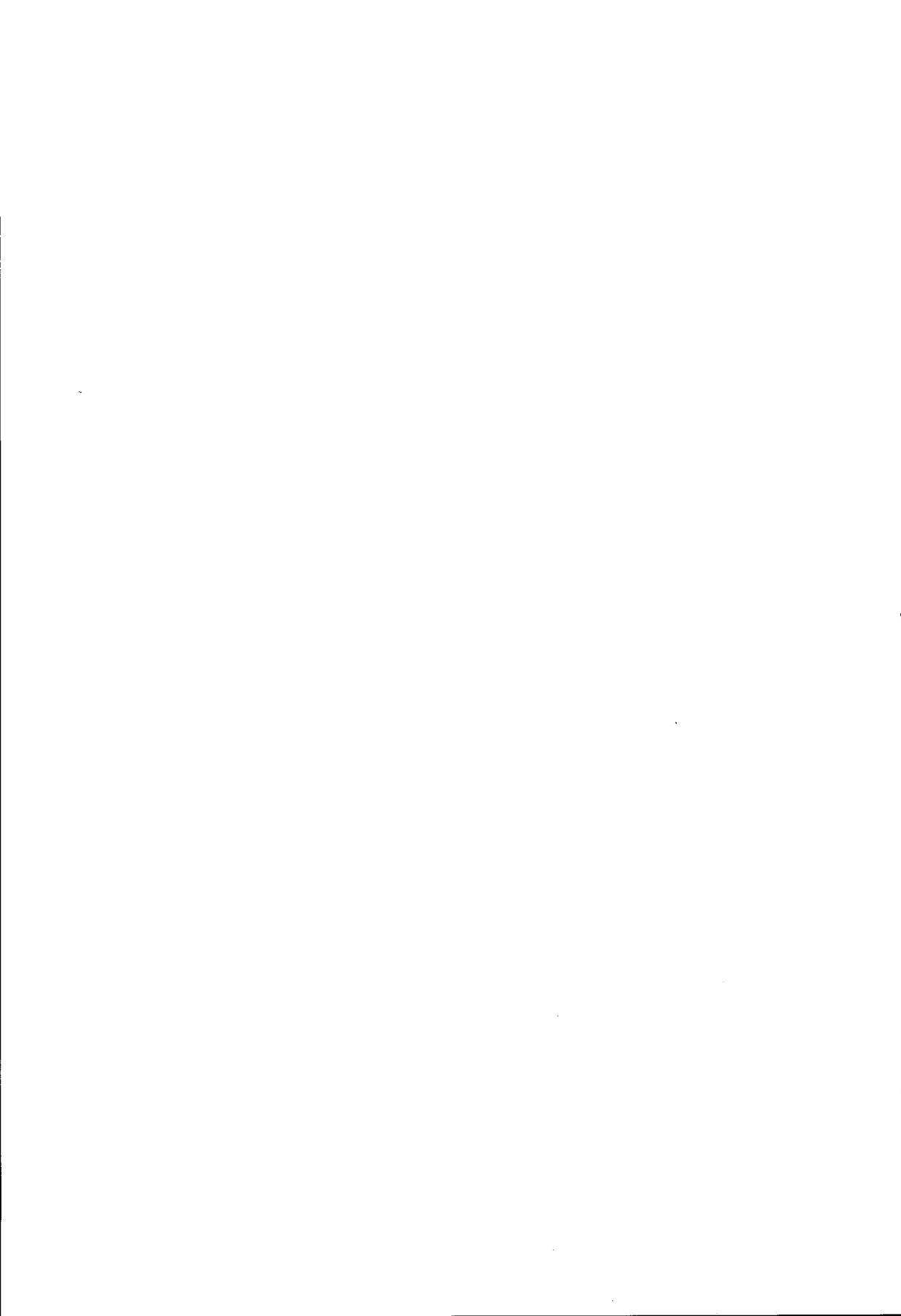
Therefore, as a general rule, you should concentrate on the drawdown data of piezometers at short distances from the pumped well. In SATEM the decision about whether drawdown data from piezometers at relatively large distances should be discarded from your analysis is facilitated by displaying a critical  $r$  value together with the analysis. Note that you should use this information only as an indication. The transition from unsteady state to steady state is gradual, which means that there is no single value for  $u$  (Thiem-Jacob method) or  $r/L$  (Hantush-Jacob method) that you can take as universal threshold value. The decision to discard any drawdown data from your analysis should be based on the match between observed and calculated drawdowns and not primarily on the displayed critical  $r$  value.

If the drawdown in the pumped well itself was also observed during the test, you should not include its data in a distance-drawdown analysis. The reason is that in addition to the laminar aquifer losses, the observed drawdown also includes linear and non-linear well losses. When such a value is plotted together with the drawdown data observed in the piezometers, this results in a drawdown that is too large. In the case of step-drawdown tests (Chapter 5), the non-linear well loss component can be estimated. Even when the observed drawdown in the pumped well has been corrected for this non-linear well loss, due to the linear well loss component its data point may still be located above the straight line as determined from the drawdown data of the piezometers. This, unfortunately, cannot be assessed from step-drawdown analyses.

Finally, you cannot perform distance-drawdown analyses if the pumped well only partially penetrates the tested aquifer. This is because contraction of flow lines towards the well screen causes the observed drawdowns in such tests to exhibit an additional head loss. Because this effect is strongest at the well face, and decreases with increasing distances from the pumped well, a distance-drawdown analysis would yield erroneous results, i.e. the transmissivity value will be lower - sometimes substantially lower - than it should be. You will see this when you analyse the data stored in the Jaipur file. With the Thiem-Jacob method, such an analysis would yield a transmissivity of 2343



$\text{m}^2/\text{d}$  and an unrealistically high specific yield of 55 per cent. Time-drawdown analyses performed for the same test (see Chapter 8, Section 3) yielded a transmissivity value ranging from 14 000 to 17 000  $\text{m}^2/\text{d}$  and a specific yield value of 1 to 2 per cent.



## 10 Step-drawdown analyses

Step-drawdown analyses are done for two reasons. In the case of exploration wells, aquifer tests are commonly preceded by step-drawdown tests to determine the proper discharge rate for the subsequent aquifer test. In the case of exploitation wells, the results of step-drawdown analyses are used to determine the optimum production capacity and to analyse the well performance over time, for the purpose of maintenance and rehabilitation.

The analysis of step-drawdown analyses uses diagnostic plots in which ratios of the steady-state drawdowns at the end of each step and the discharge rate are plotted against the discharge rate on linear paper. According to theory, such a plot should exhibit either a straight or a curved line. When the data points fall on a straight line under a slope, Jacob's method should be applied; in all other cases, Rorabaugh's method is to be used.

Below, field data will be used to show how step-drawdown data can be analysed with SATEM. Both analysis methods may be applied to confined, unconfined, and leaky aquifers.

### 10.1 Using Jacob's method

The way the Jacob method is used in SATEM will be illustrated using the step-drawdown data in Kruseman and de Ridder (1990), which are stored in the 'Clark' file. Select Analysis from the main menu bar of SATEM. Make sure that in the Window Open dialogue box the folder is c:\Satem50\ilripu57 and the file type is *Step-drawdown*. Select the file 'Clark' from the list of existing files and select *Jacob's method* in the method selection form.

The first screen shows you the time-drawdown data plotted in semi-log format during Step 1. This graph shows you that the drawdowns had not yet stabilised at the end of this step, i.e. no steady state developed during Step 1. This implies that the observed drawdown value at the end of Step 2 needs to be corrected. In SATEM, the Hantush-Bierschenk method is used for this purpose (see Chapter 5, Section 3). On the basis of visual inspection you now indicate which part of the late data exhibit a straight line. You can do this by entering numerical values for the lower and upper time limits, after the question marks. SATEM then shows you the best-fitting straight line through the selected points; this is done by linear regression. Next, use the arrow keys to indicate which drawdown will be used for the extrapolation: choose a drawdown value at the end of Step 1 which is on or close to the straight-line segment. Time limits of 10 and 180 min have been selected for the straight-line segment and the drawdown value for 120 min has been taken for extrapolation to Step 2.

This first type of screen is repeated for all subsequent steps. No steady state developed during these steps either. All data in these time-drawdown plots were selected to determine the straight-line segments, except for Step 4 where the lower limit was taken as 2 min. The drawdown value for extrapolation was not changed and remained the one for 120 min. Note that if you change this drawdown value in a particular step, SATEM will adopt the same time value in all other steps as well.

The second type of screen shows you the diagnostic plot; the expression  $s_w/Q$  is known as the specific drawdown. The  $s$  values correspond to the time value you selected for extrapolation in the first type of screen; for Steps 2 to 6 they have been corrected by extending the slope of the straight-line segments through the drawdown values at 120 min for previous steps and subtracting them from the observed values.

Figure 10.1 shows that the six data points lie almost exactly on a sloping straight line. This implies that the Jacob method ( $P = 2$ ) can be used for this step-drawdown test. The straight line was based on the full range of discharge rates; it was determined by SATEM using linear regression. The values of  $B$  and  $C$  can be found directly from this straight line: its slope is equal to  $C$  and its intercept with the  $y$ -axis ( $Q = 0$ ) is equal to  $B$  (see Chapter 5, Section 4).

The third type of screen displays the values of  $B$  and  $C$ . The general drawdown equation for the pumped well has been calculated as

$$s_w = 3.1 \times 10^{-3} Q + 2.0 \times 10^{-7} Q^2 \quad (10.1)$$

This screen also displays a comparison between observed and calculated draw-

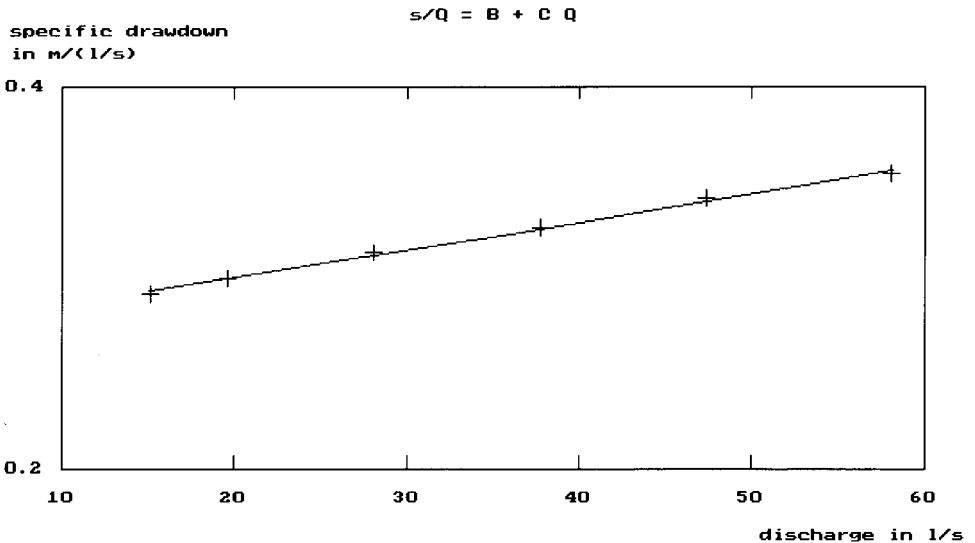


Figure 10.1 Diagnostic plot of step-drawdown data ('Clark') for an application using the Jacob method

Table 10.1 Comparison between corrected and calculated drawdown values, resulting from the 'Clark' step-drawdown analysis using the Jacob method

Discharge rate (m <sup>3</sup> /d)	Corrected drawdown (m)	Calculated drawdown from Equation 10.1 (m)
1306	4.40	4.43
1693	5.87	5.87
2423	8.78	8.75
3261	12.35	12.32
4094	16.19	16.14
5019	20.61	20.70

downs. Keep in mind that SATEM corrected the observed drawdowns for non-steady state at the end of each step. Table 10.1 shows these results. The standard deviation of the differences between corrected and calculated drawdowns has been calculated as 0.06 m. The difference between the means is always equal to zero because the line in Figure 10.1 has been determined by linear regression.

The fourth and last type of screen displays a graph showing the total drawdown in the pumped well plotted against the discharge rate. Figure 10.2 shows this relationship as plotted points; the dashed line represents the drawdown values without the contribution of the non-linear well-loss component ( $s_w = BQ$ ). This figure shows that the non-linear well-loss is negligible up to discharge rates of some 1800 m<sup>3</sup>/d. This implies that for higher discharge rates the well efficiency will start to decrease.

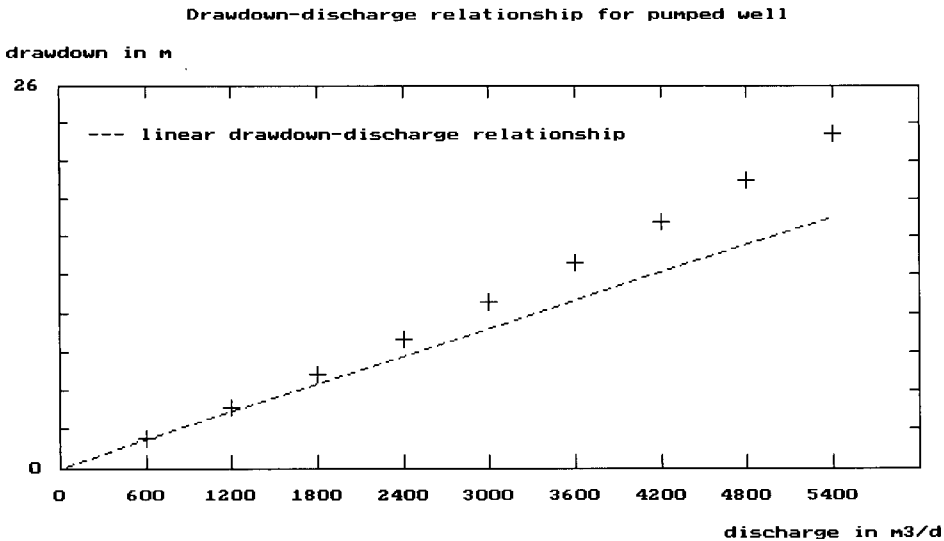


Figure 10.2 Discharge-drawdown relationship of the pumped well ('Clark') using the Jacob method

If you have only drawdown values at the end of each step, i.e. one drawdown value per step, SATEM will skip the first type of screen. With only one drawdown value per step you cannot verify whether the drawdowns did actually stabilise at the end of each step, nor can you make any corrections. To show you the differences between a series of drawdown values per step and only one drawdown value per step, the drawdown values at 180 min of the previous test have been entered in the 'Clarksv' file. If you select this file and select again *Jacob's method* in the method selection form, SATEM shows you the diagnostic plot as the first screen on your screen. You will see that the six data points now deviate more from a straight line than in Figure 10.1. When you again select the full discharge range, the general drawdown equation for the pumped well is now calculated as

$$s_w = 3.4 \times 10^{-3} Q + 2.1 \times 10^{-7} Q^2 \quad (10.2)$$

Equation 10.2 is not very different from Equation 10.1, so the fact that in this test the drawdowns were not in a steady state at the end of each step does not lead to significantly different values for B and C. The standard deviation of the differences between observed and calculated drawdowns has increased from 0.06 to 0.11 m.

Although in this example the value of the parameters did not change much, it is advisable to always use the time-drawdown data during each step. This will enable you to check whether the drawdowns at the end of each step did actually stabilise and, if not, to correct them. Such an approach will generally yield more consistent results and more reliable analyses.

## 10.2 Using Rorabaugh's method

The way the Rorabaugh method is used in SATEM will be illustrated using the step-drawdown in Kruseman and de Ridder (1990), which are stored in the 'Sheahan' file. Select this file from the list of existing files and select *Rorabaugh's method* in the method selection form.

The first screen immediately shows the diagnostic plot, because only one drawdown value per step is available for this test. This implies that you must assume that the observed drawdowns were in a steady state at the end of each step. This screen shows that the four data points are located on a concave line, indicating a P value larger than 2. The values for B, C, and P cannot be found directly from this plot. It can be shown that a plot of  $[s_w/Q - B]$  versus Q on log-log paper yields a straight line under a slope for only one particular value of B (Chapter 5, Section 5).

You need to give an initial B value. Once you have done that, the second screen shows you the corresponding log-log plot of  $[s_w/Q - B]$  versus Q for that B value, together with a straight line which is drawn through the first and last

$$s/Q = B + C Q^{(p-1)}$$

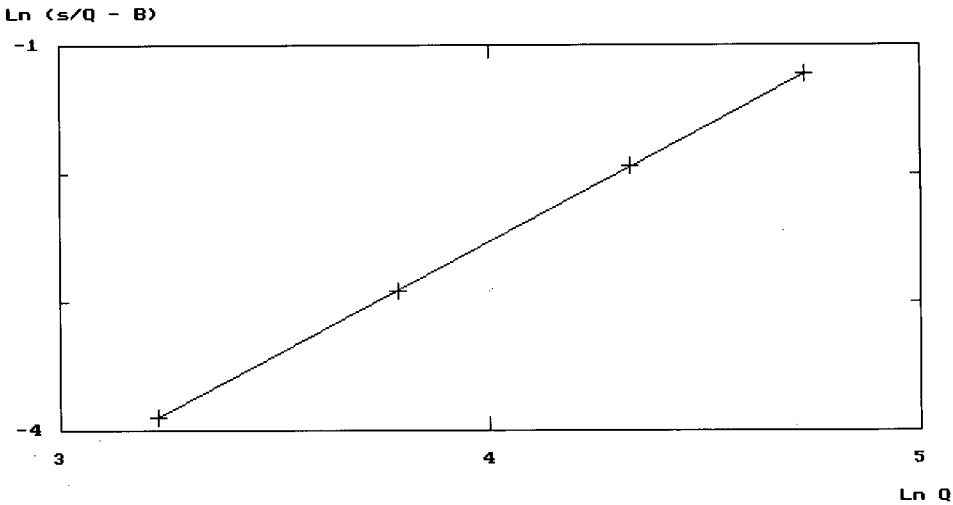


Figure 10.3 Plot of  $s_w/Q-B$  versus  $Q$  for a  $B$  value of 0.0835 ('Sheahan') for an application using the Rorabaugh method

data points. The intermediate points are usually not located on this line, so you need to change the  $B$  value repeatedly until you have found the best match. It is simple to change the  $B$  value: if the intermediate points are located above the straight line, you decrease the  $B$  value, and vice versa. A value of 0.0835 for  $B$  produced the best match; Figure 10.3 shows the resulting plot. The remaining parameters  $C$  and  $P$  can now be found from this straight line: its slope is equal to  $P-1$ , while its intercept with the  $Q = 1$  axis is equal to  $\log C$ .

The next screen displays the values of  $B$ ,  $C$ , and  $P$ . The general drawdown equation for the pumped well has been calculated as

$$s_w = 9.7 \times 10^{-4} Q + 2.7 \times 10^{-10} Q^{2.78} \quad (10.3)$$

This screen also displays a comparison between observed and calculated drawdowns. Table 10.2 shows these results. The standard deviation of the differences between observed and calculated drawdowns has been calculated as 0.03 m.

The final screen displays a graph showing the total drawdown in the pumped well versus the discharge rate. Figure 10.4 shows this relationship as plotted points; the dashed line represents the drawdown values without the contribution of the non-linear well-loss component ( $s_w = BQ$ ). This figure shows that up to discharge rates of some 1000  $\text{m}^3/\text{d}$  the non-linear well loss is negligible. For higher discharge rates, the non-linear well loss increases rapidly; above 5000  $\text{m}^3/\text{d}$ , the non-linear well loss contributes more than 50% to the total drawdown.

Table 10.2 Comparison between observed and calculated drawdown values, resulting from the 'Sheahan' step-drawdown analysis using the Rorabaugh method

Discharge rate (m <sup>3</sup> /d)	Corrected drawdown (m)	Calculated drawdown from Equation 10.3 (m)
2180	2.62	2.62
3815	6.10	6.11
6540	17.22	17.18
9811	42.98	43.01

Let's suppose that you need a capacity of 9000 m<sup>3</sup>/d for drinking-water supply. If you install one exploitation well for this purpose, the drawdown will be some 35 m according to Equation 10.3. If you were to install three wells, each with a capacity of 3000 m<sup>3</sup>/d, each well would have a drawdown of some 4 m. The total pumping costs of these three wells would be substantially lower than that of a single well of 9000 m<sup>3</sup>/d, due to the sharp increase of the non-linear well losses from such a well. Although the construction costs of three smaller capacity wells are higher than those of one high-capacity well, the increased pumping costs for the latter will be spread over the well's economic life time - say a period of 20 to 30 years. In other words, in cases as depicted in Figure 10.4, if a well field is considered there could be an economic trade-off between increased construction costs versus decreased pumping costs.

If you were to analyse the same data with the Jacob method you would

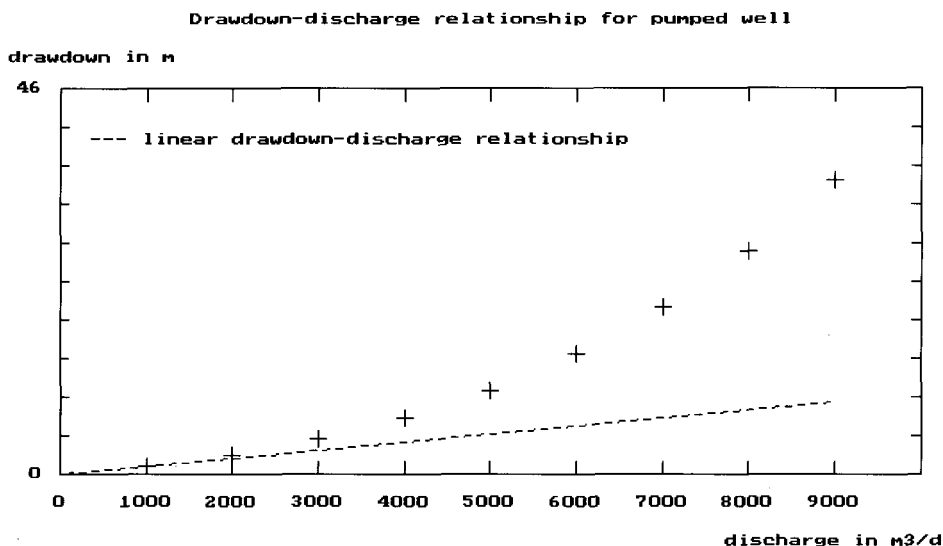


Figure 10.4 Discharge-drawdown relationship of the pumped well ('Sheahan') using the Rorabaugh method



obtain values for B and C that are orders of magnitudes lower than the values presented

$$s_w = 1.0 \times 10^{-4} Q + 4.2 \times 10^{-7} Q^2 \quad (10.4)$$

The standard deviation of the differences between observed and calculated drawdowns now increases from 0.03 to 1.24 m, also indicating that the four data points do not lie on a straight line.

So, you may conclude that the Sheahan test data can be fitted better with the Rorabaugh method than with the Jacob method; in other words, the P value differs from 2. Note that the adoption of the Jacob method would result in substantially higher non-linear well losses than according to the Rorabaugh method.

### 10.3 Guidelines

For the analysis of step-drawdown data, you may use either the Jacob method or the Rorabaugh method. It is up to you to judge which of the two methods gives the most consistent results for your data.

The best approach is always to start with the Jacob method. From the diagnostic plot you can then decide whether your data basically exhibit a straight line (yes or no). To augment visual inspection, which is of course a subjective measure, you can use the value of the standard deviation of the differences between observed and calculated drawdowns as a more objective measure. If you are satisfied with both, there is no reason to use the Rorabaugh method as well. If, however, you nonetheless decide to apply the Rorabaugh method, it will then yield a P value around 2 and a standard deviation of the same order of magnitude as that obtained by applying the Jacob method. The B value will have approximately the same value, but the C value will be different because P is different. For example, try to analyse the Clark data with the Rorabaugh method. In these cases, it is advisable to base your analysis solely on the results of the Jacob method.

If the diagnostic plot shows that the data points clearly exhibit a curved line, you are advised to use the Rorabaugh method. This method will then give you a better match and a significantly lower value for the standard deviation of the differences between observed and calculated drawdowns. With the Jacob method you may even encounter a negative B value if the P value is significantly higher than 2. Such a negative value of B is, of course, physically impossible. You will see this phenomenon if you use the Jacob method to analyse the data stored in the 'Feature1' file; its data pertain to a step-drawdown test performed in a highly conductive fracture. If, however, you analyse the same data with the Rorabaugh method – a value of 0.765 for B produces the best match - the analysis will yield the following

general drawdown equation for this pumped well

$$s_w = 8.9 \times 10^{-3}Q + 2.3 \times 10^{-14}Q^{5.57} \quad (10.5)$$

The standard deviation of the differences between observed and calculated drawdowns is now 0.01 m, whereas with the Jacob method it was 0.64 m. As was discussed at the beginning of this chapter, there will be no non-linear well losses for relatively low pumping rates. Whether such a situation did occur with your data can be verified by visually inspecting the discharge-drawdown relationship as presented in the last screen of SATEM. If you use the Jacob method to analyse the data stored in the 'Feature2' file, the analysis will yield the following general drawdown equation for this pumped well

$$s_w = 1.2 \times 10^{-2}Q + 2.0 \times 10^{-7}Q^2 \quad (10.6)$$

From the last screen you will see that up to 1800 m<sup>3</sup>/d the non-linear well losses are negligible. In such cases, you may not use the values of B, C and P from Equation 10.6 to estimate drawdowns for discharge rates higher than those used in the test itself.

If you analyse the same data with the Rorabaugh method, the analysis will yield the following general drawdown equation for this pumped well

$$s_w = 1.2 \times 10^{-3}Q + 1.0 \times 10^{-2}Q^{1.01} \quad (10.7)$$

Note that in this case the C value does not represent the non-linear well loss coefficient, but rather the linear well loss coefficient. If the value of P is taken to be 1 exactly, Equation 10.7 can be rearranged to

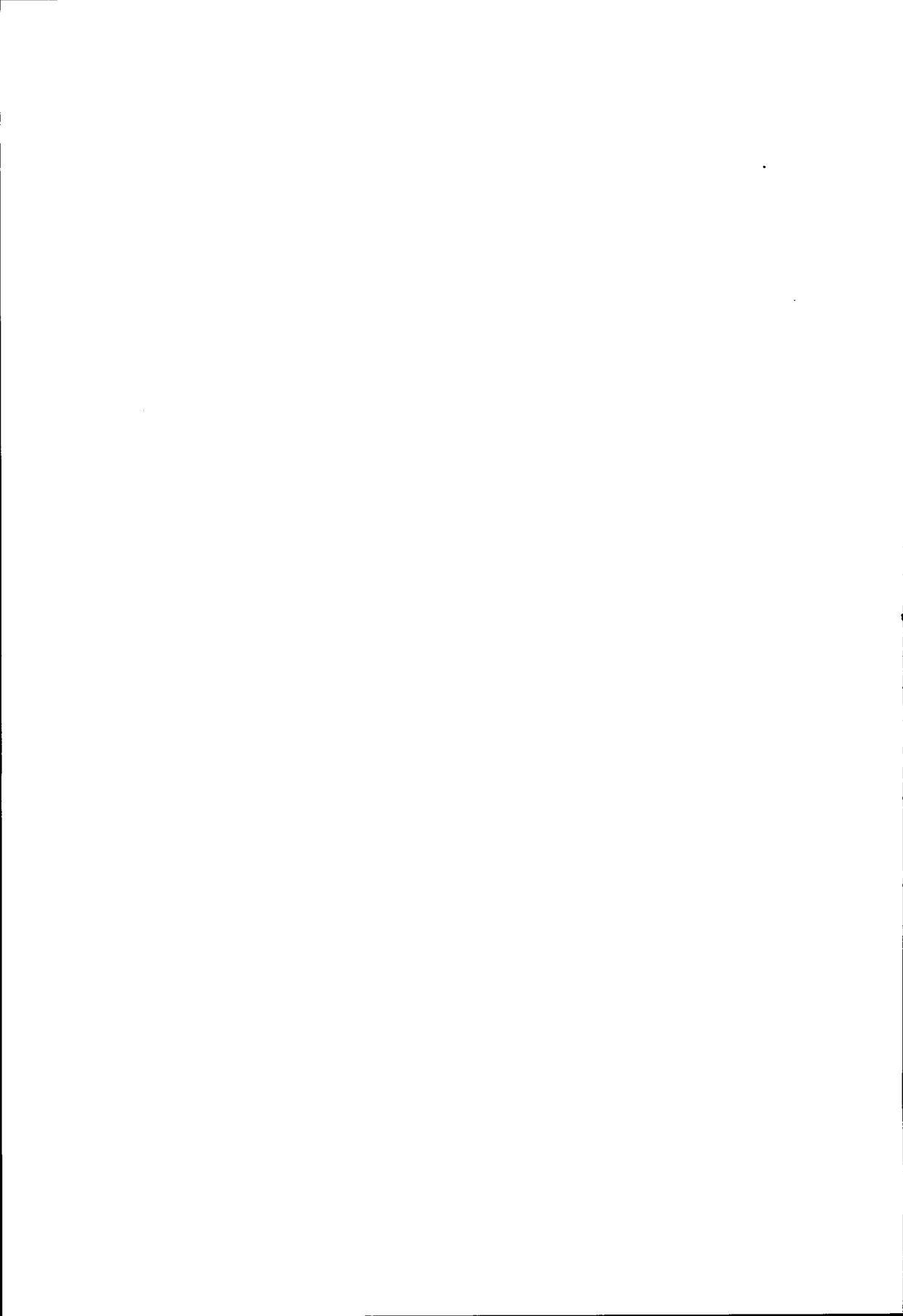
$$s_w = 1.12 \times 10^{-2}Q \quad (10.8)$$

For all practical purposes, Equations 10.6 and 10.8 yield the same linear loss coefficients. Note that in this case the dashed line in the last screen does not represent the linear well losses. It actually represents the first term of the right-hand side of Equation 10.7. Because P is almost equal to 1, the second term of the right-hand side of Equation 10.7 also represents the linear well losses. If the P value found from the analysis is significantly lower than 2 it can thus be concluded that the last screen does not provide correct information.

If non-linear well losses are very small or absent, it is impossible to judge which of the two methods will yield the most consistent results. If you are interested in a general drawdown equation for the pumped well, which you can also use for extrapolation, you must repeat the step-drawdown test, but with significantly higher discharge rates in each step.

Finally, the well may not have been properly developed before a step-draw-

down test was performed. The diagnostic plot will then reveal  $s_w/Q$  values that decrease with increasing values for  $Q$ . This will lead to negative values for  $C$  when you try to apply the Jacob method. An analysis with the Rorabaugh method is then impossible. You will encounter this phenomenon when you analyse the data stored in the 'Feature3' file.



# 11 Case studies

In the previous three chapters, field data were used to show how time-drawdown, distance-drawdown, and step-drawdown data can be analysed with the various methods in SATEM. This chapter will show how you can improve the analysis results by combining time-drawdown with distance-drawdown data, or pumping-test data with recovery-test data, or by combining step-drawdown data with single-well test data.

The data from the various aquifer tests in this chapter have already been analysed. So, once you have selected the appropriate method and data file, you should merely press <Enter> repeatedly and these analyses as we performed them will be replayed on the screen. The best way to perform your own analysis is first to use the input menu to retrieve the existing file and to save it under a different name. Because the convention used in SATEM is that the pop-up menu to save a file will only appear when you have changed the data (see Chapter 6, Section 3.5), you need to re-enter the same value for one of the input data. If you don't do this, this menu will not appear.

## 11.1 Aquifer test in an unconfined aquifer

The first case study contains data from an aquifer test conducted in the alluvial plain of the Indus Basin. A well was drilled to a depth of 105 m and was pumped at a constant rate of  $6117 \text{ m}^3/\text{d}$  for 6 consecutive days. Three piezometers were drilled to a depth of 37 m at distances of 30, 61, and 122 m and two piezometers were drilled to a depth of 55 m at distances of 61 and 122 m; in other words, at the latter two distances both a shallow and a deep piezometer were drilled. The depth to water table was recorded in the pumped well itself and in the five piezometers during the pumping period only; these data were converted to drawdown data. The data from this aquifer test are stored in the 'Pakistan' file.

### *Time-drawdown analysis*

We will start the analysis of this aquifer test with the time-drawdown data. Select Analysis from the main menu bar of SATEM. Make sure that in the Window Open dialogue box the folder is `c:\Satem50\ilripu57` and the file type is *Time-drawdown/recovery*. Select the file 'Pakistan' from the list of existing files and select *Theis-Jacob's method* in the method selection form.

Repeatedly pressing <Enter> brings up time-drawdown graphs of the various wells one by one on your screen, together with the selections already made. You will observe the following features. First, you will observe irregular behaviour in the time-drawdown graph of the pumped well itself. This is not

Time-drawdown graph of well ( $r = 61 \text{ m}$ )

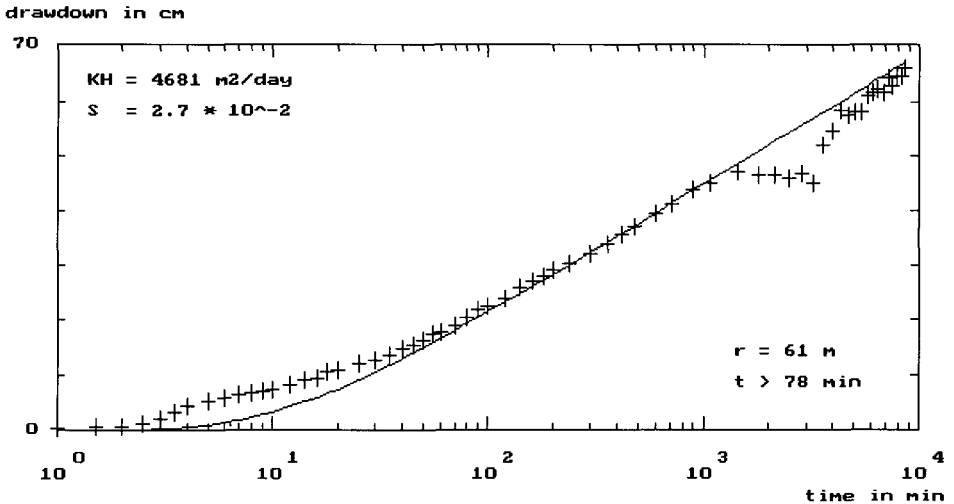


Figure 11.1 Time-drawdown analysis for the deep piezometer at distance 61 m.

unusual, because any irregularities in the discharge are, so to speak, magnified in the time-drawdown behaviour of the pumped well. Secondly, you will observe similar anomalies in all the time-drawdown graphs. Between 1000 and 3000 min of pumping the drawdowns stabilise and in some piezometers even decrease. The only explanation for this peculiar phenomenon is that during that period the discharge rate was not constant but decreased.

From the geology of the area, but also from the values of the resulting specific yield, it is clear that the tested aquifer can be considered to be acting as an unconfined aquifer. Most unconfined aquifers will exhibit a delayed-yield phenomenon when pumped. As was discussed in Chapter 4, Section 3, when analysing the data of an unconfined aquifer with delayed-yield effects the Theis-Jacob method can either be applied to the early-time drawdown data (left-hand side of Figure 4.10) or to the late-time drawdown data (right-hand side of Figure 4.10). However, the correct aquifer properties can be found if the analysis is based on the late-time drawdown data (see Figure 8.2). It was for this reason that the late-time drawdown data were selected in the time-drawdown graphs of all the wells. So, you should discard the early-time drawdown data when judging the match between observed and theoretical drawdown data (Figure 11.1). The situation is complicated by the irregularities in drawdowns during the period from 1000 and 3000 min mentioned earlier.

The final screen gives you an overview of the results we obtained from analysing the time-drawdown data from the various piezometers (see Table 11.1). This table shows that the various time-drawdown analyses produced fairly consistent results for the aquifer transmissivity and specific yield.

Table 11.1 Hydraulic properties of the 'Pakistan' unconfined aquifer, calculated with the Theis-Jacob method

Distance to pumped well (m)	Transmissivity (m <sup>2</sup> /d)	Specific yield (-)
0	4518	no value
30	4814	$3.7 \times 10^{-2}$
61	4745	$4.8 \times 10^{-2}$
61	4681	$2.7 \times 10^{-2}$
122	4624	$4.7 \times 10^{-2}$
122	4881	$5.5 \times 10^{-2}$

Neither is there a significant difference in the resulting aquifer properties between the shallow and deep piezometers at distances of 61 and 122 m from the pumped well.

*Distance-drawdown analysis*

We will continue the analysis of this aquifer test with a distance-drawdown analysis. At the end of the pumping period at 8640 min, the observed drawdowns in the various wells were selected assuming that at that time pseudo-steady state conditions prevailed (see Chapter 4, Sections 1 and 3). These data are stored in the 'Pakistan' file. Because each data file for the three different types of test in SATEM has its own unique file extension, you can give the same name to a time-drawdown, distance-drawdown, and step-drawdown file.

Select Analysis from the main menu bar of SATEM. Make sure that in the

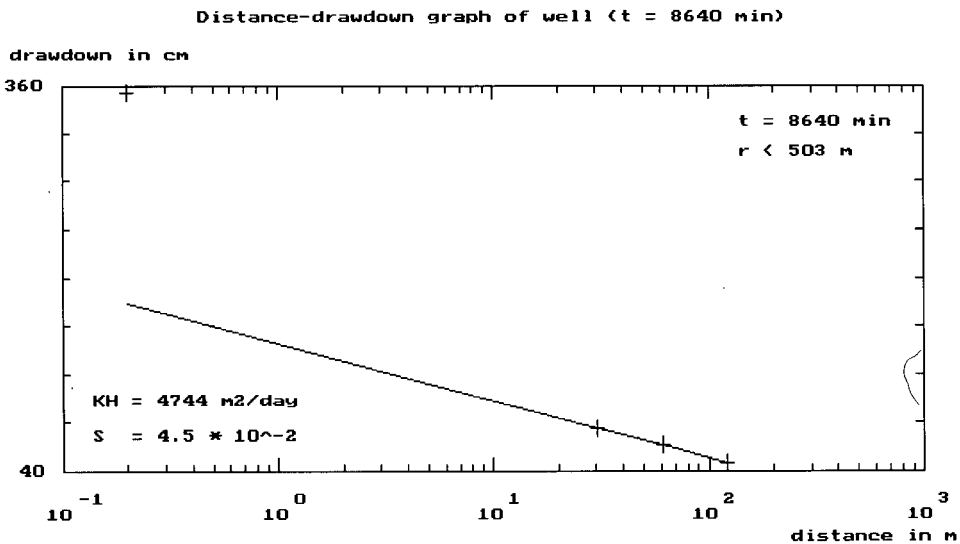


Figure 11.2 Distance-drawdown analysis of the pseudo-steady-state drawdown data based on the three piezometers and ignoring the well drawdown

Window Open dialogue box the file type is *Distance-drawdown*. Select the file 'Pakistan' from the list of existing files and select *Thiem-Jacob's method* in the method selection form.

The first screen shows you the distance-drawdown plot. The drawdown in the pumped well has been discarded for determining the straight-line segment, because of the linear and non-linear well losses (Figure 11.2). These losses result in an additional drawdown in the pumped well that is not accounted for in the analysis methods (see Chapter 9, Section 3). The resulting aquifer transmissivity ( $4744 \text{ m}^2/\text{d}$ ) and specific yield ( $4.5 \times 10^{-2}$ ) of this distance-drawdown analysis correspond very well to those of the various time-drawdown analyses as depicted in Table 11.1. The reason that in this case too a specific yield value is obtained from the distance-drawdown analysis is because in unconfined aquifers no steady state will develop in the sense of the drawdown stabilising. The drawdowns (and hence the cone of depression) will continue to deepen and expand, because theoretically aquifers of this type are not recharged by an outside source.

Suppose that a single-well test had been performed for this site instead of an aquifer test. Then, only time-drawdown data would have been available for the pumped well. Most probably, you would have selected all the observed drawdowns in determining the straight-line segment. That would have resulted in a transmissivity value of some  $6000 \text{ m}^2/\text{d}$ . This demonstrates that the results of aquifer tests are more reliable and more accurate than those of single-well tests. Aquifer tests allow estimates to be made of both the aquifer's transmissivity and its specific yield or storativity, which is not possible with single-well tests. Further, if more than one piezometer is drilled in an aquifer test, separate estimates of the aquifer properties can be made for each piezometer, allowing the various estimates to be compared. Moreover, you can obtain yet another estimate of the aquifer properties by using not only the time-drawdown relationship, but also the distance-drawdown relationships.

## 11.2 Aquifer test in a confined aquifer

The second case study contains data from an aquifer test in which only one piezometer was drilled at a distance of 90 m from the pumped well. A constant discharge rate of  $1168 \text{ m}^3/\text{d}$  was maintained for 260 min. The depth to water table was recorded in the pumped well itself and in the piezometer both during the pumping and the subsequent recovery period. These data have been converted to drawdown and residual-drawdown data and are stored in the 'Umhillal' file.

### *Time-drawdown / recovery analysis*

We will start the analysis of this aquifer test with the time-drawdown data.



Time-drawdown graph of well ( $r = 0$  m)

drawdown in cm

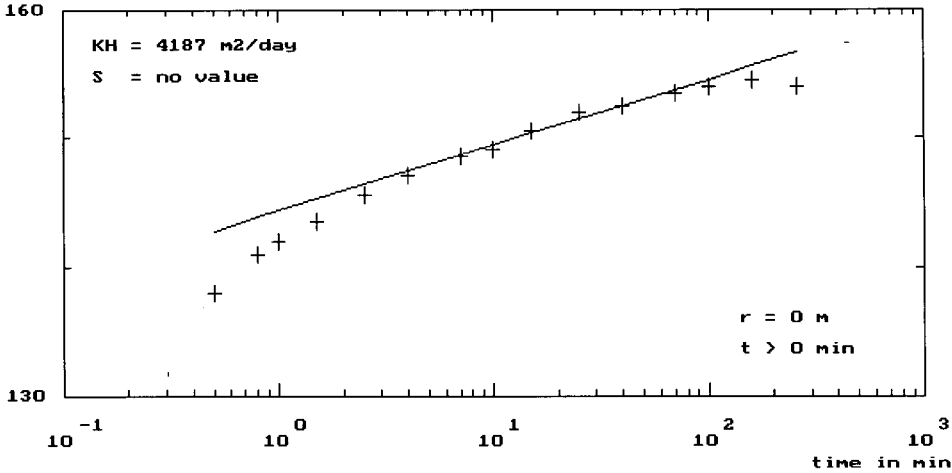


Figure 11.3 Time-drawdown analysis of the drawdown data for the pumped well

Select Analysis from the main menu bar of SATEM. Make sure that in the Window Open dialogue the file type is *Time-drawdown/recovery*. Select the file 'Umhillal' from the list of existing files and select *Theis-Jacob's method* in the method selection form.

Repeatedly pressing <Enter> brings up the various time-drawdown graphs one by one on your screen, together with the selections already made. You will observe the following features. In the first time-drawdown graph, that of the pumped well, the early drawdown data have been discarded because of assumed well-bore storage (see Chapter 8, Section 5). The last two drawdown data have also been discarded. This resulted in a transmissivity value of 4187  $\text{m}^2/\text{d}$  (Figure 11.3) and a storativity value that is not shown by SATEM (see Chapter 4, Section 6). The second data set comprises the residual drawdowns of the pumped well during the recovery period. SATEM then calculates the synthetic recovery values, as explained in Chapter 4, Section 5, and shows these in the next screen. These recovery data exhibit a fairly consistent pattern and all data were selected to determine the straight-line segment. That resulted in a transmissivity value of 4166  $\text{m}^2/\text{d}$ . For the piezometer at distance 90 m the late-time drawdown data were selected, as is common practice for confined and/or unconfined aquifers.

The final screen gives you an overview of the results of our analyses of the time-drawdown data from the various piezometers. Table 11.2 shows these results. Both the time-drawdown analyses and the analysis of the data on time and synthetic recovery produced fairly consistent results for the aquifer transmissivity and storativity.

Table 11.2 Hydraulic properties of the 'Umhillal' confined aquifer, calculated with the Theis-Jacob method

Distance to pumped well (m)	Transmissivity (m <sup>2</sup> /d)	Storativity (-)
0	4187	no value
0	4116	no value
90	3831	$3.2 \times 10^{-4}$
90	3815	$1.1 \times 10^{-4}$

*Time/residual-drawdown analysis*

Whenever you enter both drawdown data observed during a pumping period and residual-drawdown data observed during the subsequent recovery period in SATEM (see Chapter 6, Section 3.2) and save these data in a file with a particular name (see Chapter 6, Section 3.5), SATEM automatically saves an additional file under the same name, containing only the residual-drawdown data. You can use that file to perform an analysis based on the Theis recovery method. So, we will continue the analysis of this aquifer test with this method. Select now *Theis's recovery method* in the method selection form.

Repeatedly pressing <Enter> brings up the graphs of time ratio plotted against residual drawdown one by one on your screen, together with the selections already made. You will observe the following features. For both wells, the late-time residual-drawdown data have been selected, as is common practice for this analysis method. So the lower time-ratio values were selected for determining the straight-line segment (see Chapter 8, Section 4). The value entered for the aquifer storativity was the value obtained from the analysis of the time-drawdown data from the piezometer at distance 90 m:  $3.2 \times 10^{-4}$ . The final screen shows an overview of the results of our analyses of the data on time ratio and residual drawdown for the two wells. Table 11.3 summarizes the results. These aquifer transmissivity and storativity values are almost identical to those obtained from the time-drawdown analyses and the analyses of time and synthetic recovery data (Table 11.2). The results of the analysis of the data on time ratio and residual drawdown for the piezometer at distance 90 m were discussed in Chapter 8, Section 4.

The above results demonstrate why it is strongly recommended to continue to monitor the water table behaviour during the recovery period, after the pump has been shut down. This allows a second estimate of the aquifer

Table 11.3 Hydraulic properties of the 'Umhillal' confined aquifer, calculated with the Theis recovery method

Distance to pumped well (m)	Transmissivity (m <sup>2</sup> /d)	Storativity (-)
0	3839	no value
90	3816	$1.0 \times 10^{-4}$

properties to be made, which can then be compared with the one found during the pumping period. SATEM even allows a third estimate of the aquifer properties to be obtained, based on synthetic recovery data.

### 11.3 Aquifer test in a leaky aquifer

The third case study comprises data from an aquifer test in which two piezometers were drilled at distances of 20 and 40 m from the pumped well. A constant discharge rate of  $545 \text{ m}^3/\text{d}$  was maintained for 2 consecutive days. During the pumping and subsequent recovery period the depth to water table was recorded in the pumped well and in the piezometers. These data have been converted to drawdown and residual-drawdown data and are stored in the 'Kuwait' file.

#### *Time-drawdown/recovery analysis*

We will start the analysis of this aquifer test with the time-drawdown data. Select Analysis from the main menu bar of SATEM. Make sure that in the Window Open dialogue box the file type is *Time-drawdown/recovery*. Select the file 'Kuwait' from the list of existing files and select *Theis-Jacob's method* in the method selection form.

Repeatedly pressing <Enter> brings up the time-drawdown graphs of the various wells on your screen. From the shape of these graphs it is clear that the tested aquifer exhibits features of a leaky aquifer (Figure 11.4). Select now *Hantush's inflection point method* in the method selection form.

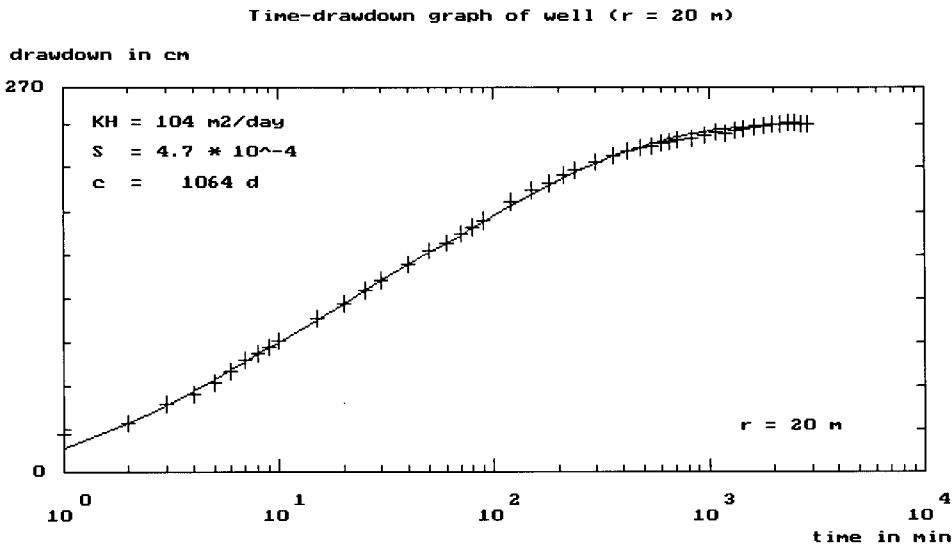


Figure 11.4 Time-drawdown analysis of the drawdown data for the piezometer at distance 20 m

Table 11.4 Hydraulic properties of the 'Kuwait' leaky aquifer', calculated with the Hantush inflection point method

Distance to pumped well (m)	Transmissivity (m <sup>2</sup> /d)	Storativity (-)	Hydraulic resistance (d)
0	116	no value	no value
0	110	no value	no value
20	104	$4.7 \times 10^{-4}$	1064
20	104	$4.3 \times 10^{-4}$	924
40	114	$1.2 \times 10^{-3}$	263
40	107	$1.3 \times 10^{-3}$	203

Now, again repeatedly pressing <Enter> brings up the time-drawdown graphs of the various wells one by one on your screen, together with the selections already made. You will observe that all graphs exhibit a stabilisation of the drawdowns at the end of the pumping period, so straightforward estimates of the steady-state drawdown can be made. All graphs except those of the pumped well also clearly show inflection points, so estimates of the tangent can be made straightforwardly. The early drawdown data have been discarded for the pumped well, because of assumed well-bore storage (see Chapter 8, Section 5). The match between observed and theoretical drawdown data is fairly good for all the wells.

The final screen gives you an overview of the results of our analyses of the time-drawdown data from the various wells. Table 11.4 shows these results. All six analyses of time versus drawdown and time versus synthetic recovery produced fairly consistent values for the aquifer transmissivity. For reasons that are unknown, the aquifer storativity and aquitard hydraulic resistance values are, however, quite different for the two piezometers.

#### *Time and residual-drawdown analysis*

We will now continue the analysis of this aquifer test with the data on time and residual drawdown. Select now *Theis's recovery method* in the method selection form.

Repeatedly pressing <Enter> brings up the graphs of time ratio plotted against residual drawdown for the various wells one by one on your screen, together with the selections already made. You will observe that for the first two wells, the upper time-ratio values have been selected for determining the straight-line segment. This is contrary to common practice (see previous section) but was necessary because in the Theis recovery method no allowance has been made for the recharge to the aquifer, resulting ultimately in steady-state conditions for leaky aquifers. For the piezometer at distance 40 m, the uppermost time-ratio values have been discarded, in line with usual practice. The values entered for the aquifer storativity were those obtained from the analysis of the time-drawdown data from the piezometers (Table 11.4).

The final screen gives an overview of the results of our analyses obtained

Table 11.5 Hydraulic properties of the 'Kuwait' leaky aquifer, calculated with the Theis recovery method

Distance to pumped well (m)	Transmissivity (m <sup>2</sup> /d)	Storativity (-)
0	113	no value
20	108	$6.5 \times 10^{-5}$
40	136	$1.6 \times 10^{-5}$

from the time ratio and residual-drawdown data from the two wells. Table 11.5 shows the results. A comparison between the values of Tables 11.4 and 11.5 shows that the transmissivity value obtained from the piezometer at distance 40 m is somewhat higher than all the other values. This can be explained by the high value of  $r/L$  (0.25); the value for the piezometer at distance 20 m is only 0.06. At large values of  $r/L$  the transmissivity will be overestimated and the storativity underestimated (compare Equations 4.4 and 4.12). The results of the analysis of the data from the piezometer at distance 20 m were discussed in Chapter 8, Section 4.

#### *Distance-drawdown analysis*

We will continue the analysis of this aquifer test with a distance-drawdown analysis. At the end of the pumping period at 2880 min, the observed drawdowns of the various wells represented the steady-state drawdowns, as can be clearly observed from the time-drawdown graphs. These data are stored in the 'Kuwait' file. Because each data file for the three types of test in SATEM has its own unique file extension, you can give the same name to a time-drawdown, distance-drawdown and step-drawdown file.

Select Analysis from the main menu bar of SATEM. Make sure that in the Window Open dialogue box the file type is *Distance-drawdown*. Select the file 'Kuwait' from the list of existing files and select *Hantush-Jacob's method* in the method selection form.

The first screen shows you the distance-drawdown plot. You will see that if you select only the drawdown data of both piezometers, contrary to expectation the theoretical drawdown in the pumped well is larger than was observed in the field. The theoretical drawdown of the pumped well ought to be smaller, because of the linear and non-linear well losses. These losses result in an additional drawdown in the pumped well that is not accounted for in the analysis methods (see Chapter 9, Section 3). Such a phenomenon was depicted in Figure 11.2.

Even if you include the drawdown in the pumped well for determining the straight-line segment, the resulting aquifer transmissivity (82 m<sup>2</sup>/d) is still lower than the transmissivities from the time-drawdown analyses. The reason for this poor result is that the storativity and, even more so, the hydraulic resistance values, are very different for the two piezometers. You should therefore discard the results of the distance-drawdown analysis.

Summarising, in this case of a leaky aquifer, you will only obtain consistent results for the aquifer transmissivity by combining the time-drawdown analyses with the analyses of time and residual-drawdown for the pumped well and for the piezometer at distance 20 m.

#### 11.4 Single-well test in an unconfined aquifer

The fourth case study comprises data from a step-drawdown test (Boonstra 1999<sup>a</sup>). The well was pumped with a step-wise increased discharge rate, with each step lasting 60 min. This test was followed by a single-well test (Boonstra 1999<sup>b</sup>). During the pumping and subsequent recovery period the depth to water table was recorded in the pumped well. These data have been converted to drawdown and residual-drawdown data. The data from both the step-drawdown test and the single-well test are stored in the 'Malleka' file.

##### *Step-drawdown analysis*

We will start the analysis with the step-drawdown data. Select Analysis from the main menu bar of SATEM. Make sure that in the Window Open dialogue box the file type is *Step-drawdown*. Select the file 'Malleka' from the list of existing files and select *Jacob's method* in the method selection form.

Repeatedly pressing <Enter> brings up the time-drawdown graphs of the various steps one by one on your screen, together with the selections already made. You will observe that the drawdowns had not yet stabilised at the end of the various steps. This implies that the observed drawdown values at the end of each step need to be corrected. The late-time drawdown data have been selected for this purpose. The resulting diagnostic plot shows that the four data points lie almost exactly on a sloping straight line (Figure 11.5). This implies that the Jacob method can be used. The next screen shows you the resulting drawdown equation for the pumped well:

$$s_w = 7.0 \times 10^{-4} Q + 1.3 \times 10^{-7} Q^2$$

This step-drawdown test was followed by a single-well test. For that test, the discharge rate of the third step was adopted: 3853 m<sup>3</sup>/d. According to Equation 5.3 the non-linear well loss  $s_3$  can be calculated as

$$s_3 = CQ^p = 1.3 \times 10^{-7} \times 3853^2 = 1.93 \text{ m}$$

##### *Time-drawdown / recovery analysis*

The observed drawdown data of the pumped well were corrected for this non-linear well loss and stored in the 'Malleka1' file. We will continue the analysis with the corrected time-drawdown data.

Select Analysis from the main menu bar of SATEM. Make sure that in the

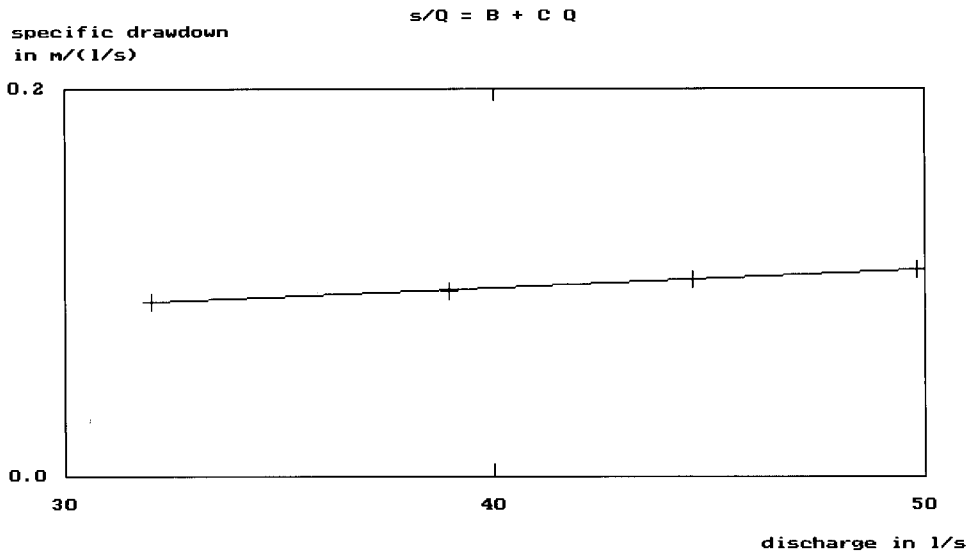


Figure 11.5 Diagnostic plot of step-drawdown data

Window Open dialogue box the file type is *Time-drawdown/recovery*. Select the file 'Malleka1' from the list of existing files and select *Theis-Jacob's method* in the method selection form.

Repeatedly pressing <Enter> brings up the time-drawdown graph of the pumped well on your screen, together with the selections already made. You will observe that the early drawdown data have been discarded because of assumed well-bore storage (see Chapter 8, Section 5). This resulted in a transmissivity value of  $1430 \text{ m}^2/\text{d}$  and a storativity value that is not shown by SATEM (see Chapter 4, Section 6). The second data set comprises the residual drawdowns of the pumped well during the recovery period. SATEM then calculates the corresponding synthetic recovery values as was explained in Chapter 4, Section 5 and shows these in the next screen. These recovery data exhibit a fairly consistent pattern and the late-time data have been selected to determine the straight-line segment. That resulted in a transmissivity value of  $1287 \text{ m}^2/\text{d}$ .

To obtain an estimate of the storativity or specific yield from a single-well test using SATEM, apply the following procedure. Retrieve the file of the corrected drawdown data, in this case 'Malleka1'. Increase the  $r$  value by a factor of 10. (This is necessary because SATEM suppresses values for storativity or specific yield for  $r$  values less than 1 m; in other words, when the  $r$  value actually represents the effective radius of the pumped well rather than the distance from a piezometer to the pumped well.) Store the data in a new file, in this case 'Malleka2'. When you now perform the analysis again, a value for the storativity is displayed (Figure 11.6). This is not the correct value, because you increased the  $r$  value artificially by a factor of 10. You therefore need to

Time-drawdown graph of well (r = 2 m)

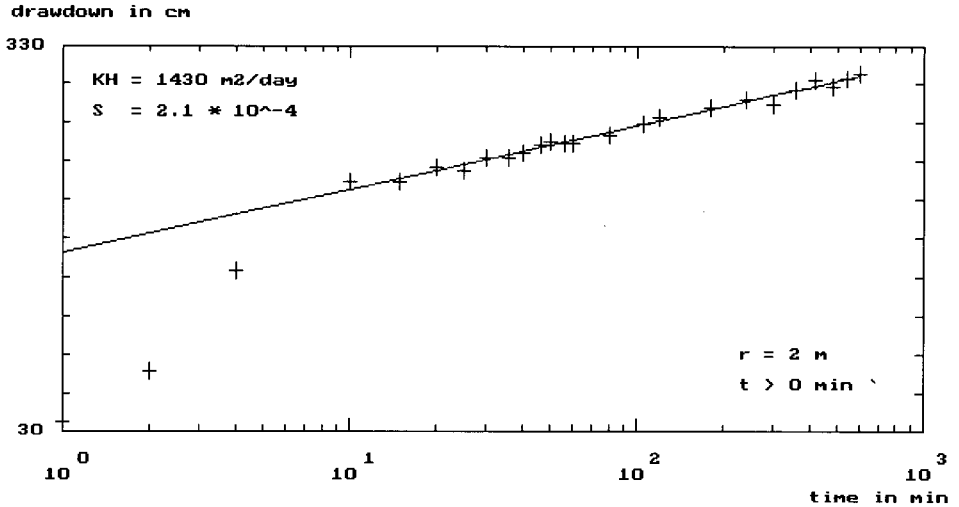


Figure 11.6 Time-drawdown data of the corrected drawdown data for the pumped well

multiply the displayed value by 100 (see Equation 4.28). Based on the drawdowns corrected for non-linear well loss, the resulting specific yield value is then  $2.1 \times 10^{-2}$  or 2.1 per cent. The synthetic recovery drawdowns yield a value of 5.8 per cent. These values should be treated with caution, because they are highly sensitive to the value of the effective radius of the pumped well, and the linear well loss is not accounted for (see Chapter 4, Section 6).

*Time/residual-drawdown analysis*

We will now continue the analysis of this single-well test with the data on time and residual drawdown. Select Analysis from the main menu bar of SATEM. Make sure that in the Window Open dialogue box the file type is *Time-residual-drawdown*. Select the file 'Malleka' from the list of existing files and select *Theis's recovery method* in the method selection form.

Repeatedly pressing <Enter> brings up the graph of time ratio plotted against residual drawdown for the pumped well on your screen, together with the selections already made. You will observe that lower time-ratio values have been selected, as is common practice for this analysis method. This resulted in a transmissivity value of 1230 m<sup>2</sup>/d, which corresponds well with the values found from the time-drawdown analysis. The application of time-drawdown and time-recovery analyses thus enables us to check the calculated transmissivity value. When the two values are close to each other, it implies that the data are consistent, i.e. that the results of the test are reliable. Together with the results of the preceding step-drawdown test, we have even obtained an estimate of the specific yield from this single-well test.



# References

- Boonstra, J. 1992. Aquifer tests with partially penetrating wells: theory and practice. *J. Hydrol.* 137: 165-179.
- Boonstra, J. 1999a. Well design and construction. In: *The Handbook of Groundwater Engineering*. Ed. Jacques W. Delleur. CRC Press, Boca Raton, USA: 9:1-9:29.
- Boonstra, J. 1999b. Well hydraulics and aquifer tests. In: *The Handbook of Groundwater Engineering*. Ed. Jacques W. Delleur. CRC Press, Boca Raton, USA: 8:1-8:34.
- Boonstra, J. and de Ridder, N.A. 1994. Single well and aquifer tests. In: *Drainage Principles and Applications*. Ed. H.R. Ritzema. Publication 16. International Institute for Land Reclamation and Improvement/ILRI. Wageningen.
- Bos, M.G. 1989. Measurement discharge structures. Publication 20. International Institute for Land Reclamation and Improvement/ILRI. Wageningen.
- Bouwer, H. 1978. *Groundwater hydrology*. McGraw-Hill series in water resources and environmental engineering. McGraw-Hill Book company, New York.
- Cooper, H.H. and Jacob, C.E. 1946. A generalised graphical method for evaluating formation constants and summarising well field history. *Am. Geophys. Union Trans.* Vol. 27, pp. 526-534.
- Darcy, H. 1856. *Les fontaines publiques de la ville de Dyon*. V. Dalmont, Paris, 647 p.
- De Glee, G.J. 1930. Over groundwaterstromingen bij wateronttrekking door middel van putten. Thesis. J. Waltman, Delft, 175 pp.
- De Glee, G.J. 1951. Berekeningsmethoden voor de winning van grondwater. In: *Drinkwatervoorziening, 3e Vakantiecursus: 38-80 Moorman=s periodeke pers*, The Hague.
- Driscoll, F.G. 1986. *Groundwater and wells*. 2nd ed. St. Paul, Johnson Division.
- Genetier, B. 1984. *La pratique des pompages d'essai en hydrogeologie*. Bureau de recherches geologique et minieres. Manuels et methodes, No. 9.
- Groundwater Manual*. 1981. A water resources technical publication. U.S. Department of the Interior; Water and Power Resources Service. U.S. Government Printing Office, Denver.
- Hantush, M.S. 1956. Analysis of data from pumping tests in leaky aquifers. *Am. Geophys. Union Trans.* Vol. 37, pp. 702-714.
- Hantush, M.S. 1962. Aquifer tests on partially penetrating wells. *Am. Soc. Civ. Eng. Trans.* Vol. 127, Part I, pp. 284-308.
- Hantush, M.S. 1964. Hydraulics of wells. In: *Advances in hydroscience*. Ed. V.T. Chow. Vol. I, pp. 281-432. Academic Press, New York and London.
- Hantush, M.S. and Jacob, C.E. 1955. Non-steady radial flow in an infinite leaky aquifer. *Am. Geophys. Union Trans.* Vol. 36, pp. 95-100
- Jacob, C.E. 1944. Notes on determining permeability by pumping tests under water table conditions. U.S. Geol. Surv. open file rept.
- Jacob, C.E. 1947. Drawdown test to determine effective radius of artesian well. *Trans. Amer. Soc. of Civil Engrs.* Vol. 112, Paper 2321, pp. 1047-1064.
- Jacob, C.E. 1950. Flow of groundwater, *Engineering Hydraulics*, ed H. Rouse. John Wiley & Sons, New York, pp. 321-386.
- Kruseman, G.P. and de Ridder, N.A. 1990. Analysis and evaluation of pumping test data. Publication 47. International Institute for Land Reclamation and Improvement/ILRI. Wageningen.
- Lennox, D.H. 1966. Analysis of step-drawdown test. *J. Hydr. Div., Proc. of the Amer. Soc. Civil Engrs.*, Vol. 92(HY6), pp. 25-48.
- Neuman, S.P. 1975. Analysis of pumping test data from anisotropic unconfined aquifers considering delayed gravity response. *Water Resources Research*, Vol. 11, No. 2, pp. 329-342.
- Papadopoulos, I.S. and Cooper, H.H., Jr. 1967. Drawdown in a well of large diameter. *Water Resources Res.* Vol. 5, pp. 817-829.

- Rorabaugh, M.J. 1953. Graphical and theoretical analysis of step-drawdown test in artesian well. Proc. Amer. Soc. Civil Engrs., Vol 79, separate no. 362, 23 pp.
- Schafer, D.C. 1978. Casing storage can affect pumping test data. Johnson Drillers' Journal, Jan/Feb, Johnson Division, UOP Inc., St. Paul, MN.
- Theis, C.V. 1935. The relation between the lowering of the piezometric surface and the rate and duration of discharge of a well using groundwater storage. Am. Geophys. Union Trans., Vol. 16, p. 519-524.
- Thiem, G. 1906. Hydrologische Methoden. Gebhardt, Leipzig.

# List of principal symbols and units

Symbol	Definition	Units
A	Cross-sectional area normal to flow direction	$m^2$
b	Penetration depth of pumped well	m
b'	Penetration depth of piezometer	m
B	Linear well loss coefficient	$d/m^2$
c	Hydraulic resistance of aquitard	d
C	Non-linear well loss coefficient	$d^2/m^5$
d	Mean pore diameter	m
d	Non-screened part of pumped well	m
d'	Non-screened part of piezometer	m
D'	Saturated thickness of aquitard	m
$E_w$	Well efficiency	-
g	Acceleration due to gravity	$m/d^2$
h	Hydraulic head	m
H	Saturated thickness of aquifer	m
i	Hydraulic gradient	-
k	Intrinsic permeability	$m^2$
K	Hydraulic conductivity	$m/d$
KH	Transmissivity of aquifer	$m^2/d$
$K_h$	Hydraulic conductivity for horizontal flow	$m/d$
$K_v$	Hydraulic conductivity for vertical flow	$m/d$
$K_0(r/L)$	Modified Bessel function	-
L	Leakage factor or characteristic length	m
$N_R$	Reynolds number	-
Q	Volume rate of flow	$m^3/d$
Q	Constant well discharge	$m^3/d$
r	Distance of piezometer from pumped well	m
$r_o$	Interception point in distance	m
$r_w$	Effective radius of pumped well	m
s	Drawdown	m
s'	Residual drawdown	m
$s_m$	Steady-state drawdown	m
$s_w$	Drawdown of pumped well	m
S	Storativity of aquifer	-
$S_s$	Specific storage of aquifer	$m^{-1}$
$S_y$	Specific yield of aquifer	-
t	Time since pumping started	d
t'	Time since recovery started	d
$t_o$	Interception point in time	d

T	Transmissivity of aquifer	$m^2/d$
u	Parameter of Theis well function	-
v	Specific discharge or Darcy velocity	$m/d$
W(u)	Theis well function	-
W(u,r/L)	Hantush well function	-
$\mu$	Dynamic viscosity of the fluid	$kg/m.d$
$\rho$	Density of fluid	$kg/m^3$

# Appendix

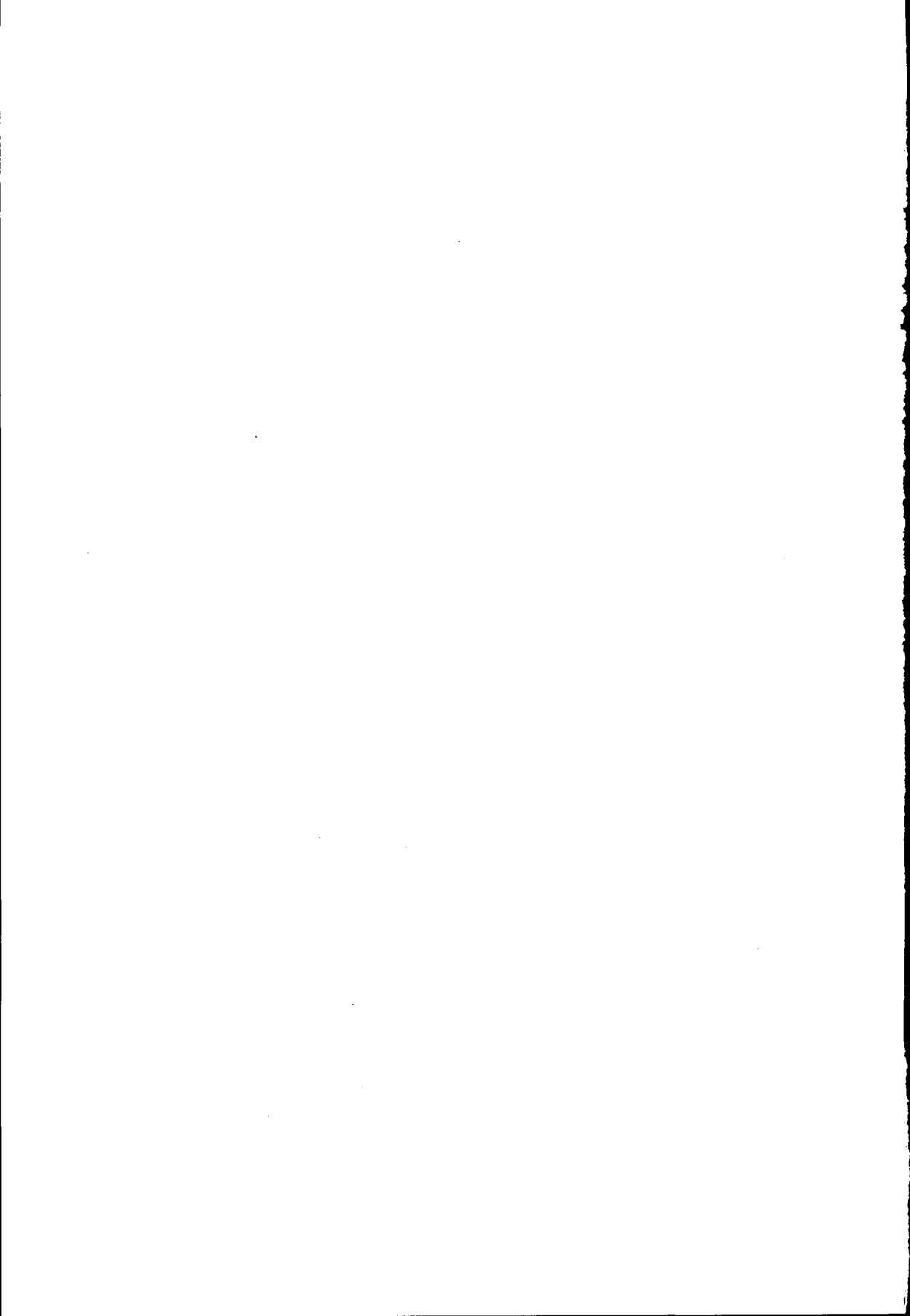
Values of  $K_0(r/L)$  and  $e^{r/L} K_0(r/L)$  as function of  $r/L$

Values of  $K_0(r/L)$  and  $e^{r/L} K_0(r/L)$  as function of  $r/L$ 

$r/L$	$K_0(r/L)$	$e^{r/L} K_0(r/L)$	$r/L$	$K_0(r/L)$	$e^{r/L} K_0(r/L)$	$r/L$	$K_0(r/L)$	$e^{r/L} K_0(r/L)$	$r/L$	$K_0(r/L)$	$e^{r/L} K_0(r/L)$
1.0(-2)	4.72	4.77	3.8(-2)	3.39	3.52	6.6(-2)	2.84	3.03	9.4(-2)	2.49	2.73
1.1(-2)	4.63	4.68	3.9(-2)	3.36	3.50	6.7(-2)	2.82	3.02	9.5(-2)	2.48	2.72
1.2(-2)	4.54	4.59	4.0(-2)	3.34	3.47	6.8(-2)	2.81	3.01	9.6(-2)	2.47	2.72
1.3(-2)	4.46	4.52	4.1(-2)	3.31	3.45	6.9(-2)	2.79	2.99	9.7(-2)	2.46	2.71
1.4(-2)	4.38	4.45	4.2(-2)	3.29	3.43	7.0(-2)	2.78	2.98	9.8(-2)	2.45	2.70
1.5(-2)	4.32	4.38	4.3(-2)	3.26	3.41	7.1(-2)	2.77	2.97	9.9(-2)	2.44	2.69
1.6(-2)	4.25	4.32	4.4(-2)	3.24	3.39	7.2(-2)	2.75	2.96	1.0(-1)	2.43	2.68
1.7(-2)	4.19	4.26	4.5(-2)	3.22	3.37	7.3(-2)	2.74	2.95	1.1(-1)	2.33	2.60
1.8(-2)	4.13	4.21	4.6(-2)	3.20	3.35	7.4(-2)	2.72	2.93	1.2(-1)	2.25	2.53
1.9(-2)	4.08	4.16	4.7(-2)	3.18	3.33	7.5(-2)	2.71	2.92	1.3(-1)	2.17	2.47
2.0(-2)	4.03	4.11	4.8(-2)	3.15	3.31	7.6(-2)	2.70	2.91	1.4(-1)	2.10	2.41
2.1(-2)	3.98	4.06	4.9(-2)	3.13	3.29	7.7(-2)	2.69	2.90	1.5(-1)	2.03	2.36
2.2(-2)	3.93	4.02	5.0(-2)	3.11	3.27	7.8(-2)	2.67	2.89	1.6(-1)	1.97	2.31
2.3(-2)	3.89	3.98	5.1(-2)	3.09	3.26	7.9(-2)	2.66	2.88	1.7(-1)	1.91	2.26
2.4(-2)	3.85	3.94	5.2(-2)	3.08	3.24	8.0(-2)	2.65	2.87	1.8(-1)	1.85	2.22
2.5(-2)	3.81	3.90	5.3(-2)	3.06	3.22	8.1(-2)	2.64	2.86	1.9(-1)	1.80	2.18
2.6(-2)	3.77	3.87	5.4(-2)	3.04	3.21	8.2(-2)	2.62	2.85	2.0(-1)	1.75	2.14
2.7(-2)	3.73	3.83	5.5(-2)	3.02	3.19	8.3(-2)	2.61	2.84	2.1(-1)	1.71	2.10
2.8(-2)	3.69	3.80	5.6(-2)	3.00	3.17	8.4(-2)	2.60	2.83	2.2(-1)	1.66	2.07
2.9(-2)	3.66	3.76	5.7(-2)	2.98	3.16	8.5(-2)	2.59	2.82	2.3(-1)	1.62	2.04
3.0(-2)	3.62	3.73	5.8(-2)	2.97	3.14	8.6(-2)	2.58	2.81	2.4(-1)	1.58	2.01
3.1(-2)	3.59	3.70	5.9(-2)	2.95	3.13	8.7(-2)	2.56	2.80	2.5(-1)	1.54	1.98
3.2(-2)	3.56	3.67	6.0(-2)	2.93	3.11	8.8(-2)	2.55	2.79	2.6(-1)	1.50	1.95
3.3(-2)	3.53	3.65	6.1(-2)	2.92	3.10	8.9(-2)	2.54	2.78	2.7(-1)	1.47	1.93
3.4(-2)	3.50	3.62	6.2(-2)	2.90	3.09	9.0(-2)	2.53	2.77	2.8(-1)	1.44	1.90
3.5(-2)	3.47	3.59	6.3(-2)	2.88	3.07	9.1(-2)	2.52	2.76	2.9(-1)	1.40	1.88
3.6(-2)	3.44	3.57	6.4(-2)	2.87	3.06	9.2(-2)	2.51	2.75	3.0(-1)	1.37	1.85
3.7(-2)	3.41	3.54	6.5(-2)	2.85	3.04	9.3(-2)	2.50	2.74	3.1(-1)	1.34	1.83

Values of  $K_0(r/L)$  and  $e^{r/L} K_0(r/L)$  as function of  $r/L$ 

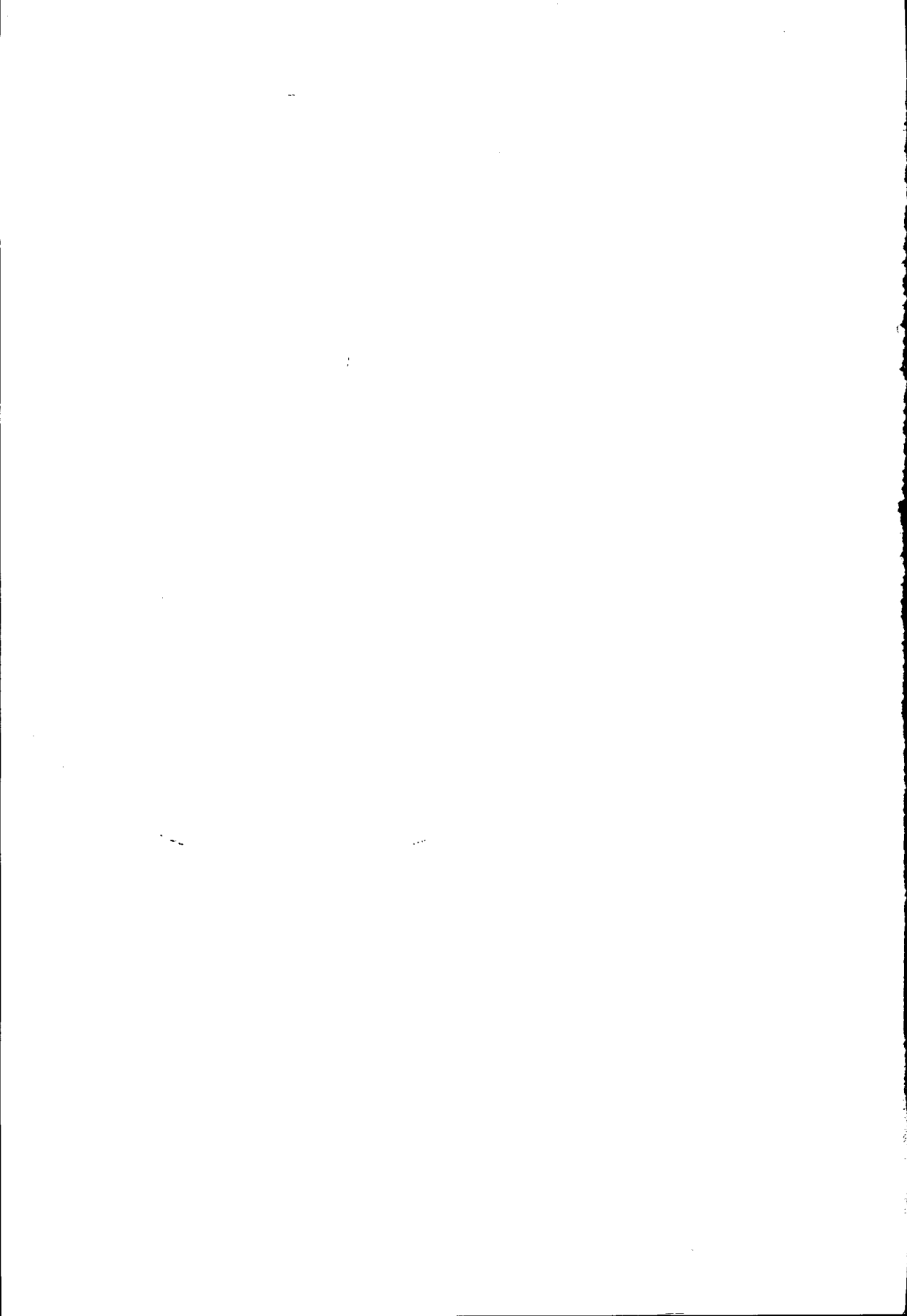
$r/L$	$K_0(r/L)$	$e^{r/L} K_0(r/L)$	$r/L$	$K_0(r/L)$	$e^{r/L} K_0(r/L)$	$r/L$	$K_0(r/L)$	$e^{r/L} K_0(r/L)$	$r/L$	$K_0(r/L)$	$e^{r/L} K_0(r/L)$
3.2(-1)	1.31	1.81	6.0(-1)	7.78(-1)	1.42	8.8(-1)	5.01(-1)	1.21	2.6	5.54(-2)	7.46(-1)
3.3(-1)	1.29	1.79	6.1(-1)	7.65(-1)	1.41	8.9(-1)	4.94(-1)	1.20	2.7	4.93(-2)	7.33(-1)
3.4(-1)	1.26	1.77	6.2(-1)	7.52(-1)	1.40	9.0(-1)	4.87(-1)	1.20	2.8	4.38(-2)	7.21(-1)
3.5(-1)	1.23	1.75	6.3(-1)	7.40(-1)	1.39	9.1(-1)	4.80(-1)	1.19	2.9	3.90(-2)	7.09(-1)
3.6(-1)	1.21	1.73	6.4(-1)	7.28(-1)	1.38	9.2(-1)	4.73(-1)	1.19	3.0	3.47(-2)	6.98(-1)
3.7(-1)	1.18	1.71	6.5(-1)	7.16(-1)	1.37	9.3(-1)	4.66(-1)	1.18	3.1	3.10(-2)	6.87(-1)
3.8(-1)	1.16	1.70	6.6(-1)	7.04(-1)	1.36	9.4(-1)	4.59(-1)	1.18	3.2	2.76(-2)	6.77(-1)
3.9(-1)	1.14	1.68	6.7(-1)	6.93(-1)	1.35	9.5(-1)	4.52(-1)	1.17	3.3	2.46(-2)	6.67(-1)
4.0(-1)	1.11	1.66	6.8(-1)	6.82(-1)	1.35	9.6(-1)	4.46(-1)	1.16	3.4	2.20(-2)	6.58(-1)
4.1(-1)	1.09	1.65	6.9(-1)	6.71(-1)	1.34	9.7(-1)	4.40(-1)	1.16	3.5	1.96(-2)	6.49(-1)
4.2(-1)	1.07	1.63	7.0(-1)	6.61(-1)	1.33	9.8(-1)	4.33(-1)	1.15	3.6	1.75(-2)	6.40(-1)
4.3(-1)	1.05	1.62	7.1(-1)	6.50(-1)	1.32	9.9(-1)	4.27(-1)	1.15	3.7	1.56(-2)	6.32(-1)
4.4(-1)	1.03	1.60	7.2(-1)	6.40(-1)	1.31	1.0	4.21(-1)	1.14	3.8	1.40(-2)	6.24(-1)
4.5(-1)	1.01	1.59	7.3(-1)	6.30(-1)	1.31	1.1	3.66(-1)	1.10	3.9	1.25(-2)	6.17(-1)
4.6(-1)	9.94(-1)	1.57	7.4(-1)	6.20(-1)	1.30	1.2	3.19(-1)	1.06	4.0	1.12(-2)	6.09(-1)
4.7(-1)	9.76(-1)	1.56	7.5(-1)	6.11(-1)	1.29	1.3	2.78(-1)	1.02	4.1	9.98(-3)	6.02(-1)
4.8(-1)	9.58(-1)	1.55	7.6(-1)	6.01(-1)	1.29	1.4	2.44(-1)	9.88(-1)	4.2	8.93(-3)	5.95(-1)
4.9(-1)	9.41(-1)	1.54	7.7(-1)	5.92(-1)	1.28	1.5	2.14(-1)	9.58(-1)	4.3	7.99(-3)	5.89(-1)
5.0(-1)	9.24(-1)	1.52	7.8(-1)	5.83(-1)	1.27	1.6	1.88(-1)	9.31(-1)	4.4	7.15(-3)	5.82(-1)
5.1(-1)	9.08(-1)	1.51	7.9(-1)	5.74(-1)	1.26	1.7	1.65(-1)	9.06(-1)	4.5	6.40(-3)	5.76(-1)
5.2(-1)	8.92(-1)	1.50	8.0(-1)	5.65(-1)	1.26	1.8	1.46(-1)	8.83(-1)	4.6	5.73(-3)	5.70(-1)
5.3(-1)	8.77(-1)	1.49	8.1(-1)	5.57(-1)	1.25	1.9	1.29(-1)	8.61(-1)	4.7	5.13(-3)	5.64(-1)
5.4(-1)	8.61(-1)	1.48	8.2(-1)	5.48(-1)	1.25	2.0	1.14(-1)	8.42(-1)	4.8	4.60(-3)	5.59(-1)
5.5(-1)	8.47(-1)	1.47	8.3(-1)	5.40(-1)	1.24	2.1	1.01(-1)	8.25(-1)	4.9	4.12(-3)	5.53(-1)
5.6(-1)	8.32(-1)	1.46	8.4(-1)	5.32(-1)	1.23	2.2	8.93(-2)	8.06(-1)	5.0	3.69(-3)	5.48(-1)
5.7(-1)	8.18(-1)	1.45	8.5(-1)	5.24(-1)	1.23	2.3	7.91(-2)	7.89(-1)			
5.8(-1)	8.04(-1)	1.44	8.6(-1)	5.16(-1)	1.22	2.4	7.02(-2)	7.74(-1)			
5.9(-1)	7.91(-1)	1.43	8.7(-1)	5.09(-1)	1.21	2.5	6.23(-2)	7.60(-1)			





# Index

- Analysis
  - distance-drawdown, 63, 127, 133
  - time-drawdown, 63, 125, 128, 131, 134
  - time-recovery, 63, 128, 131, 134
  - time residual-drawdown, 130, 132, 136
- Anisotropy, 18
- Aquiclude, 13
- Aquifer, 13
  - confined, 13, 128
  - leaky, 15, 36, 131
  - losses, 55
  - multi-layered, 15
  - semi-confined, 15
  - unconfined, 15, 42, 125, 134
- Aquitard, 15
- Artesian well, 13
- Darcy's law, 16
- Delayed yield, 42, 93, 103
- Diagnostic plots, 58, 91, 107, 115
- Discharge rate, 26
- Drainable pore space, 21
- Drawdown, 23
  - corrected, 44
  - residual, 48, 73
- Effective
  - porosity, 21
  - radius, 53, 105
- Equation
  - De Glee, 40
  - Hantush, 44
  - Thiem-Dupuit, 35
  - Theis, 31
- Flow
  - pseudo-steady state, 27
  - steady-state, 28
  - unsteady-state, 27
- Function
  - Hankel, 38
  - Hantush well, 37, 45
  - Modified Bessel, 38
  - Theis well, 32
- Guidelines, 102, 111, 121
- Heterogeneous, 18
- Hydraulic
  - conductivity, 19
  - head, 16
  - resistance, 22
- Intrinsic permeability, 17
- Late-time slope
  - flattening, 104
  - steepening, 104
- Leakage factor, 22
- Method
  - Hantush-Bierschenk, 59, 115
  - Hantush's inflection point, 37, 76, 85, 95
  - Hantush-Jacob, 40, 110
  - Jacob, 59, 115
  - Jacob-Hantush, 46, 79, 87, 98
  - Rorabaugh, 61, 118
  - Thiem-Jacob, 34, 107
  - Theis-Jacob, 32, 73, 83, 91
  - Theis's recovery, 49, 81, 100
- Partially penetration, 44, 112
- Piezometer, 16
- Pumping duration, 26
- Reynold's number, 17
- Saturated thickness, 20
- Specific
  - capacity, 57
  - drawdown, 116
  - storage, 20
  - yield, 21
- Storativity, 21
- Synthetic
  - Data Generator, 82
  - recovery, 49, 75
- Test
  - aquifer, 11
  - pumping, 23
  - recovery, 23, 48
  - single-well, 11, 52, 134
  - step-drawdown, 55, 134
- Time sequence, 25
- Transmissivity, 20
- Trend correction, 25
- Unconfined storativity, 21
- Well
  - bore storage, 52, 95, 97, 103
  - efficiency, 57
  - losses, 52, 105
    - linear, 56, 122
    - non-linear, 57, 122
  - observation, 16
  - pumped, 112



## Currently available ILRI publications

No	Publications	Author	ISBN No.
16	Drainage Principles and Applications (second edition, completely revised)	H.P. Ritzema (Ed.)	90 70754 339
17	Land Evaluation for Rural Purposes	R. Brinkman and A.J. Smyth	90 70260 859
19	On Irrigation Efficiencies	M.G. Bos and J. Nugteren	90 70260 875
20	Discharge Measurement Structures (third edition)	M.G. Bos	90 70754 150
21	Optimum Use of Water Resources	N.A. de Ridder and E. Erez	—
24	Drainage and Reclamation of Salt-Affected Soils	J. Martínez Beltrán	—
25	Proceedings of the International Drainage Workshop	J. Wesseling (Ed.)	90 70260 549
26	Framework for Regional Planning in Developing Countries	J.M. van Staveren and D.B.W.M. van Dusseldorp	—
29	Numerical Modelling of Groundwater Basins: A User-Oriented Manual	J. Boonstra and N.A. de Ridder	90 70260 697
31	Proceedings of the Bangkok Symposium on Acid Sulphate Soils	H. Dost and N. Breeman (Eds.)	90 70260 719
32	Monitoring and Evaluation of Agricultural Change	J. Murphy and L.H. Sprey	90 70260 743
33	Introduction to Farm Surveys	J. Murphy and L.H. Sprey	90 70260 735
38	Aforadores de caudal para canales abiertos	M.G. Bos, J.A. Replogle, and A.J. Clemmens	90 70260 921
39	Acid Sulphate Soils: A Baseline for Research and Development	D. Dent	90 70260 980
40	Land Evaluation for Land-Use Planning and Conservation in Sloping Areas	W. Siderius (Ed.)	90 70260 999
41	Research on Water Management of Rice Fields in the Nile Delta, Egypt	S. El Guindy and I.A. Risseeuw; H.J. Nijland (Ed.)	90 70754 08 8
44	Selected Papers of the Dakar Symposium on Acid Sulphate Soils	H. Dost (Ed.)	90 70754 13 4
45	Health and Irrigation, Volume 1	J.M.V. Oomen, J. de Wolf, and W.R. Jobin	90 70754 21 5
45	Health and Irrigation, Volume 2	J.M.V. Oomen, J. de Wolf, and W.R. Jobin	90 70754 17 7
46	CRIWAR 2.0 A Simulation Model On Crop Irrigation Water Requirements	M.G. Bos, J. Vos, and R.A. Feddes	90 70754 39 8
47	Analysis and Evaluation of Pumping Test Data (second edition, completely revised)	G.P. Kruseman and N.A. de Ridder	90 70754 20 7
48	SATEM: Selected Aquifer Test Evaluation Methods: A Computer Program	J. Boonstra	90 70754 19 3
49	Screening of Hydrological Data: Tests for Stationarity and Relative Consistency	E.R. Dahmen and M.J. Hall	90 70754 27 4
51	Influences on the Efficiency of Irrigation Water Use	W. Wolters	90 70754 29 0
52	Inland Valleys in West Africa: An Agro-Ecological Characterization of Rice Growing Environments	P.N. Windmeijer and W. Andriessse (Eds.)	90 70754 32 0
53	Selected Papers of the Ho Chi Minh City Symposium on Acid Sulphate Soils	M.E.F. van Mensvoort (Ed.)	90 70754 31 2

54	FLUME: Design and Calibration of Long-Throated Measuring Flumes	A.J. Clemmens, M.G. Bos, and J.A. Replogle	90 70754 30 4
55	Rainwater Harvesting in Arid and Semi-Arid Zones	Th.M. Boers	90 70754 36 3
56	Envelope Design for Subsurface Drains	W.F. Vlotman, L.S. Willardson and W. Diericks	90 70754 53 3

### Bulletins

1	The Auger Hole Method	W.F.J. van Beers	90 70754 816
4	On the Calcium Carbonate Content of Young Marine Sediments	B. Verhoeven	—
8	Some Nomographs for the Calculation of Drain Spacings	W.F.J. van Beers	—
10	A Viscous Fluid Model for Demonstration of Groundwater Flow to Parallel Drains	F. Homma	90 70260 824
11 <sup>S</sup>	Análisis y evaluación de los datos de ensayos por bombeo	G.P. Kruseman and N.A. de Ridder	—
11 <sup>F</sup>	Interprétation et discussion des pompages d'essai	G.P. Kruseman and N.A. de Ridder	—
13	Groundwater Hydraulics of Extensive Aquifers	J.H. Edelman	90 70260 794

### Bibliographies

18	Drainage: An Annotated Guide to Books and Journals	G. Naber	90 70260 93 X
----	----------------------------------------------------	----------	---------------

### Special Reports

Liquid Gold Paper 1	Scarcity by Design: Protective Irrigation in India and Pakistan	M. Jurriëns and P. Wester	
Liquid Gold Paper 2	Irrigation Water Division Technology in Indonesia: A Case of Ambivalent Development	L. Horst	90 70754-24-8
Liquid Gold Paper 3	Water Control in Egypt's Canal Irrigation A discussion of institutional issues at different levels	P.P. Mollinga, D.J. Merrey, M. Hvidt, and L.S. Radwan	9070754 45 2
Liquid Gold Paper 4	Coping with Water Water management in flood control and drainage systems in Bangladesh	P. Wester, and J. Bron	9070754 47 9
Liquid Gold Paper 5	The Response of Farmers to Political Change Decentralization of irrigation in the Red River delta, Vietnam	J.P. Fontenelle	9070754 48 7
	Water and Food Security in Semi-Arid Areas	A. Schrevel	
	Public Tubewell Irrigation in Uttar Pradesh, India A case study to the Indo-Tubewell Project	J.H. Alberts	
	Sustainability of Dutch Water Baords: Appropriate design characteristics for self-governing water management organisations	B. Dolfing, and W.B. Snellen	
	Em38 Workshop Proceedings	W.F. Vlotman	90 7075451 7
	SALTMOD: Description of Principles, User Manual, and Examples of Application	R.J. Oosterbaan	90 70754 52 5